Novel Intelligent Infra-Red Thermal Image Processing for Monitoring and Screening of Some Critical Ailments in Humans

Thesis submitted by

Asok Bandyopadhyay

Doctor of Philosophy (Engineering)

Department of Instrumentation & Electronics Engineering,
Faculty Council of Engineering & Technology,
Jadavpur University,
Kolkata, India

2024

Novel Intelligent Infra-Red Thermal Image Processing for Monitoring and Screening of Some Critical Ailments in Humans

Thesis submitted by

Asok Bandyopadhyay

Doctor of Philosophy (Engineering)

Department of Instrumentation & Electronics Engineering,
Faculty Council of Engineering & Technology,
Jadavpur University,
Kolkata, India

2024

To my parents, my wife and daughter

Jadavpur University

Kolkata-700032, India

REF. NO. D-7/E/549/17
INDEX NO. 179/17/E

1. Title of the thesis:

"Novel Intelligent Infra-Red Thermal Image Processing for Monitoring and Screening of Some Critical Ailments in Humans"

2. Name, Designation, & Institution of the Supervisors:

Dr. Bivas Dam

Professor,

Department of Instrumentation & Electronics Engineering,

Jadavpur University, Kolkata-700098, India

Dr. Dipak Chandra Patranabis

Professor (Retired)

Dept. of Instrumentation and Electronics Engineering

Jadavpur University, Kolkata-700098, India

Publication of the Author

3. Publication of the Author:

1. Asok Bandyopadhyay, Himanka Sekhar Mondal, Abhisekh Hazra. "Infrared Imaging of Stress Level Monitoring for Intelligent Diagnosis System", 2nd International Conference on Biomedical Engineering and Assistive Technologies, BEATS-2012, December 6-7, 2012, NITJalandhar.
2. Asok Bandyopadhyay, Himanka Sekhar Mondal, Bhaswati Mukherjee, Amit Chaudhuri. "Infrared Imaging of Stress and Diabetic Level Monitoring for Intelligent Healthcare System", CSI Journal of Computing Vol. 2 No. 1-2, 2013,66-73
3. Asok Bandyopadhyay, Himanka Sekhar Mondal, Amit Chaudhuri. "Thermal Imaging Based Diabetes Screening using Medical Image Processing Techniques", International Journal of Engineering Research & Technology (IJERT) ISSN: 2278-0181 Vol. 3 Issue 11, November- 2014
4. Asok Bandyopadhyay, Himanka Sekhar Mondal, Amit Chaudhuri. "Intelligent IR based image processing techniques for medical application", SAI Computing Conference 2016, July 13-15, 2016, London, UK
5. Asok Bandyopadhyay, Himanka Sekhar Mondal, Bivas Dam &Dipak Chandra Patranabis. "Efficient infrared image processing and machine learning algorithm for breast cancer screening". Computer Methods in Biomechanics and Biomedical Engineering: Imaging & Visualization, Taylor & Francis, Published online: 26 Jun 2023, VOL. 11, NO. 6, 2226–2238, https://doi.org/10.1080/21681163.2023.2225639
6. Asok Bandyopadhyay, Himanka Sekhar Mondal, Barnali Pal, Bivas Dam, Dipak Chandra Patranabis. "Exploring the potential use of infrared imaging in medical diagnosis: comprehensive framework for diabetes & breast cancer screening". Proceedings of 4th International Conference on Image Processing & Capsule Networks (ICIPCN 2023),10-11 August 2023, Bangkok, Thailand, pp388-402.
7. Asok Bandyopadhyay, Himanka Sekhar Mondal, Bivas Dam, and Dipak Chandra Patranabis, (2023). "An Overview of Infra-red Image Processing Based Oral Cancer

Detection Technique". Archives of Advanced Engineering Science, 1–9. https://doi.org/10.47852/bonviewAAES32021844

8. Asok Bandyopadhyay, Himanka Sekhar Mondal, Bivas Dam, and Dipak Chandra Patranabis, "Revolutionizing Breast Cancer Screening: Comprehensive System with Angiogenesis Correlations through Rotational Thermography and Dynamic Temperature-Based Infrared Imaging". Communicated to the Journal of Medical Engineering &Technology Print ISSN: 0309-1902 Online ISSN: 1464-522X on 02-08-2023 and is under review.
9. Asok Bandyopadhyay, Himanka Sekhar Mondal, Barnali Pal, Bivas Dam, Dipak Chandra Patranabis, " Innovative Infrared Imaging Approach for Breast Cancer Screening: Integrating Rotational Thermography and Machine Learning Analysis". Communicated to the Journal of "Artificial Intelligence in Health" Electronic ISSN: 3029-2387 on 28-03-2024 and is under review.

4. Patent claimed through this research:

1. Patent: Title: "A ROTATIONAL THERMO-GRAPHIC IMAGING BASED BREAST CANCER SCREENING SYSTEM"

   Patent Application No: 202031036632

   Filing Date: 25/08/2020

   Patent Inventors: Asok Bandyopadhyay, Himanka Sekhar Mondal, Debabrata Pal, Sayantani Banerjee, Mamata Chakaraborty, Barnali Pal, Amit Chaudhuri

   STATUS: Reply Filed. Application in amended examination

   Novelty of the patent claimed as follows:

1.A rotational thermo-graphic imaging based breast cancer screening system, the system comprises: a temperature controlled enclosure having an adjustable grooved hole in the front wall to accommodate one breast, wherein a set temperature is maintained by an air-conditioning unit controller ; an image capturing sub-unit , provided in the temperature-controlled enclosure , to

capture thermo-graphic images of the breast accommodated in the adjustable grooved hole of the temperature-controlled enclosure , the image capturing sub-unit comprising an infra-red camera provided at an end of a rotating arm to facilitate capturing of the thermo-graphic image of breast from different angles and from both axilla; and a computer , electronically connected to the image capturing sub-unit and air conditioning unit controller , to operate the movement of the image capturing sub-unit and capturing the thermo-graphic images from different angles, wherein the captured image is analysed for detection of abnormalities of the breast at each angle.

2. The system as claimed in claim 1, wherein movement of the image capturing sub-unit is controlled using a motor controller configured to be operated via the computer.

3.The system as claimed in claim 2, wherein the image capturing sub-unit preferably move in a semi-circular path, with adjustable grooved hole as center to capture the thermo- graphic images of the breast from different angles and from both axilla.

4.The system as claimed in claim 1, wherein the image capturing sub-unit rotates, such that, the distance between the IR camera and the adjustable grooved hole in the temperature-controlled enclosure, where breast is accommodated, remains constant resulting in focusing of the IR camera on the adjustable grooved hole.

5.The system as claimed in claim 4, wherein the distance between the IR camera and the adjustable grooved hole in the temperature-controlled enclosure, where breast is accommodated, depends on the minimal focus distance of the IR camera.

6. The system as claimed in claim 1, wherein at least two sets of images from different angles and both axilla are taken, each set being taken at two different temperatures, to extract the dynamic nature of thermogram due to angiogenesis in malignant breast.

7. The system as claimed in claim 1, wherein the temperature of the room where the system is kept is maintained at a constant temperature via an external air conditioning unit controller.

8. The system as claimed in claim 1, wherein the adjustable grooved hole is preferably semi-circular.

9. The system as claimed in claim 1, wherein the adjustable grooved hole is made adjustable to different size of breast by providing different templates.

10.The system as claimed in claim 1, wherein a table top mechanical arrangement is provided in the system to facilitate capturing of thermo-graphic image of one breast at a time by covering the other breast behind an infra-red proof wall.

11.The system as claimed in claim 1, wherein a temperature sensor is placed inside the temperature-controlled enclosure to provide the temperature of the enclosure to the air conditioning unit controller.

12.The system as claimed in claim 1, wherein the air conditioning unit controller controls an internal air conditioning unit provided on the temperature-controlled enclosure based on the temperature provided by the temperature sensor to maintain constant temperature inside the temperature-controlled enclosure.

5. List of Copyright:

1. Copyright: Title: Copyright: IR based Breast Cancer Screening software
   Copyright Registration no: SW-12853/2019
   Copyright Dated: 23.09.2019
   Copyright Inventors: Asok Bandyopadhyay, Himanka Sekhar Mondal, Amit Chaudhuri
   STATUS: Copyright received: on 23.09.2019

6. List of Book Chapter:

1. Exploring the Potential Use of Infrared Imaging in Medical Diagnosis: Comprehensive Framework for Diabetes and Breast Cancer Screening" has been published in the springer book series "Lecture Notes in Networks and Systems volume 798" pp 411-424.

7. List of Presentations in National /International/ Conferences/ Workshops:

1. Presented the paper titled “Infrared Imaging of Stress Level Monitoring for Intelligent Diagnosis System”, in the 2nd International Conference on Biomedical Engineering and Assistive Technologies, BEATS-2012, December 6-7, 2012, NIT Jalandhar.
2. Presented the paper “Intelligent IR based image processing techniques for medical application” at SAI Computing Conference 2016, July 13-15, 2016, London, UK.
3. As invited Speaker delivered a talk on “Development of breast cancer screening system using efficient infrared image processing and machine learning algorithm” in the 7th International Conference on Cancer Research and Oncology organized by Cancer 2023 Scientific Meditech July 29-30,2023.
4. Presented the paper “Exploring the potential use of infrared imaging in medical diagnosis: comprehensive framework for diabetes and breast cancer screening” in the 4th International Conference on Image Processing & Capsule Networks (ICIPCN 2023),10-11 August 2023, Bangkok, Thailand(online).
5. As invited Speaker delivered a talk on “Intelligent System for Infrared Imaging Based Breast Cancer Screening using Angular Views” in the 8th International Conference on Cancer Research and Oncology (Online) organized by Cancer 2023 Scientific Meditech November 25-26, 2023.
6. As invited speaker delivered a talk on “Breast cancer screening system using efficient infrared image processing and machine learning algorithm” on 16th December, in the 3rd International Conference on Cancer Science and Therapy (online) during December 15-17,2023.

“Statement of Originality”

I, Asok Bandyopadhyay registered on 02/08/2017 (Ref. No. **D-7/E/549/17,** Index No.**179/17/E**) do hereby declare that this thesis entitled “Novel intelligent infra-red thermal image processing for monitoring and screening of some critical ailments in humans” contains literature survey and original research work done by the undersigned candidate as part of Doctoral studies.

All information in this thesis have been obtained and presented in accordance with existing academic rules and ethical conduct. I declare that, as required by these rules and conduct, I have fully cited and referred all materials and results that are not original to this work.

I also declare that I have checked this thesis as per the “Policy on Anti Plagiarism, Jadavpur University, 2019”, and the level of similarity as checked by iThenticate software is 5 %.

Asok Bandyopadhyay

Signature of Candidate:

Date: 30/04/2024

Certified by Supervisor(s):

(Signature with date, seal)

1. 30/04/2024

Professor
Dept. of Instrumentation & Electronics Engg
Jadavpur University
Saltlake, 2nd Campus
Kolkata-700098

2. 30/04/2024

Professor (Rtd.)
Dept. of Instrumentation & Electronics Engg
Jadavpur University
Saltlake, 2nd Campus
Kolkata-700098

CERTIFICATE FROM THE SUPERVISORS

*This is to certify that the thesis entitled "***Novel intelligent infra-red thermal image processing for monitoring and screening of some critical ailments in humans***" submitted by* ***Shri Asok Bandyopadhyay****, who got his name registered on 02/08/2017 (Ref. No.* ***D-7/E/549/17,*** *Index No.****179/E/17****) for the award of Ph.D. (Engineering) degree of Jadavpur University is absolutely based upon his own work under the supervision of* ***Prof. (Dr) Bivas Dam*** *and* ***Prof. (Retd.) (Dr) Dipak Chandra Patranabis*** *and that neither his thesis nor any part of the thesis has been submitted for any degree/diploma or any other academic award anywhere before.*

Bivas Dam 20/04/2024

1.Prof. (Dr) Bivas Dam

Signature of the Supervisor

and date with Office Seal

Professor
Dept. of Instrumentation & Electronics Engg
Jadavpur University
Saltlake, 2nd Campus
Kolkata-700098

D. Patranabis 20/04/2024

2. Prof. (Retd.) (Dr) Dipak Chandra Patranabis

Signature of the Supervisor

and date with Office Seal

Professor (Retd.)
Dept. of Instrumentation & Electronics Engg
Jadavpur University
Saltlake, 2nd Campus
Kolkata-700098

ABSTRACT

Advancements in medical imaging techniques have led to the development of novel strategies for improving healthcare services and addressing the complexities inherent in medical diagnostics. This thesis focuses on the innovative application of infra-red (IR) thermal imaging in the non-invasive monitoring and screening of critical human ailments, such as diabetes, breast cancer, and oral cancer. Intricate nature of medical measurements and the complexity involved in managing patient diagnostics, shows that there is need for research to find robust and intelligent imaging systems in medical practice.

The study validates the novel infra-red imaging techniques through meticulous research conducted in various medical settings and climatic conditions in India, incorporating an enhanced software version tailored to accommodate diverse populations and environmental variations. The thesis highlights the significant contributions made towards establishing IR imaging as a valuable screening tool, emphasizing its non-invasive nature and intelligent processing capabilities are expected to make it widely acceptable in medical diagnostics.

Integral to the research is the development of an IR image acquisition and analysis system, featuring automatic image segmentation for precise Region of Interest (ROI) selection. This system incorporates a statistical analysis algorithm, capturing essential parameters from the extracted ROI, which subsequently serve as discriminating features in a machine learning algorithm. Notably, the study showcases the efficacy of a modified IR pattern recognition system and advanced machine learning techniques, facilitating accurate diagnosis and treatment assessment based on IR imaging.

The research also presents a novel approach for breast cancer screening, incorporating rotational thermography and dynamic temperature measurements. The work has further considered the transformative impact of infra-red imaging in diabetic condition diagnosis, stress assessment and the early detection of oral cancer, demonstrating its versatility in a multitude of medical applications.

It is believed that the research findings make a significant contribution towards the development of infra-red imaging techniques providing a comprehensive framework for enhancing medical diagnostics and targeted patient care.

ACKNOWLEDGEMENT

A remarkable expedition for carrying out the PhD and writing this thesis in the Department of Instrumentation and Electronics Engineering at Jadavpur University is very memorable due to the support and encouragement of many outstanding people. First,I would like to thank God for the kind blessings and being my ultimate protector.Foremost, I would like to express my sincere gratitude to my supervisors, **Prof. Bivas Dam** and **Prof. Dipak Chandra Patranabis** for the continuous support of my PhD study and research, for their patience, motivation, enthusiasm, and immense knowledge. Their guidance and attitude towards excellence helped me in all the time of research and writingof this thesis. I could not have imagined having better supervisors and advisers for my PhD study. I would also like to thank the authorities and administrative staff of Jadavpur University for being very helpful and supportive throughout my tenure at Jadavpur University. Special thanks to Head of Department, Instrumentation and Electronics Engineering for the valuable support. I would also like to thank **Late** Amit Chaudhuri of C-DAC, Kolkata for his initial support as a supervisor.

In addition, the author would also like to take this opportunity to express gratitude to the Centre for Development of Advanced Computing, Kolkata for support, without which, I would not have been able to go on this enlightening journey. However, I will remain grateful to **Sankar Prasad Banerjee**, my father, and **Gouri Banerjee,** my mother, for whom I got courage and patience to step forward. Initially, the journey for my PhD work starts with my dear teachers of my post graduate college. The support of my colleagues Himanka Sekhar Mondal, Barnali Pal of CDAC, Kolkata established a path at the midway of the journey that gives me additional energy for the PhD work.

No words would ever do justice to express my deepest thanks and gratitude to my beloved wife **Indrani** and my daughter **Rupsa** for being there for me at all times. Their continuous love, sacrifice, supports and encouragement have allowed me to pursue my ambitions. I would also like to thank my brothers and my sister for the constant support and encouragement. Finally, I dedicate my work to my parents, my wife, my daughter and teachers, whom I owe all my successes and achievement.

Jadavpur University

AsokBandyopadhyay

(**Asok Bandyopadhyay**)

30/04/2024

Kolkata-700098

CONTENTS

LIST OF FIGURES

LIST OF TABLES

Chapter I

INTRODUCTION

1.1 Introduction

1.1.1 Motivation for the Research

In the progressive landscape of modern society, the pervasive integration of Information and Communication Technology (ICT) systems has led to a marked transformation in various sectors, including healthcare. This transformation has highlighted the need for advanced, innovative diagnostic tools that facilitate accurate and reliable medical assessment and extend the reach and accessibility of healthcare services. Consequently, integrating new-generation diagnostic technologies has become of paramount interest, aiming to enhance the quality of medical services and improve patient care.

Amidst this paradigm shift, infra-red thermal imaging has emerged as a promising avenue for non-invasive monitoring and screening of critical human ailments. The pressing need for such advancements in medical technology arises from the intricate nature of medical measurements, which involves a complex interaction between the human body as the subject and the physician as the orchestrator of the diagnostic process. This complexity suggests that there is scope for employing sophisticated computational models and intelligent processing techniques to ensure accurate and reliable biomedical measurements.

The motivation for this research stems from the above and various other factors, each contributing to realizing the crucial role that intelligent infra-red thermal image processing can play in advancing the usefulness and spread of medical diagnostic systems. This motivation can broadly be attributed to several factors, including:

1.1.1.1 Inspiration from Previous Research

The impetus for this research finds its roots in the seminal contributions of previous researchers, whose ground breaking work has not only propelled the field of infrared thermal imaging forward but also illuminated the impending use for its integration into advanced medical diagnostics. The insights from the earlier discussions emphasized the need to build upon the existing knowledge base and push the boundaries of infrared imaging applications towards developing a system conducive to providing practical solutions for medical breakthroughs. Notably, the literature review highlighted the works of Dr Lykken, Dr Steinbrook, and Dr Furedy, all of which underline the inadequacies of traditional stress

assessment techniques, thereby pointing towards the critical need for more reliable and non-invasive methodologies, such as those enabled by infra-red thermal imaging [1].

1.1.1.2 Identified Gaps in Current Diagnostic Practices

Analysis of current healthcare diagnostic practices has some gaps and limitations, particularly in accurate and non-invasive ailment monitoring. These gaps, as found in research documents, prompted a critical reassessment of the existing methodologies and deserved a need for innovative approaches that could offer more accurate assessments of critical ailments. Notably, the works of S. Sivanandam et al. shed light on the challenges faced in precise diabetes monitoring, emphasizing the prospective use of infra-red imaging to bridge the existing gaps and provide a more nuanced understanding of physiological changes [2].

1.1.1.3 Interaction with Industry Experts and Medical Practitioners

The engagement and collaboration with experts from industry and medical practitioners in diagnostics provided invaluable insights into the practical challenges and requirements of the healthcare ecosystem. These interactions facilitated a deeper understanding of the intricacies of infra-red imaging applications. They suggested a more tailored and user-friendly approach to infrared thermal imaging integration. The inputs received from these stakeholders played a significant role in shaping the research direction and emphasizing the critical importance of developing a solution that aligns seamlessly with the practical needs of healthcare professionals and the broader patient community.

1.1.1.4 Technological Advancements and Workforce Availability

The rapid advancements in infra-red imaging technologies and the increasing availability of a skilled workforce proficient in handling sophisticated diagnostic tools have provided a fertile ground for pursuing innovative research endeavours. Integrating state-of-the-art infra-red cameras with advanced image processing software has opened up new possibilities for developing a robust and efficient diagnostic framework that can cater to the evolving demands of the healthcare landscape. This synergy of technological advancements and a skilled workforce has helped to develop an intelligent infra-red thermal image processing into the existing medical diagnostic ecosystem, ensuring a more streamlined and practical approach to critical ailment monitoring and screening.

By addressing these motivating factors, this research aspires to contribute to advancing a novel intelligent infra-red thermal image processing for monitoring and screening critical ailments in humans, thereby ensuring a significant stride forward in modern medical diagnostics.

1.2 Review of Earlier Works

A widespread review of prior research in infra-red thermal imaging for medical applications illuminates the trajectory of advancements and limitations that have shaped the current landscape of diagnostic technologies. The synthesis of earlier works emphasizes the critical role of infra-red thermal imaging in addressing complex medical conditions, highlighting the challenges that have impeded its widespread implementation.

The pioneering works of Dr Lykken, Dr Steinbrook, and Dr Furedy reflect the limitations of classical polygraph tests in reliably monitoring sudomotor activity [1]. Their research serves as a foundational reference point, shedding light on the inefficiencies of conventional stress assessment techniques and paving the way for exploring more robust and non-invasive methodologies, such as infrared thermal imaging.

Similarly, the research conducted by S. Sivanandam [1] et al. in 2012 has demonstrated a negative correlation between HbA1c levels and the carotid region, indicating the potential for infrared imaging to facilitate diabetes monitoring [2]. This research serves as a testament to the feasibility of employing infrared imaging for precise physiological measurements, thereby bolstering the credibility of its application in critical ailment monitoring.

Furthermore, Dr Roeland Van Wijk, Dr Masaki Kobayashi, and Dr Eduard P.A. Van Wijk have contributed significantly to the exploration of human biophoton emission using cryogenically cooled CCD camera systems, showcasing the potential of infrared imaging in capturing ultra-weak photon emissions from living organisms [3], [4],[5],[6],[7]. These seminal studies have highlighted the complex relationship between bio-photonic or bio-electromagnetic phenomena and the functional coherence within biological systems, thus emphasizing the broad scope and potential applications of infrared imaging in medical diagnostics.

Most researchers have reported the use of conventional methods for IR cameras for this purpose [8], [9], [10], but they still need to apply appropriate image processing techniques. An intelligent infrared thermal imaging method was proposed in [11],[12], [13], [14], [13].

The applications of infrared imaging techniques for breast cancer screening have been depicted as an essential part of the thesis [8][9][15][9], [16][16][16][17][18][10]

Additionally, the cumulative knowledge derived from various studies, as highlighted by Kandlikar et al. in their review of the current status, protocols, advantages, and limitations of infrared imaging techniques for breast cancer detection, has shed light on the intricate nuances of utilizing infra-red imaging for early detection and screening of malignant diseases [19]. The synthesis of this extensive body of work serves as a foundational basis for the present research, enabling a complete understanding of the capabilities and limitations of infrared thermal imaging in the context of critical ailment diagnosis.

Various research teams have investigated the selection of regions of interest (ROIs) for infrared (IR) image capture within their respective studies. Notably, Sodi et al. conducted a study comparing ocular surface temperature (OST) among patients with non-proliferative diabetic retinopathy (NPDR) [2], while Roback and Johansson explored the study investigated the potential of using thermographic imaging as an early detection method for foot disorders in diabetic patients.[20]. Additionally, Nishide et al. focused on identifying latent inflammation within foot calluses using thermography and ultrasonography. At the same time, Minamishima et al. conducted a treadmill walking stress test combined with thermography to elucidate characteristic patterns of diabetic autonomic neuropathy in the toes [21]. Fujiwara, Inukai, and Armstrong utilized thermographic measurement of skin temperature for type 2 diabetes [22], Fushimi et al. investigated abnormal vasoreactions in hands [23], and Sivanandam et al. explored various body regions, including the face, forehead, and hand, foot, and neck [24].

Using a system of IR pattern recognition, digital geometry, and signal processing techniques, it has been established that a diagnostic tool can be created to increase the accuracy of risk analysis for patients with mental stress and correlate with their body emissions [23]. In addition to its clinical applications, the proposed system can be used for healthcare and stress management issues in hospitals and offices and by physicians to evaluate the condition of patients with manageable costs and non-invasive techniques.

Chapter III describes research on monitoring the autonomic nervous system's response to mental stress, involving the measurement of periodic changes in skin perfusion (with blood) in the face and ear, which are associated with regulating skin temperature by an Infrared Camera integrated with a computer system. It is well known that the autonomic nervous system is affected by mental stress, resulting in changes in some physiological parameters. These include higher heart rate, blood pressure, pale or blushing, and excessive perspiration (enhanced sudomotor activity). The latter is often detected by decreased galvanic skin resistance. As Dr Lykken, Dr Steinbrook and Dr Furedy pointed out, the classical polygraph tests based primarily on monitoring sudomotor activity are unreliable [1]. Electroencephalography (EEG) to monitor event-related brain potentials is more reliable than the conventional polygraph [1]. Still, it is impractical as a routine technique from the standpoints of the cost and time involved. The same applies to magneto-encephalography, which can measure brain activity without contact but only in a sophisticated, highly controlled and costly environment.

The infrared camera or other thermal imager detects changes in the subject's skin temperature by continuously monitoring the modulation (i.e., increase or decrease) of skin temperature. The mechanism by which infrared cameras can measure skin temperature caused by stress is described well. [25].

Researchers have done similar work with different technologies on the effects of human body emissions. Measurement of the human body emission in the ELF (Extremely low frequency) band can be done using the loop antennae of the type used in bands ranging from ELF to UHF (ultra-high frequencies) from the very beginning of radio communication, which works on measurement and recording of electrical human body emission component in the stage of already designed dedicated measurement devices. [26]. Many molecular mechanisms can be assessed quantitatively in vivo using radionuclide techniques such as single photon emission computed tomography (SPECT) and positron emission tomography (PET). [27]

During research work done by Dr Roeland Van Wijk, Dr Masaki Kobayashi, and Dr Eduard P.A. Van Wijk [28], a cryogenically cooled CCD camera system that incorporates a CCD42-40 NIMO back illuminated high-performance CCD Sensor having full-frame architecture was used for imaging of human biophoton emission. Ultra-weak photon Emission using CCD is developed using these principles. The primary purpose was to research some

"integrative biophysics" that pays attention to the properties of coherence, long-range interactions, information and communication in living organisms with bio-photonic or bio-electromagnetic techniques. The research activities can be recognized by the increasing literature in this field, which is presented in different reviews and books [3], [29], [4],[6],[7]. These literary works demonstrate the richness of information that can be retrieved from photon emission measurements. The present review offers the opportunity to participate in the discussion to understand radiation from (and within) biological matter. [7]. All these technologies have specific positive impacts and cost-effective and purpose-specific applications. In comparison, IR imaging has tremendous probabilities in general-purpose low-cost solutions in different types of applications.

1.2.1 Correlation between Pathology and Infrared Imaging

Early research explored the association between underlying breast cancer and regional skin surface temperature alterations. In a study conducted in 1963 by Lawson and Chughtai, surgeons from McGill University, demonstrated that the increase in regional skin surface temperature associated with breast cancer links to venous convection [30]. This pioneering quantitative study bolstered previous research, indicating that findings of infrared imaging correlated with heightened vascularity. Infrared breast imaging holds significant predictive potential as it may correlate with various pathologic prognostic factors such as tumour size, grade, lymph node involvement, and markers of tumour growth [31]. Ongoing investigations seek to elucidate the pathologic mechanisms underlying these infrared findings. One proposed mechanism involves increased blood flow due to vascular proliferation, as assessed by microvascular density (MVD) reflecting tumour-associated angiogenesis. However, a study by [32] found no correlation between MVD and abnormal infrared findings. Notably, the imaging technology used in that study, contact plate technology and liquid crystal thermography (LCT), lacked the capability for modern computerized analysis. Therefore, digital processing is deemed essential for correlating histological and discrete vascular changes [33].

In 1993, Head and Elliott [34] reported that advancements in second-generation infrared systems facilitated more objective and quantitative analysis [38], highlighting a strong association between infrared image interpretation and prognostic indicators related to tumour growth rates. In a comprehensive review, Anbar [35] proposed utilizing a sophisticated biochemical and immunological cascade to explain the observed infrared changes in small

tumours, which could be attributed to enhanced perfusion over a significant area of the breast surface via regional tumour-induced nitric oxide (NO) vasodilation. Nitric oxide, synthesized by nitric oxide synthesis (NOS), exerts potent vasodilating effects and plays a crucial role in tumorigenesis, particularly in breast carcinoma [36].

Nitric oxide diffuses readily through tissues and induces various biochemical changes upon binding to endothelial receptors, leading to vasodilation. Most neoplasms exhibit a lower cellular metabolic demand in the early stages of tumour growth.

In a comprehensive review, Anbar [35] proposed that angiogenesis, stimulated by angiogenesis factors (AF) released from precancerous or cancerous cells, further contributes to increased blood supply and vascular asymmetry observed in infrared images.

The concept of angiogenesis as an early event in breast cancer development was underscored by Guido and Schnitt in 1996 [37]. They observed that angiogenesis may precede morphological evidence of carcinoma, emphasizing its significance in early detection. Additionally, Gamagami, in his 1996 textbook, highlighted the utility of infrared imaging in detecting hypervascularity and hyperthermia associated with nonpalpable breast cancers, aiding in their detection [38]. The substantial body of evidence supporting the efficacy of infrared imaging in detecting precancerous and cancerous breast lesions lies in its ability to capture angiogenesis and the recruitment of existing vascularity, which is crucial for sustaining malignant cellular growth. Biomedical engineering studies have further validated the value of infrared imaging in both in vitro and in vivo settings [39][40].

1.2.2 Infrared Imaging as a Prognostic Indicator

Studies exploring the biology of cancers have shown that the amount of thermo-vascular activity in the breast is directly proportional to the tumour's aggressiveness. As such, infrared imaging provides the clinician with an invaluable prognosis and treatment monitoring tool.

In a study of 209 breast cancer patients, Dilhuydy and associates [41] found a positive correlation between the degree of abnormalities and the existence of positive axillary lymph nodes. It was reported that the amount of thermovascular activity seen in the breast was directly related to the prognosis. The study concluded that infrared imaging is a significant factor in prognosis and should be included in the pre-therapeutic assessment of breast cancer.

1.2.3 Different Regions of Infrared in Energy Spectrum

The International Commission on Illumination (CIE) proposed categorizing infrared radiation into three main bands:

IR-A: Ranging from 700 nm to 1400 nm (0.7 μm – 1.4 μm, equivalent to frequencies between 215 THz and 430 THz).

IR-B: Spanning from 1400 nm to 3000 nm (1.4 μm – 3 μm, corresponding to frequencies from 100 THz to 215 THz).

IR-C: Extending from 3000 nm to 1 mm (3 μm – 1000 μm, with frequencies between 300 GHz and 100 THz).

One commonly adopted sub-division is Near-infrared (NIR, IR-A DIN), which covers the wavelength range of 0.75-1.4 μm. This range is defined by water absorption and finds extensive use in fiber optic telecommunications, particularly in adverse weather conditions. Outdoor activities are often rescheduled due to inclement weather conditions, with low attenuation losses observed in the silica (SiO_2) glass medium. Devices such as image intensifiers are highly sensitive to this spectrum, with night vision goggles being prominent examples.

Another sub-division is Short-wavelength infrared (SWIR, IR-B DIN), which spans from 1.4 to 3 μm. Notably, water absorption increases significantly around 1,450 nm. The spectral region between 1,530 to 1,560 nm is widely utilized in long-distance telecommunications.

The third sub-division is Mid-wavelength infrared (MWIR, IR-C DIN) and intermediate infrared (IIR), covering the range from 3 to 8 μm. In guided missile technology, this band's 3-5 μm portion is the atmospheric window utilized by passive infrared "heat-seeking" missiles' homing heads. These missiles typically track target aircraft by detecting their infrared signatures, often associated with the jet engine exhaust plume.

Long-wavelength infrared (LWIR, IR-C DIN): 8–15 μm. This region is solely for "thermal imaging", and the sensors are limited to obtaining a passive picture of the outside world based solely on thermal emissions., requiring no external light or thermal sources. The spectrum offers a range of options for technology, such as the sun, moon, or infrared

illuminator. FLIR systems take advantage of this spectrum area to provide forward-looking infrared capabilities. Which is sometimes also called the "far infrared ".

Far infrared (FIR): region 15 - 1,000 μm.

NIR and SWIR are sometimes called "reflected infrared", while MWIR and LWIR are sometimes referred to as "thermal infrared. "Hot objects appear brighter in the MW than in the LWIR due to blackbody radiation curves.

1.2.4 Infra-Red Radiation from Human Skin

IR light has longer wavelengths than visible light, starting at 0.74 micrometres and extending to 300 micrometres. IR light is emitted or absorbed by molecules when they change their movements. It covers a 1-400 THz frequency range and includes thermal radiation from objects at room temperature.

1.2.5 Mammography and Infrared Imaging

From a scientific perspective, it is important to differentiate between mammography and infrared imaging as screening tests. Mammography primarily serves as a structural imaging procedure, focusing on detecting architectural tissue shadows, whereas infrared imaging functions as a functional imaging technology, observing changes in the metabolic activity within the breast tissue. Despite these distinct approaches, research has enabled statistical comparisons between the two technologies. While previous studies have extensively examined the efficacy of infrared imaging, this discussion will concentrate on the current status of mammography.

In a study conducted by Rosenberg [42], a comprehensive analysis was undertaken involving 183,134 screening mammograms to assess changes in sensitivity attributed to various factors such as age, breast density, ethnicity, and estrogen replacement therapy. Among these screenings, 807 cases were detected as cancerous. The findings indicated varying sensitivities across different demographic groups: 54% sensitivity in women under 40, 77% in the 40–49 age group, 78% in the 50–64 age group, and 81% in women over 64. Additionally, sensitivity was noted to be 68% in women with dense breasts and 74% in users of estrogen replacement therapy.

In a separate investigation into the cumulative risk of false-positive results in mammographic screening, Elmore and colleagues [43] conducted a 10-year retrospective study involving 2,400 women aged 40 to 69. A total of 9762 mammograms were investigated. It was found that a woman had an estimated 49.1% cumulative risk of having a false-positive result after ten mammograms. Even though no breast cancer was present, over one-third of the women screened were required to have additional evaluations.

A study by Head [44] assessed the accuracy of mammography and infrared imaging in detecting breast cancer. Based on the study, mammography has an average sensitivity rate of 86% and a specificity rate of 79%. As per the information provided, the diagnostic test has a positive predictive value of 28% and a negative predictive value of 92%. These values represent the accuracy of the test in determining true positives and true negatives. Although the PPV is relatively low, the NPV is high, indicating that the test is more effective in ruling out the condition than confirming it. Conversely, infrared imaging showed an average performance of 86% sensitivity, 89% specificity, 23% positive predictive value, and 99.4% negative predictive value.Keyserlingk et al. [45] conducted a study to evaluate the relative usefulness of clinical examinations, mammography, and infrared imaging in detecting ductal carcinoma in situ, stage I and II breast cancers for 100 subjects. The study revealed that clinical examination achieved a sensitivity of 61%, while mammography attained 66%, and infrared imaging reached 83% when findings were suspicious or equivocal. Combining mammograms increased sensitivity to 85%, while a sensitivity of 95% was achieved by combining doubtful and equivocal mammograms with abnormal infrared images. Further amalgamation of clinical examination reports, mammography, and infrared images led to a sensitivity of 98%.

A review of the cumulative literature database shows that mammography's average sensitivity and specificity are 80 and 79%, respectively, for women over 50. Below a certain age threshold, there is a notable decline in sensitivity and specificity among women. Additionally, studies indicate that mammography frequently fails to detect interval cancers (those occurring between screening exams), whereas infrared imaging may prove effective in their detection. Overall, when examining the collective evidence, it becomes evident that mammography needs to catch up in various aspects... The current gold standard leaves much to be desired for breast cancer screening. As a standalone screening procedure, there may be better choices than mammography. In the same light, infrared imaging should not be used alone as a screening test. The two technologies are complementary. Neither used alone is sufficient,

but when combined, each build on the deficiencies of the other. In reviewing the literature, it seems evident that a multimodal approach to breast cancer screening would serve women best. Combining clinical examination, mammography, and infrared imaging would provide the most significant breast conservation and survival potential.

From previous studies, Sodi A et al. Johansson M and Roback K investigated the feasibility of thermal imaging-based ocular surface temperature in patients with diabetic foot disease and non-proliferative diabetic retinopathy (NPDR). [46] [47]. Nishide K et al. worked on using thermal imaging and ultrasound techniques to identify underlying inflammation of foot calluses [21]. To elucidate the typical pattern features of diabetic autonomic neuropathy in the toes, Fujiwara Y et al. Perform treadmill walking stress testing and thermal imaging [22]. Fushimi H et al. worked on the measurement of skin temperature in type 2 diabetic patients using thermal imaging [23]. S. Sivanandam et al. worked on investigating abnormal vasovagal responses in the hand [2]. It acts on different body parts, such as the face, forehead, hands, feet, and neck [2]. Sivanandam, M. Anburajan et al. investigated the potential of infrared thermography (IR) in diagnosing type 2 diabetes [2]in their early works.

In the first part of Chapter V, Diabetes Screening using IR imaging techniques has been described. Further, the selection of the ear cavity region as a critical body region for Diabetes screening has been explained along with advances in image processing, data acquisition, and machine learning contributing to its accuracy and validity. In this thesis, the importance of automated image processing and analysis methods to improve the accuracy and efficiency of infrared imaging for Diabetes and Breast Cancer screening has been highlighted.

The second part of Chapter V is focused on detecting breast cancer using infrared imaging.

Previously, various methods for detecting breast cancer using thermal imaging have been proposed. Etehad Tavakol et al. [8] introduced bi-spectral invariant features and achieved high detection rates in their study [15], [9]. They also compared colour segmentation techniques and found that K-means clustering performs better than other methods [9]. Gadugno Ramon et al. [16] developed a non-invasive tool for breast cancer diagnosis using a thermal imaging camera, using temperature and texture features with promising results [16]. Prakash et al. Comparing K-means, Fuzzy C-means and the EM algorithm, it is concluded that the EM algorithm has the highest segmentation accuracy [17]. Venkataramani et al. [18] proposed a semi-automated

method using thermal video imaging and achieved high sensitivity and specificity through morphological filtering and thresholding. Pramanik et al. proposed a deep learning-based level-set method for segmenting suspicious regions in chest thermograms and achieved high accuracy [10]. In brain tumour detection, Wu et al. proposed a colour-based K-means clustering segmentation method [48], which Kandlikar et al. reviewed [19]. The current status, protocols, advantages and limitations of infrared imaging techniques for breast cancer detection have been discussed [19]. These methods and studies demonstrate the potential of thermal imaging in breast cancer detection and provide insights into different methods and techniques of image processing and analysis [20].

The second part of Chapter V also addresses challenges such as quantifying suitable temperature values for malignant diseases and the lack of qualified medical professionals for infrared imaging-based screening systems. To address the above issues, a novel, non-contact, non-invasive breast imaging method based on rotational thermography and dynamic temperature has been developed, which detects any abnormalities found in the subjects [49], [50],[51]. The developed rotating thermal imaging device makes the affected area more visible, improving breast cancer detection accuracy. The machine learning algorithm is trained on the extracted features and predicts normal vs. abnormal values for the subjects.

Researchers have been able to develop efficient infrared image processing and machine learning algorithms for breast cancer screening. In their study, Etehad Tavakol et al. proposed bi-spectral invariant features for breast cancer detection from thermal images [15]. They achieved a reasonable detection rate by applying their proposed method to a dataset of thermal images. In another study, the same author compared different colour segmentation techniques for breast thermograms and found that K-means clustering outperformed other methods [9].

In a different approach, Garduño-Ramón et al. developed a supportive, non-invasive tool for the diagnosis of breast cancer using a thermographic camera as a sensor [16]. They used temperature and texture features for breast cancer detection and achieved promising results.

Several studies have been made on image segmentation for breast cancer detection using thermal images. Etehad Tavakol et al. applied K- and fuzzy c-means algorithms to colour-segment thermal infrared breast images [8]. Similarly, Prakash et al. compared K-means, fuzzy c-means, and EM algorithms to segment thermal infrared breast images [17]. They concluded that the EM algorithm had the highest segmentation accuracy.

Venkataramani et al. proposed a semi-automated breast cancer tumour detection method using thermographic video imaging [18]. They used morphological filtering and a thresholding method for image preprocessing and achieved high sensitivity and specificity.

Deep learning methods have shown remarkable performance in medical image analysis in recent years. For example, Pramanik et al. proposed a deep learning-based level set method for suspicious-region segmentation from breast thermograms [10]. As a result, they achieved high accuracy in segmenting the suspicious regions of breast thermograms.

In addition to breast cancer, thermal imaging has been used for brain tumour detection as well. Wu et al. proposed a colour-based K-means clustering segmentation method for brain tumour detection.[48]

Kandlikar et al. [19] reviewed the current status, protocols, and new directions of infrared imaging technology for breast cancer detection. The authors provided insights into the advantages and limitations of this imaging technology and discussed various protocols used for breast cancer detection using infrared imaging. They also discussed the potential of using new directions for improving the sensitivity and specificity of the infrared imaging technique in breast cancer detection.

Regarding filtering techniques, Patel et al. [52] present a methodology for predicting the surface roughness of machined components using image processing, computer vision, and machine learning. The authors highlight the importance of surface roughness in identifying the functional capability of a component during operating conditions and the difficulty in manually checking the surface roughness of each component being manufactured on a manufacturing line[52]. The issue of texture analysis of machined surfaces in the manufacturing industry was addressed by V.Vakharia et al. [53]. The authors propose a methodology for identifying textured surface images using wavelet transform and artificial intelligence techniques [53].

Recently, some researchers have been investigating using optimization algorithms for medical image analysis. Emam et al. proposed a modified reptile search algorithm for global optimization and image segmentation with a case study of brain MRI images [8]. Houssein et al. proposed an optimized deep-learning architecture for breast cancer diagnosis based on the improved marine predator's algorithm [54]. They achieved high accuracy in detecting breast cancer using their proposed method. In another study, Houssein et al. discussed the state-of-

the-art challenges and future vision of machine learning in the quantum realm [55]. They also highlighted the potential of quantum machine learning in improving the accuracy and speed of breast cancer detection and diagnosis. They also proposed several efficient optimization-based methods for cancer diagnosis, segmentation, and classification using deep learning, thresholding, and support vector machines.[54], [56], [57], [58], [59]

Use of different datasets, these methods achieve high accuracy in detecting breast abnormalities and masses. However, some studies have not included an appropriate algorithm for data analysis and integrated image processing techniques, which may lead to the failure of instrument-level development for breast cancer screening systems.

Data collection protocols and image processing techniques must be appropriately integrated with machine learning algorithms to develop efficient and accurate breast cancer screening software.

Chapter VI of the thesis describes rotational thermographic imaging, colour-based infrared image processing, and machine learning algorithms to detect the hottest regions of abnormal breasts, called suspected regions. Machine learning algorithms then train the extracted features and achieve regular and abnormal predictions at different viewing angles. Proper understanding and adaptation of the imaging process are essential for generating appropriate synergy related to temperature variations and other physical conditions. Without such intelligent data collection, analysis plays a significant role in giving importance to algorithmic perfection and improved machine learning performance. Therefore, developing a breast cancer screening system requires an integrated approach to data collection, image processing, and machine learning algorithms to achieve accurate and efficient results.

By assimilating the findings and insights from the above-referenced works, our current research endeavours to build upon the existing knowledge and address the gaps and challenges identified in the domain of intelligent infra-red thermal image processing for the monitoring and screening of critical ailments in humans.

1.3 Scope and Organisation of the Thesis

Motivated by the imperative need to enable non-invasive monitoring and screening of critical human ailments, like mental stress, diabetes, breast cancer, and oral cancer, this research

embarks on the development of an intelligent infrared thermal image processing system. Given the intricate dynamics between the patient, a multifaceted entity, and the physician, the orchestrator of care, the inherent complexities of medical measurements necessitate implementing sophisticated computational models and imaging techniques to ensure precise biomedical assessments. Thus, the central aim of this research revolves around establishing a framework facilitating the intelligent processing of infrared thermal images for monitoring and screening crucial human ailments.

In the current research, ‘Infrared camera-based temperature changes' have been monitored on the face and ear during a computerized "Paced Stroop Test" on the subjects.

The changes during the steps of "The Stroop Test" on the proposed area of interest of subjects are further analyzed. The observations lead to the development of a non-invasive mental stress analysis system.

The imaging approach utilized in this study was established following the guidance provided by technical sessions conducted by biomedical experts, physicians, and engineers and the initial findings from collected infrared (IR) data. To ensure consistent temperature readings of subjects, the methodology involved identifying the nearest value to the core temperature of each subject. Specifically, regions of interest included the ear lobe, inner canthus points, inner posterior buccal cavity, and palm. Later on, the study focused on ear (Tympanic membrane) images for diabetic screening systems after rigorous testing in different areas in India in different climatic situations. The cross-sectional design method captures and analyses images of specific regions of interest in diabetic subjects. Then, a comparative analysis was conducted using images from normal (non-diabetic) subjects to assess differences. Another set of infrared images is collected from Cachar Cancer Hospital, Silchar, Assam, for a pilot study on breast and oral cancer subjects to utilize the system in multipurpose medical problems and extract different angles of infrared imaging.

Current research captures thermal images using an IR camera (FLIR SC325) manufactured by FLIR Systems, Inc., USA.

Further, images are captured at a proper focusing distance from the body region, namely the face, forehead and ear regions. The images are analyzed using the Labview thermo vision toolkit of Virtual Instrumentation (VI) software (www.flir.com) customized for the present

system. Throughout this investigation, special care has been taken to explore the potential of IR thermal Imaging systems for better medical diagnosis. This thesis is comprised of seven chapters. The first chapter briefly introduces to the need for Infrared imaging for critical ailments in humans and corresponding solutions. The chapter concludes with the scope and organization of the present thesis. The subsequent outline offers a concise preview of the key chapters that constitute the core of the presented research:

Chapter II: Innovative Approach in Infra-red Imaging for Medical Applications

- This chapter broadens the scope by exploring innovative infrared imaging applications in the medical field.
- It discusses the correlation between pathology and infra-red imaging, research planning, thermal image acquisition, image processing techniques, and intelligent image segmentation.
- By examining these innovative approaches, the chapter emphasizes the potential of infra-red imaging for a wide range of medical applications.

Chapter III: Application of Infra-red Imaging for Stress and Diabetic Level Monitoring

- This chapter contains work on applying infrared thermal imaging in the context of stress assessment and diabetic level monitoring.
- Experimental procedures, setup, and observations involving infrared imaging to monitor the autonomic nervous system's response to mental stress have been presented here.
- The results show how infrared imaging can provide intelligent diagnosis for stress-related conditions.

Chapter IV: Development of Oral Cancer Detection Technique Using IR Image Processing

- This chapter focuses on oral cancer and details the image acquisition process, processing features, system workflow, and results.
- It provides in-depth discussions regarding the performance of the developed system for detecting oral cancer using infrared image processing.

Chapter V: Exploring the Potential Use of Infra-red Imaging in Medical Diagnosis - Comprehensive Framework for Diabetes & Breast Cancer Screening

- This chapter presents the work on the ‘generalized’ format of infra-red imaging in medical diagnosis.
- It discusses methodologies for diabetes and breast cancer screening using infrared imaging and presents the results.

Chapter VI: Efficient Infra-red Image Processing and Machine Learning Algorithm for Breast Cancer Screening

- This chapter presents the work that covers the technical aspects of efficient infra-red image processing and machine learning algorithms.
- It outlines a sophisticated approach to using these technologies for breast cancer screening.
- The chapter presents the work on developing an intelligent system that combines image processing and machine learning to enhance breast cancer diagnostics.

Chapter VII: Concluding Remarks and Glimpses for Future Works

- The final chapter of the thesis offers a summary of the essential findings and contributions made throughout the research.
- It provides an inclusive conclusion and reflects on the significance of the research within the broader context of medical diagnostics.
- Glimpses of potential future research directions and advancements in the field are also provided.

Chapter II

Innovative Approach in Infrared Imaging for Medical Applications

2.1 Introduction

In contemporary healthcare, Infrared Imaging has emerged as a pivotal tool, revolutionizing the landscape of medical diagnostics. This innovative technology is based on some unique properties of infrared radiation. It allows for non-invasive, real-time, and contactless temperature measurements within the human body.

Infrared Imaging's most notable attribute is its ability to provide precise and instantaneous thermal Information without invasive procedures or physical contact. By capturing and analyzing the subtle variations in temperature patterns, this imaging technique offers healthcare professionals a window into the physiological processes beneath the skin's surface.

One of the pressing concerns that has propelled the widespread adoption of Infrared Imaging in healthcare is the escalating global prevalence of diabetes. Diabetes, in its various forms, has emerged as a critical healthcare challenge affecting millions worldwide. With its capacity to detect temperature anomalies and thermoregulatory changes, Infrared Imaging has shown immense promise as a diagnostic and monitoring tool for diabetes and related conditions.[49].

2.1.1 Technology Development Using Infrared Imaging

Biopsy analysis stands as the conventional gold standard for cancer detection. However, the proposed integrated methodology utilizing thermal Imaging offers a promising avenue for a cost-effective and non-invasive early detection technique, specifically for oral and breast cancers. This methodology involves onsite thermal detection to pinpoint lesion locations and determine their extent. Integrating ultrasound/mammography images and biopsy analysis enhances the specificity of thermal findings. The process begins with acquiring thermal images to establish a database for subsequent analysis. Following image preprocessing, feature extraction and selection are carried out, and machine learning algorithms are trained based on these features. The fusion of classifier output with ultrasound/mammography images and biopsy expression culminates in an inference that is compared with biopsy findings. The iterative process intelligently enhances accuracy.

Based on the above guideline, the following technology development plan has been prepared, as shown in Fig. 2.1.

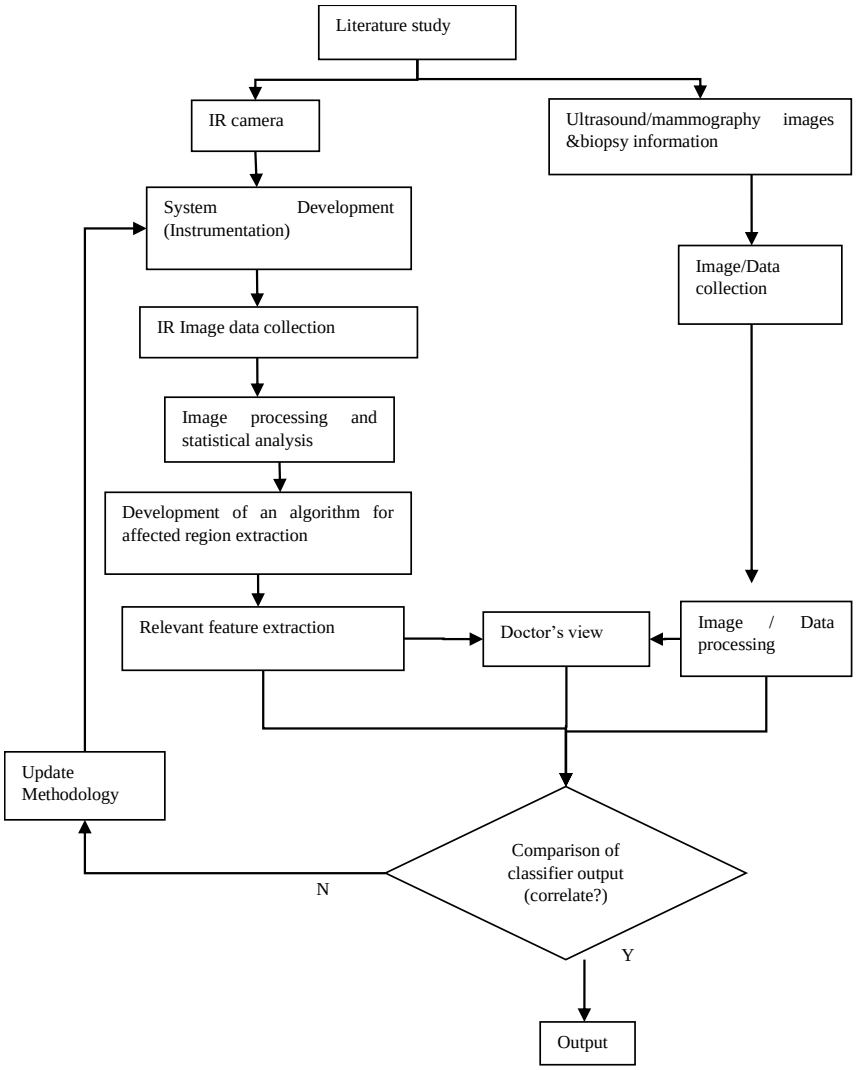

Fig. 2.1: Planning for Technology Development using Infrared Imaging

2.1.2 Thermal Image Acquisition Techniques

Infrared cameras and thermal imagers monitor skin temperature changes, allowing continuous observation of temperature modulation. The current research employs an 'Infrared Camera-based temperature profiles' approach, capturing data from facial areas, ears, buccal cavities, etc., during diabetic camps and on cancer patients for pilot studies. The FLIR SC325 IR camera captures infrared image data and analyses reports. Ear and interior buccal cavities

are selected as Region of Interest (ROIs) and provide unique features, indicating significant temperature profile differences for diabetic and non-diabetic subjects. An automated ear zone selection module is developed, enabling online system functionality for sample collection and data preparation. The image acquisition process is depicted in Fig. 2.2. below:

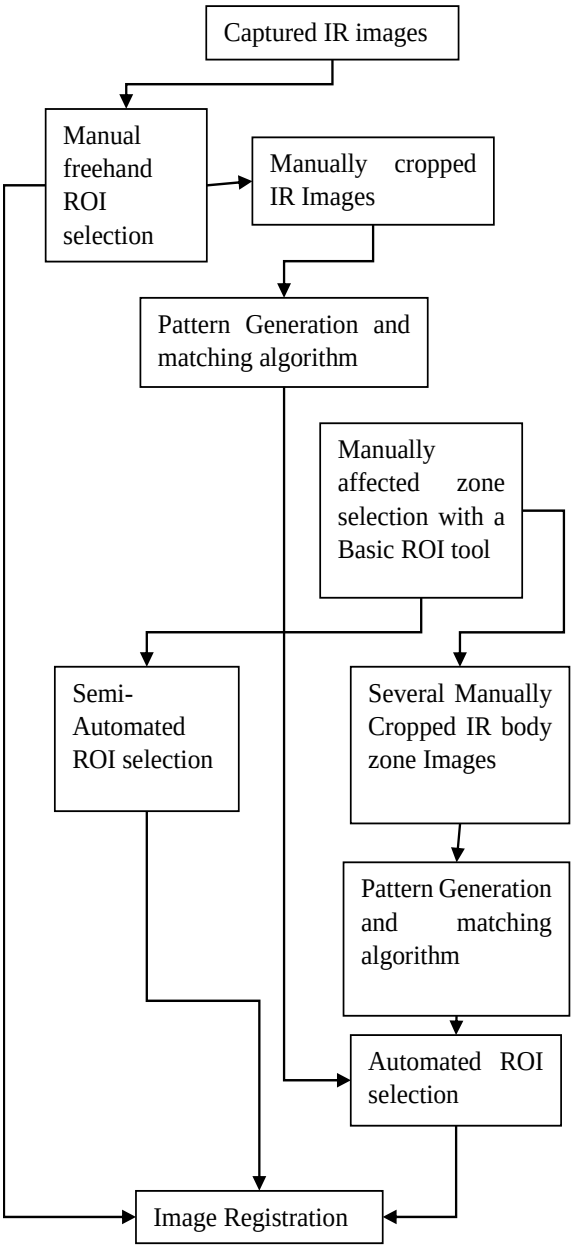

Fig. 2.2: Infrared Image acquisition

Imaging is conducted in hospital environments at different times of the year in various Indian regions with diverse climatic conditions. A data acquisition system integrated with an

LM-35 temperature sensor and an Arduino Uno microcontroller monitors ambient temperature fluctuations during image capture. This setup helps to mitigate the influence of environmental changes on body temperature.

2.1.3 Infrared Image Processing Techniques

The main challenge in this phase is the extraction of thermal Information for medical purposes by selecting the proper Region of Interest (ROI) from infrared images. ROI extraction can be accomplished manually, semi-automatically, or fully automatically. The detailed process is illustrated in Fig. 2-3.

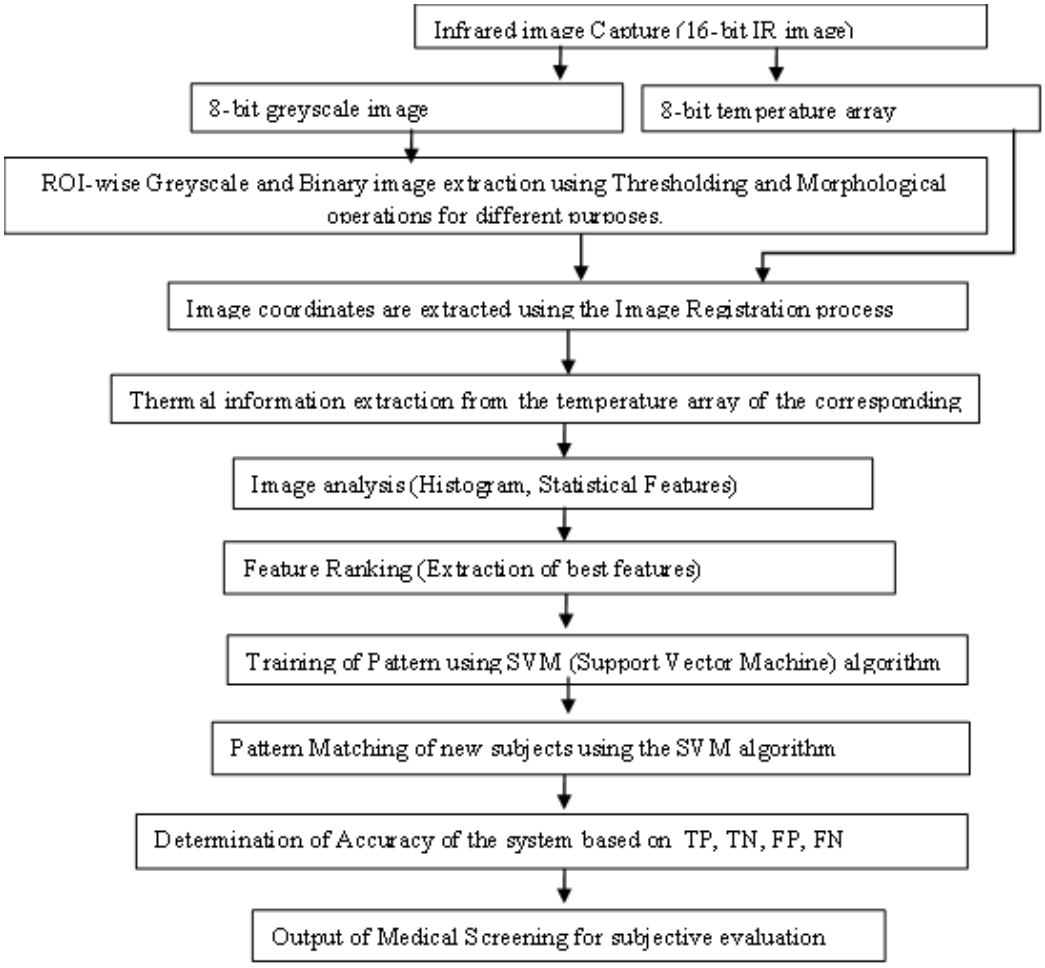

Fig. 2.3: Flow Diagram of Infrared image processing and Machine vision system

Thermal Information from the affected area is extracted using the selected ROI, either manually or automatically, through the image registration process. The overall system flow, depicted in Fig. 2.3, involves converting 16-bit raw IR images to 8-bit grayscale images and temperature arrays using the FLIR thermo-vision SDK (Software Development Kit). The SDK is customized in the Labview platform to meet specific requirements. Image processing algorithms and operations, such as thresholding and morphological operations [20], are utilized for image registration. The extracted temperature data is then fed into machine learning algorithms [14] for further analysis.

2.2 RoI detection using Dynamic Contour Evolution

2.2.1 Level-Set and Active Contour Models

Here, an automated LabView-based virtual instrument is developed that segments out Region of Interest (ROI) to get the temperature of different body parts. Firstly, the ear lobe is chosen from the side of the face to do this.

After the IR image acquisition of 85 subjects, we converted the 16-bit floating images to 8-bit grayscale images. Now, on the 8-bit image, we have taken ear templates to match each of the 85 subjects. In the program, two stages of dynamic thresholding have been done before using the Geometrical Pattern Matching algorithm [60].

IMAQ (Image Acquisition System) user Look up2 sub-VI (Virtual Instrumentation System) has been used for the dynamic thresholding in National Instrument’s LabView Software [60]. In its very first step, it increases contrast using a power of 1.50 for the image's background so that it will get a uniform background. Fig 2.4 A shows the original image, and Fig 2.4 B shows the uniform background image.

Fig.2.4: A-B-C uniform background

In the second step of the dynamic thresholding, using a power of 1/1.60 for the image's foreground increases the image's brightness, as shown in Fig 2.4 C, so that the edge of the image becomes more apparent.

After the above two steps of dynamic thresholding, LabView's NI Vision Assistant applied the Geometric pattern-matching algorithm. This algorithm works in two methods: Feature-based geometric pattern matching and edge-based geometric matching. Here, edge-based geometric pattern matching extracts the ear as an ROI to match the ear templates. As previously discussed, the algorithm has essential functions such as Row Step, Column Step, curve tracing, curve refining, edge point extraction, R-Table generation, and matching. The following table (Table 2.1) shows how these parameters have been set in the program for curve setting.

Table 2.1: Curve Setting Table

Number of Matches to find	1
Minimum Score	600
Contrast Reversal	Original
Search Strategy	Balanced
Rotation	0 to 360
Occluded	0 to 25
Extraction Mode	Normal
Edge Threshold	75
Edge filter size	Normal
Row Search Step Size	15
Column Search Step Size	15
Minimum Length	25

The algorithm generates a result on the settings of these parameters and gives a score based on which we can see how a template is matched on a subject from 6 templates. A score

of 800 is considered an excellent score to match a template. Out of six templates in the program, the best score template has been taken to be a perfect match for a particular IR image. To select the best score template, our program sorted the scores and chose the best one to match the IR image. Fig. 2.5 shows a template matching the image with its parameters.

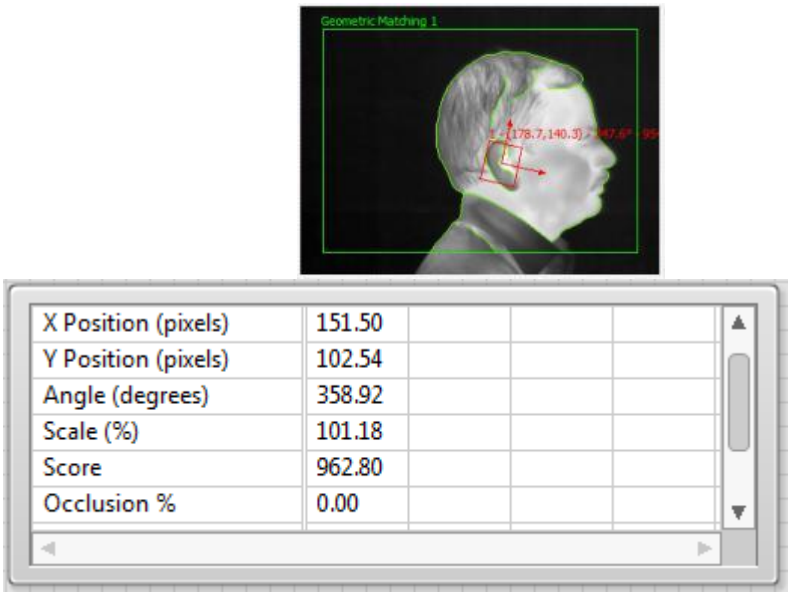

Fig. 2.5: Template matching image with it's parameters

In this process, the system gives results of almost 59%, which means that out of 85 subjects, only 50 ears match the 6 templates. The following Figures show some template images that match Fig. 2.6 and some that do not match any of the templates in Fig. 2.7.

Fig. 2.6: Some matched templates

Fig. 2.7: Some unmatched templates

In this stage of the program, some of the IR images did not find any match from the given templates. One reason is that the templates may be unable to locate the starting point for extracting the edge, or the image may have an edge that falls below the threshold. Therefore, templates get matched at the shoulder or neck instead of precisely at the ear lobe.

Now, the question of why these templates cannot find seed points arises. This is because templates find the matches through the entire image, and as a result, they get the seed point in another position rather than getting at the exact ear lobe. The solution to this problem is to match the templates on the side face of every subject instead of finding the matches through the entire image [61]. To do this, four side face templates are taken to match all 85 subjects. Fig 2.8 shows the four side face templates.

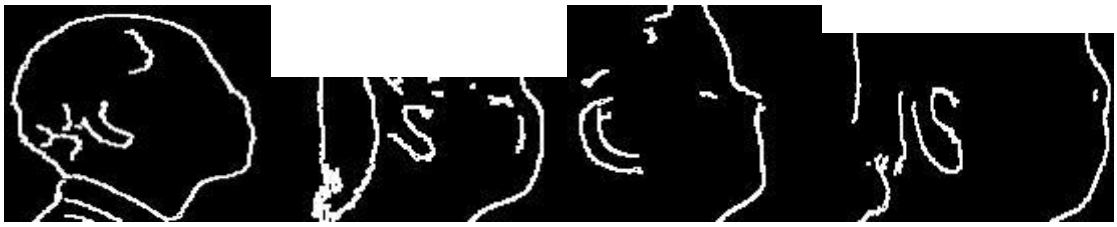

Fig. 2.8: Four side face templates

This template matching followed the previous process discussed for the Ear template matching. For side face matching, a geometric pattern matching algorithm was used. Before applying the Geometric Pattern Matching algorithm, two-stage dynamic thresholding was done to prepare the image. Two filters were used to get four templates from the 85 IR images. Fig. 2.9 shows how a side face template is segmented from the image.

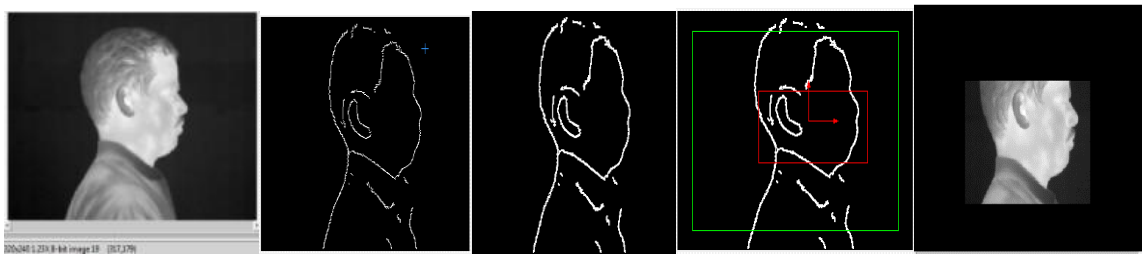

(a) (b) (c) (d) (e)

Fig. 2.9: Side face template after segmented from the image

In Fig. 2.9 (a), dynamic thresholding has been done on the original image. In Fig. 2.9 (b), a canny edge threshold filter (refer to point 2.2.5.) is used for its low error rate and high accuracy to get the boundary edge [29]. After getting the edge, a differentiation filter (refer to point 2.2.6.) was used to sharpen the edge correctly, as shown in Fig. 2.8(c). Finally, a geometric pattern matching algorithm was used to match a template on an image, as shown in Fig. 2.9(d). Fig. 2.9(e) shows a matched image of the original image.

2.2.2 Shape tracking through canny edge detection algorithm

The definition of *edges* is significant local changes in intensity within an image. Edges tend to occur at the boundary between two regions within an image. The goal of edge detection, then, is to produce a line drawing of a scene by tracing the boundaries/edges of the objects within an image. Edges can be caused by two different situations: geometric events, such as an object or surface boundary, or non-geometric events, such as reflections of light and shadows within the image.

The Canny edge detector performs these steps in the following stages [20], [60].

Smoothing/Enhancement: This is achieved by convolving a Gaussian mask with the image.

Detection: This is done simply by convolving a Sobel filter with the image.

Non-maximum suppression is an edge-thinning process that analyses the direction of the edge to determine precisely where an edge is and then clears the pixels adjacent to the edge.

Hysteresis/Thresholding is an edge-linking process that only keeps edges above a certain level. The algorithm is the same as a Schmidt trigger buffer.

The first step of the Canny Filter is to convolve a Gaussian mask over each pixel in the image. The mask is a 2D array calculated using the following Gaussian equation. The Gaussian function is a filter that removes unwanted noise from the image. The equation is given as follows.

$$F(x,y) = \frac{1}{2\pi\sigma^2} e^{\frac{-(x^2+y^2)}{2\sigma^2}} \tag{2.1}$$

After applying the Gaussian mask, it is time to detect the edges. There are several ways to do this. If we think of an edge as a rapid change in intensity in an image, then that means that it is a high-frequency signal within the image. We could take the Fourier transform of the image's 2D array and then apply a high filter to leave only the pixels within a specific frequency.

Using a high-pass filter would work but takes more computing power to accomplish, and in real-world scenarios where efficiency and speed are critical, that could be more desirable. To get around this edge, derivatives can be used. An edge can be found by detecting the first derivative's local maxima and minima or by the second-order derivative's zero-crossing. The derivative is found by approximation using finite differences.

$$\frac{\partial f}{\partial x} = \lim_{h\to 0} \frac{f(x+h,y)-f(x,y)}{h} \tag{2.2}$$

$$\frac{\partial f}{\partial y} = \lim_{h\to 0} \frac{f(x,y+h)-f(x,y)}{h} \tag{2.3}$$

For h= 1

$$\frac{\partial f}{\partial x} = \lim_{h\to 0} \frac{f(x+h,y)-f(x,y)}{h} = f(x+h, y) - f(x, y) \tag{2.4}$$

$$\frac{\partial f}{\partial x} = \lim_{h\to 0} \frac{f(x+h,y)-f(x,y)}{h} = f(x, y+h) - f(x, y) \tag{2.5}$$

df/dx and df/dy could then be calculated by convolving the following masks over the image.

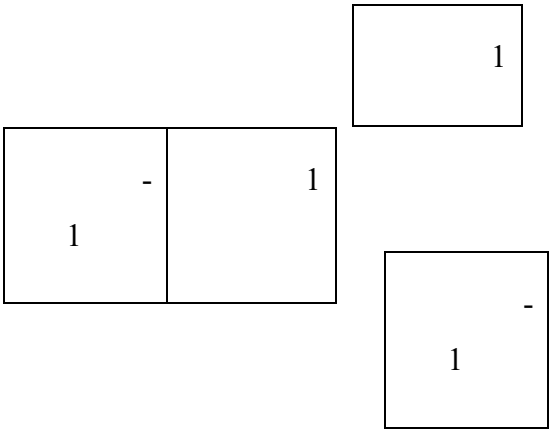

Consider the pixel arrangement around the pixel (x,y) below

P_0	P_1	P_2
P_7	[X, Y]	P_3
P_6	P_5	P_4

The partial derivatives:

$D_x = (a2 + Ca3 + a4) - (a0 + Ca7 + a6)$ (2.6)

$D_y = (a6 + Ca5 + a4) - (a0 + Ca1 + a2)$ (2.7)

The constant C implies an emphasis on pixels closer to the centre of the mask. The Sobel mask is obtained by setting C = 2. Give the two masks below.

$$D_x = \begin{matrix} -1 & 0 & 1 \\ -2 & 0 & 2 \\ -1 & 0 & 1 \end{matrix}$$

$$D_y = \begin{matrix} -1 & -2 & -1 \\ 0 & 0 & 0 \\ 1 & 2 & 1 \end{matrix}$$

These two masks are convolved with the original image to create two new images, one with the x-value of the gradient of each pixel and one with the y-value of the gradient of each pixel. The magnitude of the gradient is then found by using this equation.

$$magn(x,y) = \sqrt{D_{y^2} + D_{x^2}} \tag{2.8}$$

The direction of the edge is found by taking the inverse tangent of each pixel.

$$\mathrm{dir(x,y)} = \tan^{-1}\left(\frac{D_y}{D_x}\right) \tag{2.9}$$

Using the edge direction, non-maximum suppression can be applied. Since this is an array, there are only four directions that the edge can run in from the point [x,y]. Once the direction is known, the pixels perpendicular to the edge are set to zero. This leaves a thin line representing the edge.

2.2.3 Differentiation Filter

The differentiation filter creates smooth outlines by accentuating every pixel with a change in intensity compared to its three neighbouring pixels at the upper-left corner.

The updated pixel value is determined by taking the maximum absolute difference between the deviation of its upper-left neighbour and its two remaining neighbours.

$$P_{(i,j)} = \max\left[\left|P_{(i-1,j)} - P_{(i,j)}\right|, \left|P_{(i-1,j-1)} - P_{(i,j)}\right|, \left|P_{(i,j-1)} - P_{(i-1,j)}\right|\right] \tag{2.10}$$

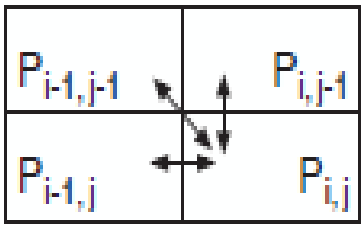

Application of edge-based active contour models with Distance Regularized Level Set (DRLSE) formulation.

2.2.4 Edge-based active contour model in the distance regularized level set formulation

Let I be an image on a domain Ω; we define an edge indicator

Function g by

$$g \triangleq \frac{1}{1+\nabla G_\sigma * |I|} \tag{2.11}$$

The convolution in (2.11) smooths the image and reduces noise. This function usually takes smaller values at object boundaries than at other locations.

For an LSF $\phi: \rightarrow \mathcal{R}$, we have an energy function $\varepsilon(\phi)$ by

$$\varepsilon(\phi) = \mu\, \mathcal{R}(\phi) + \lambda\, \mathcal{L}_g(\phi) + \alpha\, \mathcal{A}_g(\phi) \tag{2.12}$$

Where> 0 and $\alpha \epsilon \mathscr{R}$ are the coefficients of energy functions$\mathscr{L}_g(\phi)$ and $\mathcal{A}_g(\phi)$.

This energy function can be minimized by solving the following gradient flow:

$$\varepsilon(\phi) = \mu\, \mathrm{div}\,(d_p(\nabla\phi|)\nabla\phi) + \lambda\delta_\varepsilon(\phi)\mathrm{div}\left(g\,\frac{\nabla\phi}{\nabla\phi|}\right) + \alpha g\delta_\varepsilon(\phi) \tag{2.13}$$

Given an initial LSF $\phi(\mathrm{X}, 0) = \phi_0(X)$. The first term on the right-hand side of equation (2.13) is associated with the distance regularization energy$R_p(\phi)$.In contrast, the second and

third terms are associated with the energy terms $\mathscr{L}_g(\phi)$ and $\mathcal{A}_g(\phi)$, respectively. Equation (2.13) is an edge-based geometric active contour model applying the general DRLSE formulation. This section uses this active contour model as a DRLS model for simplicity.

This section shows the results of the DRLSE model of equation (2.13) for natural images. In this model, there are parametersλ,μ, and the time step Δfor the implementation. The model is not sensitive to the choice ofλandμ, which can be fixed for most applications. Unless otherwise specified, these parameters are fixed as$= 5$, $\mu = 0.09$, $\alpha = 3.5$, $\varepsilon = 1.5$ and σ = 1.5 for our application. The parameter needs to be adjusted for different images, as it plays a crucial role in driving the motion of the contour. Introducing a nonzero value provides an additional external force to guide the contour. However, it is essential to note that in specific scenarios, the final contour might not precisely align with the object boundary due to the impact of the weighted area term, which can either shrink or expand the contour. To mitigate this deviation, it is advisable to refine the contour further by allowing it to evolve for several iterations using the parameter. For images with weak object boundaries, using a significant value for the parameter may lead to boundary leakage, wherein the active contour easily breaches the object boundary.

After setting these parameters for our application to get the highest temperature area, we initialize the LSF by drawing a rectangle on the image to indicate the desired area. This rectangle is a binary step function

$$\phi_0(X) = -c_0 \text{if } X \varepsilon \mathcal{R}_0 \quad (2.14)$$

$$= c_0 \text{ otherwise.}$$

It means that when we take the positive value of its final LSF, it will move outside the rectangle, and when this value is negative, it will move inside the rectangle to find the lowest pixel value. Figs. 2.10 and 2.11 show some initial LSF and corresponding LSF.

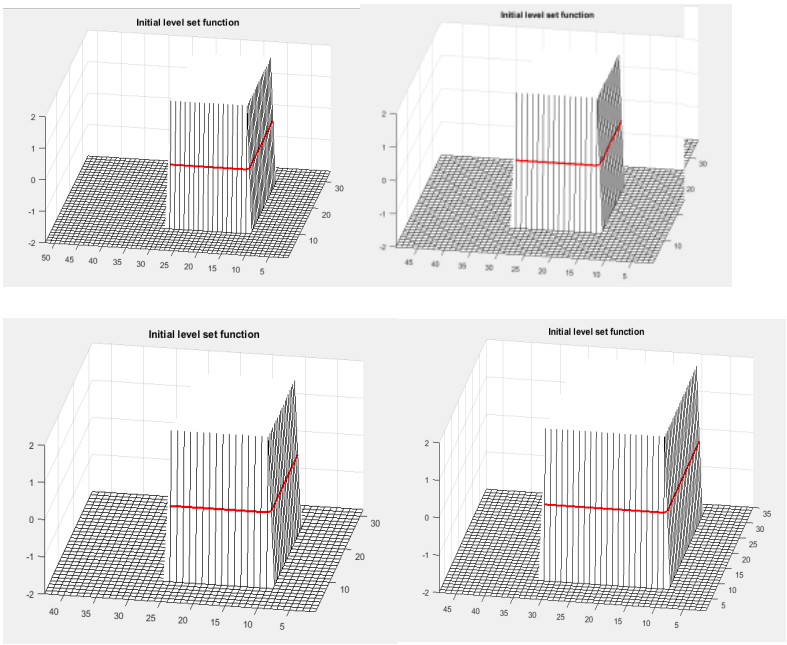

Fig.2.10 : Some initial LSF

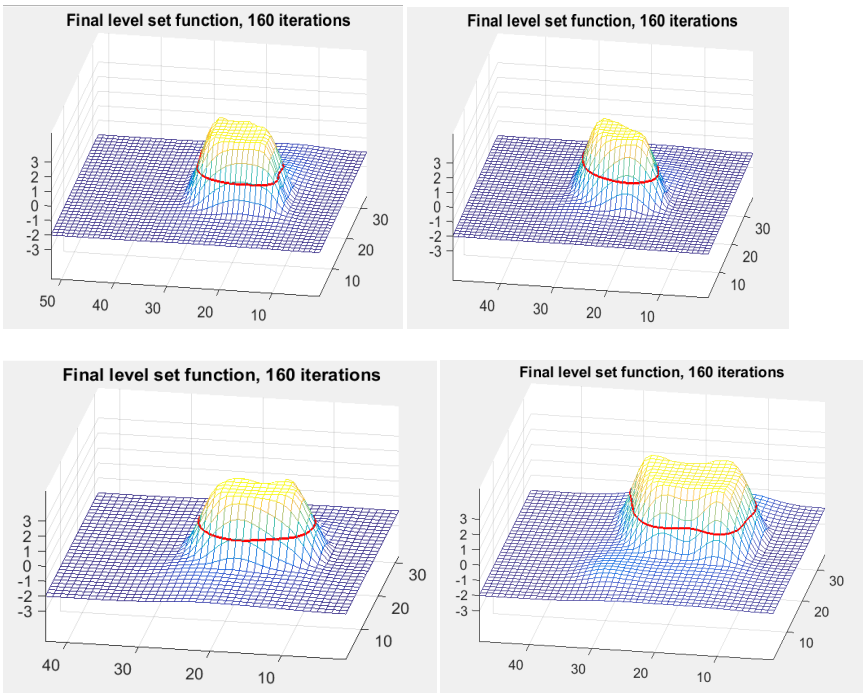

Fig.2.11: corresponding LSF

Fig.2 .11 shows how to draw the rectangle to get our desired ROI or the initial zero-level contour, and Fig.2.12 shows our desired ROI and final level set contour.

Fig. 2.12: Transition of the rectangle to get the desired contour of ROI

Fig.2.13 shows the edge detected image and the masked image.

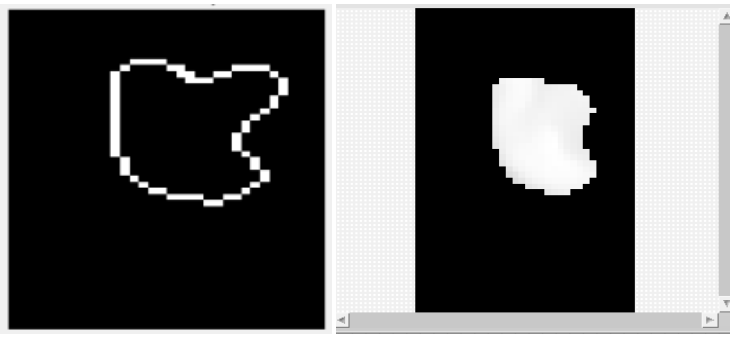

Fig.2.13 (a) Fig.2.13 (b)

Fig. 2.13: Edge detection and masking of image

From image Fig. 2.13, we extracted all the statistical features of the temperature profile for further analysis. The extracted features are mean, maximum, minimum, standard deviation, second-order central moments or variance, third-order central moments or kurtosis and fourth-order central moments or skewness.

2.2.5 Implementing DRLSE: Parameters and Real Image Results

After extracting the ear, we use a unique image segmentation method called Distance Regularized Level Set Evolution (DRLSE) [62], which has been used to get the highest temperature area within the ear. The DRLSE method is an improved version of the

classical Level Set Method. A detailed explanation of the DRLSE method was discussed earlier. Fig.2.14 and Fig.2.15 shows the method of getting the highest temperature area.

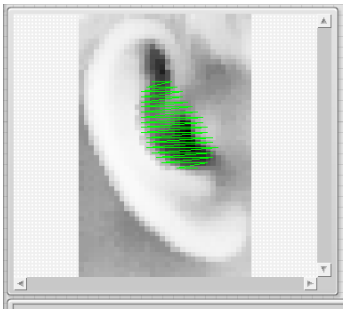

Fig. 2.14: Highest temperature image

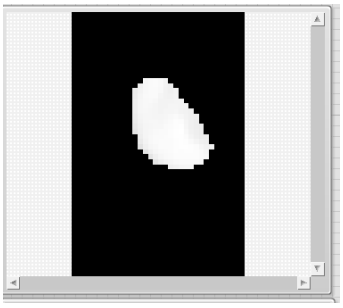

Fig. 2.15: Highest temperature area

This DRLSE image segmentation method has been implemented using the LabView MATLAB Script. This LabView MATLAB script can run on the MATLAB program, and MATLAB functions directly on the LabView platform. An explanation of extracting the highest temperature zone within the area is given below. After extracting the ear using Labview, as shown in Fig. 2.12, it is inverted in Fig.2.13. This image is inverted because it makes the DRLSE method to get the desired segmented region. Next, the lowest pixel value is extracted, as shown in Fig.2.13 (b), as the image is inverted, and this image is taken as input by the MATLAB Script to apply the DRLSE Method.

The level-set method, initially introduced independently by Caselles et al. [63] and Malladi et al. [64], brought significant advancements to the field of image segmentation, particularly within the domain of active contour models, also known as snakes. These models, first proposed by Kass et al. [29] and later refined by Malladi et al. [3], depict dynamic parametric contours with spatial parameters typically constrained within the interval [0,1]. These spatial parameters parameterize the points along the contour, while a temporal variable

signifies the contour's evolution over time. Mathematically, the curve evolution in these models is expressed as

$$\frac{\partial C(s,t)}{\partial t} = FN \tag{2.15}$$

In equation (2.15), F is the function that controls how fast the curve moves, and N is the normal average vector pointing inside the curve C. By using a time-dependent level set function (LSF) f(x, y, t), we can represent the dynamic contour C(s, t) as the zero level set. This transforms the curve evolution into a level formulation. If the LSF takes negative values inside the contour and positive values outside, we can express the inward average vector using the gradient operator. By doing this, we can transform equation (2.15) for curve evolution into a partial differential equation (PDE).

$$\frac{\partial \phi}{\partial t} = F|\nabla \phi| \tag{2.16}$$

This equation is called a level-set evolution equation. Level set methods have a valuable advantage in that they can accurately portray contours with complex topology and handle topological changes like splitting and merging naturally and efficiently [64], [65], [66]. Another benefit of level set methods is that numerical computations can be done on a fixed Cartesian grid without parameterizing points on a contour line in parametric active contour models. However, in traditional level set methods, the LSF can develop irregularities during its evolution, which can generate numerical errors and ultimately disrupt the stability of the evolution. To address this issue, a numerical remedy known as re-initialization [67],[68] was introduced to restore the regularity of the LSF and maintain stable level set evolution. Re-initialization is performed by periodically stopping the evolution and reshaping the degraded LSF as a signed distance function [69], [67].

2.2.6 Presentation of actual image results and their implications

In this program, we applied ear templates only on the side faces of every image. Six ear templates are taken to match every IR image. This process was done in parallel with the previous program. Two stages of dynamic thresholding have been done to match every ear template, after which the Geometric Pattern Matching algorithm is used to match every

template. This method gives a better result, about 89%. Out of 85 subjects, 75 images matched with the six ear templates. Fig. 2.16 A and 2.16 B show template-matched and unmatched images. Finally, Fig 2.17 shows the optimized samples of six ear templates used in this process.

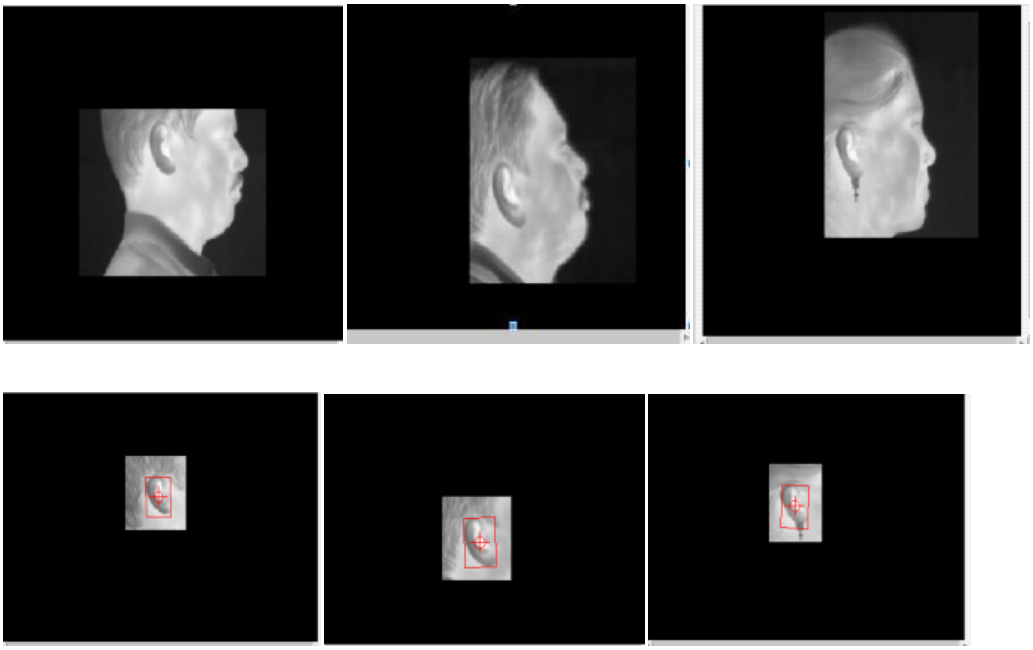

Fig. 2.16 A: Three head templates and their corresponding matched ear templates

Fig. 2.16 B: Two head templates and their corresponding unmatched ear templates

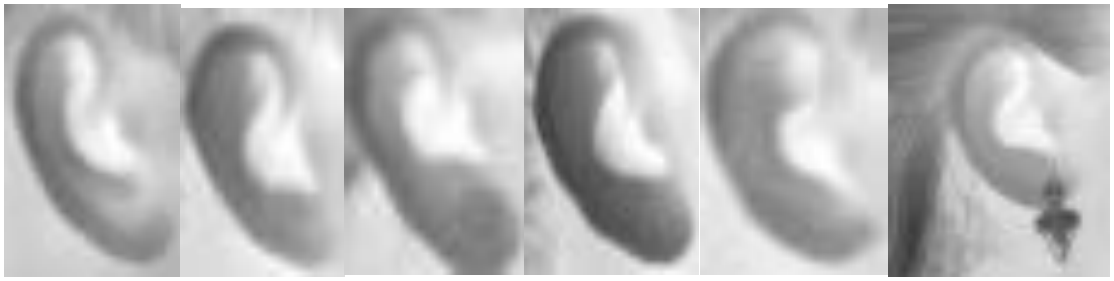

Fig. 2.17: Six ear templates.

2.2.7 Improvement in accuracy of ROI extraction

In this work, we got approximately 95% accurate results. Firstly, we did two steps of dynamic thresholding for pre-processing the image. Then, we used a local averaging filter with a kernel size 13 to smooth the image and a canny filter with a variance of 2 to detect edges. This two-stage processing gives the following result, shown in Figs. 2.18 and 2.19.

Fig. 2.18: Stage-1of Two-stage IR Image Processing

Fig. 2.19: Stage -2 of Two-stage IR Image Processing

Fig.2.19 shows that in stage 2, we get very sharp edges, which helps us find a perfectly matched head template from the side face image. The templates are given in the following Fig.

Fig. 2.20: Position of the ear in the head template

From Fig.2.20, it is clear that the position of the ear in the head template is almost in the centre, which results in the perfect matching of ear templates. This method also has some systematic errors, which could not be removed during the image processing. A standard protocol must be followed during the image acquisition to get the best of it, which will nullify most errors.

Fig.2.20 shows how an ear template matches with the side face. To get the ear's highest temperature region, we extracted the ear from the side face using the Global Rectangle, as shown in Fig.2.20

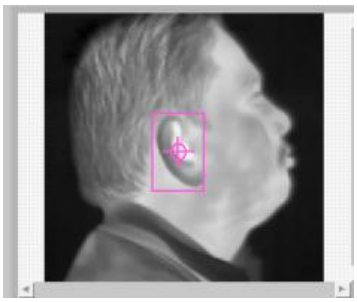

Fig. 2.21: Extracted ear part using Global Rectangle

2.3 Feature Extraction, Statistical Analysis, and Neural Network Modelling

2.3.1 Statistical analysis of extracted features for diabetes diagnosis

The statistical analysis primarily aimed to find the differentiating factors between the samples collected. Another aspect was checking the repeatability of the feature data of the subjects across different days. Several data collection programs were conducted in-house on about 15 subjects on different aspects to accomplish this purpose. The statistical analysis was done primarily by SPSS and Unscrambler software; later, the modified analysis was done using Matlab and Labview statistical tools. Fig 2.22 represents the SPSS analysis output on 12 subjects for IR image analysis to determine the significance of different zones to differentiate between diabetic and non-diabetic subjects.

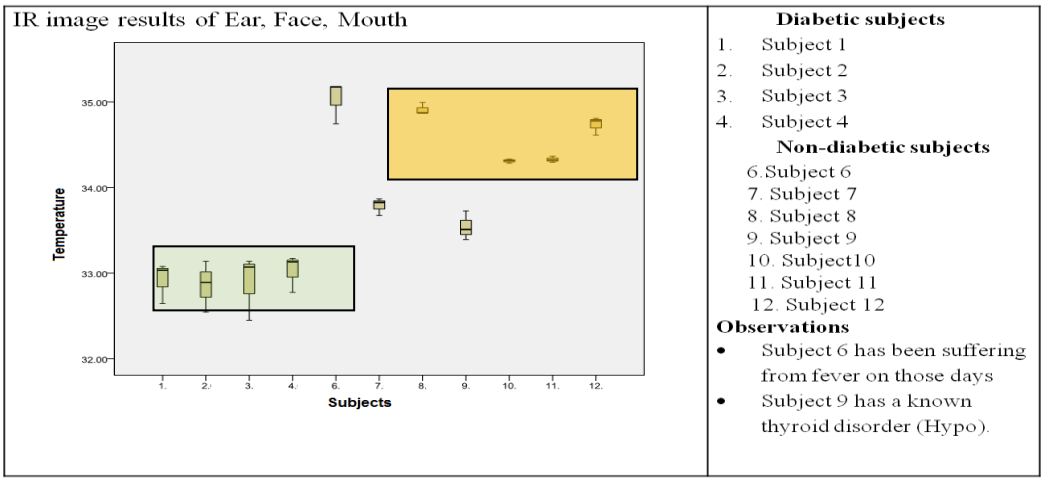

Fig. 2.22: Significance of different zones to differentiate between diabetic and non-diabetic subjects

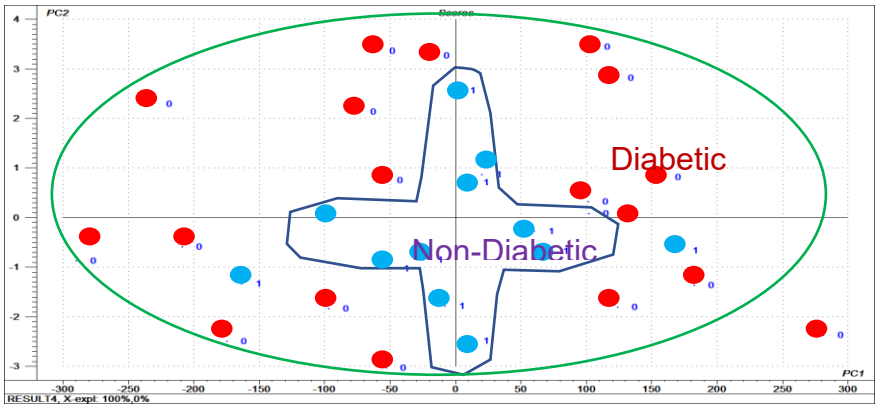

Fig. 2.23: A Model for the diabetic non-diabetic pattern classification in PCA

Infrared image output among diabetic and non-diabetic subjects reveals that diabetic subjects have lower temperature profiles than non-diabetic subjects. A Model for the diabetic non-diabetic pattern from PCA using "Unscrambler" software has been developed for classification between the subjects. The model is shown in Fig 2.23. Later, another investigation was done on IR image vs glucose levels for diabetic and non-diabetic subjects. The analysis output has been shown in Fig 2.24 using the Labview statistical analysis tool. The figure below shows a significant correlation between the populations.

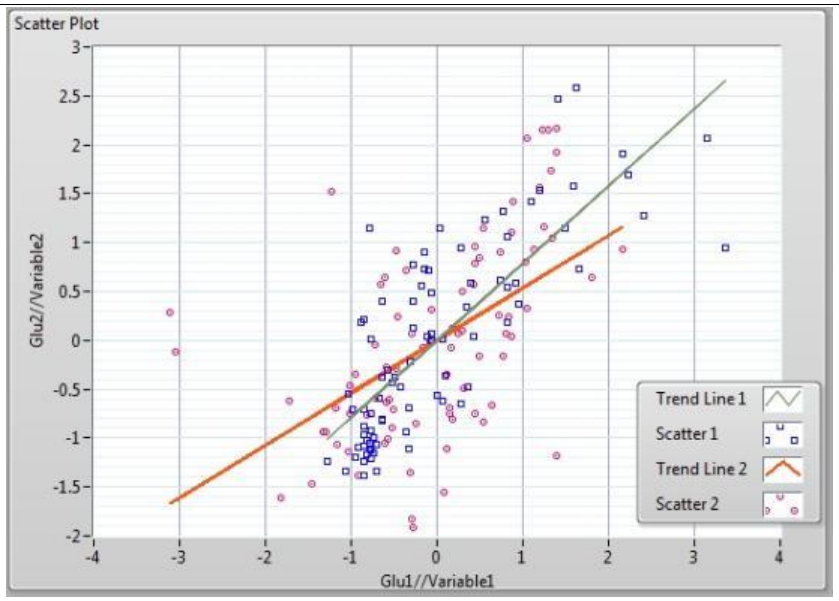

Trendline1: 38.239489

Trend Line2: 28.209728

Angle Difference: 10.029761

Correlation: 0.984717

Description: Blue dots are the diabetic person's data from the clinical report, and red dots are the IR output from mouth images collected from each subject

Fig. 2.24: Correlation between clinical report and IR data of diabetic person

From the above analysis, the primary outcome was identifying some significant features to extract from the IR images. Those features are ranked to get better classification between Diabetic and Non-diabetic subjects. The recent work on statistical analysis was performed based on the above criteria. Feature ranking from the most significant body zone, the ear zone, shows the significant classification results using different machine learning algorithms. The algorithms are developed using Matlab statistical and Machine learning tools. The outputs are discussed below.

2.3.2 Feature Extraction

The feature is a measurable property that quantifies a pattern. Multiple features construct a feature vector where the feature collectively quantifies a particular pattern. The feature vector is a group of features. In the present work, features are numerical. Fifteen statistical features

have been extracted from the ear zone thermal distribution. The features extracted from the ear zone are tabulated in Table 2.2.

Table 2.2: Extracted Features

Mean	Skewness	Entropy (Norm)
Standard Deviation	Kurtosis	Shannon Entropy
Mode	Second order Moment	Energy
Median	Third Order Moment	
Root Mean Square		
Maximum Value		
Normalized mean		

2.3.3 Feature Ranking

The extracted features have been ranked. The information Gain parameter [70] has been applied for feature ranking. Table 2.3 shows the ranked features for the female group. Table 2.4 shows the ranked features for the male group based on the information gain measure. For the female group, mean, median, root mean square (r.m.s), standard deviation (std. dev.) and skewness are the first five best-ranked features.

Algorithm:

- Find the total Information of the sample data set.
- For a particular attribute in the data set, split the original data set into child datasets.
- Find the summation of the total Information of child data sets.
- Find the difference between the total Information of the original data set and the total Information of child sets for that particular attribute.
- Repeat steps 2 to 4 for each attribute.

- Sort the attributes in descending order based on the information gain values.
- The first element in the sorted array of attributes is the best feature. Rank the feature as the best feature.
- The rest of the elements are ranked based on their corresponding information gain values.Fig. 2.25 shows the Flow chart of the Feature ranking algorithm.

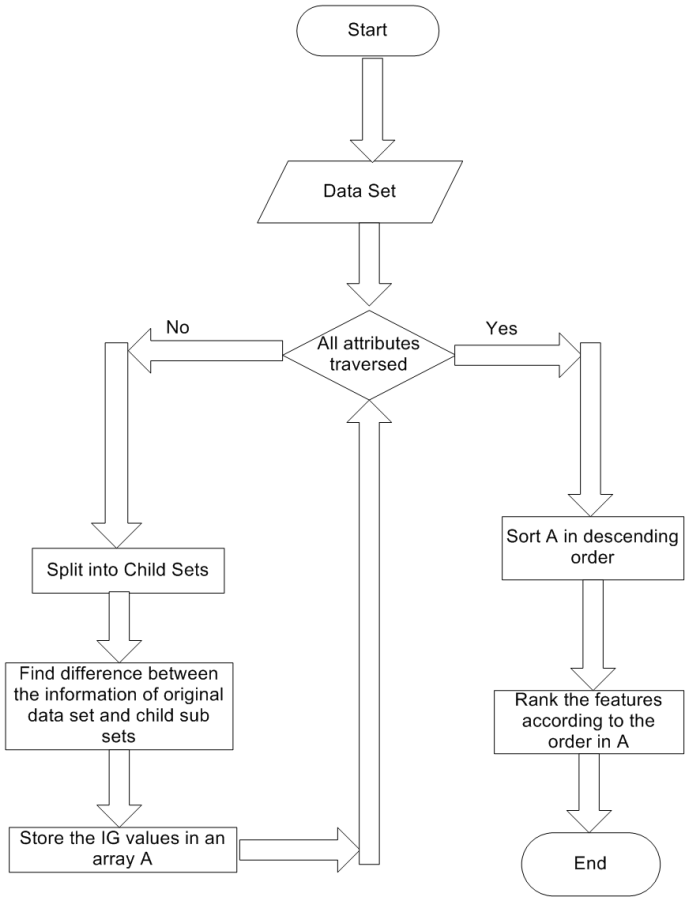

Fig. 2.25: Flow chart of the Feature ranking algorithm

2.3.4 Machine learning

Five classifiers are implemented on the extracted features of IR images. They are Support Vector Machine (SVM), Back Propagation Neural Network (BPNN), Radial Basis Function Neural Network (RBF-NN), Probabilistic Neural Network (PNN) and Bayes Classifier. The classifier performances have been evaluated based on three parameters: Accuracy (Acc.),

Sensitivity (Sen.) and Specificity (Spc.). Five-fold cross-validations have been performed. The models are applied to categorize two groups: diabetic and non-diabetic.

2.3.5 Significant Features

Table 2.3: Significant features (Female)

Feature Name	Information Gain
Std. dev.	0.163741
Mean	0.265637
r.m.s.	0.217437
Skewness	0.161612
Median	0.217437

Table 2.4: Significant features (Male)

Feature Name	Information Gain
Std. dev.	0.423924
Mean	0.330333
R. M. S	0.330333
Skewness	0.329682
Median	0.284809

Table 2.4 shows the first five best-ranked features for the male group. The best features are std. dev, mean, r.m.s, Skewness and median. The two tables show that males and females have common best-ranked features.

2.3.6 Classifier performance

Table 2.5: Comparison of Classifier Performances

Sl. No.	Classifier name	Performance Parameters	Combined Male –Female (%)	Male (%)	Female (%)
1.	SVM	Avg. Acc	67.8788	78.2143	71.1111
		Avg. Sen.	68.4524	81.6667	73.5714
		Avg. Spc.	65.5952	68.3333	62.0000
2.	BPNN	Avg Acc	51.8182	63.5714	65.5556
		Avg Sen.	100	100	90
		Avg Spc.	0	0	20
3.	RBF NN	Avg Acc.	64.7059	75.7143	71.5556
		Avg. Sen.	81.2088	80.3333	75.1429
		Avg. Spc.	42.8182	65	62
4.	PNN	Avg. Acc.	69.4118	83.5714	73.7778
		Avg. Sen.	89.7862	88.6667	88.5000
		Avg. Spc.	26.1905	85.3333	52
5.	Bayes	Avg. Acc.	70.5882	86.7857	75.7778
		Avg. Sen.	91.1888	89.3333	88.4524
		Avg. Spc.	28.3333	80	46.6667

Table 2.5 shows that the overall performances of all the classifiers are better in the case of male groups. Bayes classifier has provided the highest average accuracy among all the classifiers.

2.4 Development and results of Neural Network predictive models

2.4.1 Experimental Results and Discussion

This section shows the experimental results obtained from the extracted features. Seven features of the temperature profile of all 85 **diabetic (type 2)** and **non-diabetic** subjects are extracted. To reduce dimensionality, Principal Component Analysis in Unscrambler is used, from which four features are the mean, minimum, maximum and standard deviation of the temperature taken. Also calculated the mean temperature of all Diabetic subjects as well as non-diabetic subjects, and it was found that the **temperature of Diabetic (type 2) subjects is lower than that of non-diabetic subjects** as changes in blood flow such as ischemia, inflammation-induced vasodilatation, and neovascularization are reflected as a change in the overlying skin temperature [71]

These data have been used to feed Neural Networks to get a predictive model. To do this, the NPR tool in MATLAB 2017a is used, which gives results with **81.2%** overall accuracy.

Fig.2.26 shows the confusion matrix, which gives the performance analysis of the classification model, and Fig.2.27 shows the Receiver Operating Characteristic Curve (ROC curve).

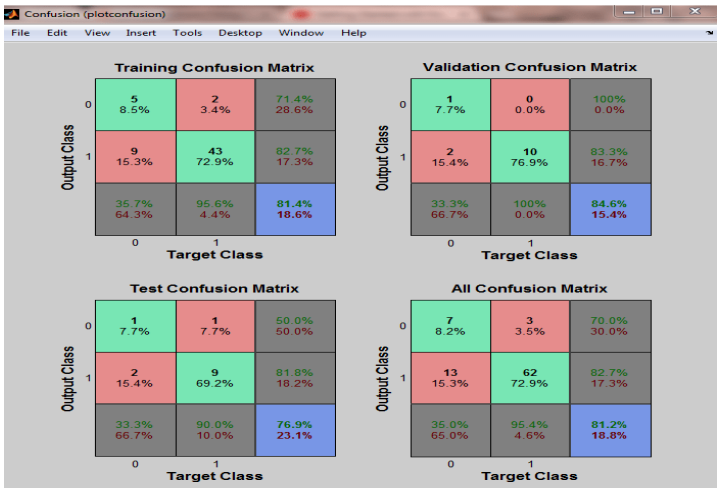

Fig. 2.26: Confusion matrix for performance analysis

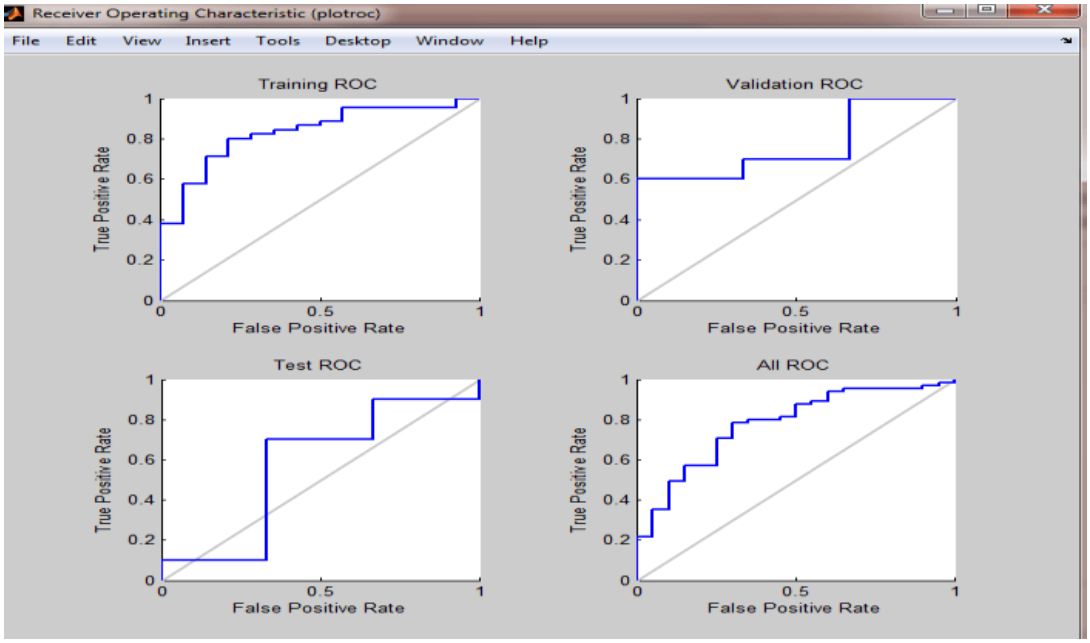

Fig. 2.27: Receiver Operating Characteristic Curve (ROC curve) of predictive model

The confusion matrix is formed from the four outcomes produced due to binary classification (or prediction): true positive, false positive, true negative and false negative.

True positive (TP): correct optimistic prediction

False positive (FP): incorrect optimistic prediction

True negative (TN): correct pessimistic prediction

False negative (FN): incorrect pessimistic prediction

Confusion matrix:

		Predicted Class	
		Negative	Positive
Actual Class	Negative	TN	FP
	Positive	FN	TP

The confusion matrix calculates the error rate, accuracy, sensitivity, specificity, precision, and false positive rate.

$$\text{Accuracy} = \frac{TP+TN}{TP+FP+TN+FN} = \frac{7+62}{62+13+7+3} = 81.2\% \quad (2.17)$$

$$\text{Error Rate} = \frac{FP+FN}{TP+TN+FN+FP} = 18.82\ \% \quad (2.18)$$

$$\text{Sensitivity} = \frac{TP}{TP+FN} = \frac{62}{62+13} = 82.66\ \% \quad (2.19)$$

$$\text{Specificity} = \frac{TN}{TN+FP} = \frac{7}{7+3} = 0.7 \quad (2.20)$$

$$\text{False Positive Rate} = \frac{TN}{TN+FP} = 1\text{- Specificity} = 0.3 = 30\ \% \quad (2.21)$$

The above results plotted the ROC curve as shown in Fig.2.27. The ROC plot uses a False Positive Rate (FPR) on the X-axis and a True Positive Rate (TPR) on the Y-axis. This plot gives a meaningful performance result of the classification model. Results were analyzed, and performance comparison was done using various classification algorithms. Table 2.6 explains the overall accuracy of the results for different classifiers.

Table 2.6: Overall accuracy of the results for different algorithms

SL. No	Classification Algorithm	Overall Accuracy (%)
1.	Complex Tree	69.4
2.	Medium Tree	69.4
3.	Simple Tree	70.6
4.	Linear SVM	77.6
5.	Quadratic SVM	71.8
6.	Cubic SVM	67.1
7.	Fine Gaussian SVM	76.5
8.	Medium Gaussian SVM	77.6
9.	Coarse Gaussian SVM	77.6
10.	Fine KNN	62.4
11.	Medium KNN	77.6
12.	Coarse KNN	77.6
13.	Cosine KNN	74.1
14.	Cubic KNN	77.6
15.	Weighted KNN	72.9
16.	Ensemble Boosted Trees	74.1
17.	Ensemble Bagged Trees	74.1
18.	Ensemble Subspace Discriminant	77.6
19.	Ensemble RUS Boosted Trees	57.6
20.	Ensemble Subspace KNN	64.7

The study was done on 243 human subjects in three diabetic camps at different places and climatic conditions in India. A collaborative Infrared data collection camp with SRM Medical College Hospital and Research Centre, Chennai, has led to new openings of the research and two more data collection programs were arranged in collaboration with Cachar Cancer Hospital following the same data collection planning validate the outcome of new findings with the enhanced version of the software to accommodate the variations in image data of the population in different climatic conditions. A statistical image analysis algorithm has been included in the "infrared image analysis module" from the beginning where Mean, Standard Deviation, Median, Mode, Skewness, Kurtosis, First, Second, Third order Moment, Root Mean Square (RMS), Norm & Shanon Entropy, Energy and Maximum temperature value of the extracted Region of Interest are automatically recorded with every snap. These statistical values are treated as discriminating features for classification in machine learning algorithms. Instead of using all the features in the machine learning algorithm, the best three significant features are ranked using information gain theory and trained for the machine learning system. The best three features for male subjects (f1= Std Deviation, f2= Mean and f3= RMS) and female subjects (f1= Mean, f2= Median and f3= RMS) are different. So, the machine learning algorithm is developed differently for males and females. The overall accuracy (F-70.62%, PP-67.08%), positive predictivity (F-65.38%, PP-61.40%), negative predictivity (F-73.14%, PP-70.29%), sensitivity(F-53.97%, PP-53.85%), specificity (81.44%, 76.34%) of the system is obtained from all male subjects (n1=36:Fasting High=23, Control=13 & PP High=23,

Control=13, n2=44:Fasting High=16, Control=28 & PP High=16, Control = 28, n3=48:Fasting High=22, Control=26 & PP High=24, Control = 24) and female subjects (n1=47:Fasting High=33, Control=14 & PP High=33, Control=14, n2=26:Fasting High=10, Control=16 & PP High=8, Control = 18, n3=41:Fasting High=16, Control=25 & PP High=16, Control = 25) separately by population-based cross-sectional and case-control study in Table 2.7 and 2.8.

Table 2.7: The population-based cross-sectional and case-control study outputs for Fasting

	Population-based cross-sectional and case-control study on Fasting		
	Female	Male	Male+ Female
Sensitivity (%)	61.538	48.649	53.968
Specificity (%)	82.927	80.357	81.443
Positive predictive value (PPV)%	69.565	62.069	65.385
Negative predictive value (NPV)%	77.273	70.313	73.148
Accuracy (%)	74.627	67.742	70.625
FNR	38.462	51.351	46.032
FPR	17.073	19.643	18.557
LR+	3.604	2.477	2.908
LR-	0.464	0.639	0.565
Diagnostic Odd Ratio (DOR)	7.771	3.876	5.146

Table 2.8: Population-based cross-sectional and case-control study outputs for PP

Population-based cross-sectional and case-control study for PP	**Population-based cross-sectional and case-control study on PP**		
	Female	Male	Male + Female
Sensitivity (%)	45.833	58.537	53.846
Specificity (%)	83.721	70.000	76.344
Positive predictive value (PPV)%	61.111	61.538	61.404
Negative predictive value (NPV)%	73.469	67.308	70.297
Accuracy (%)	70.149	64.835	67.089
FNR	54.167	41.463	46.154
FPR	16.279	30.000	23.656
LR+	2.815	1.951	2.276
LR-	0.647	0.592	0.605
Diagnostic Odd Ratio (DOR)	4.352	3.294	3.765

2.5 Development of Pattern recognition tools for IR Imaging based Health Monitoring Software

This thesis presents the development of crucial software modules and tools to monitor and measure human health. These software modules involve the integration of image processing and pattern recognition algorithms. The initial iterations of these modules have undergone refinement based on feedback obtained from the statistical analysis of data collected during hospital-based data collection activities [12].

Utilizing feature ranking methodologies, selected the most compelling features were selected from various feature sets. Furthermore, comparisons between different classification techniques were also conducted. This thesis enhances pattern recognition tools tailored for body emission imaging software [13].

Body emission measurement combines hardware and software components, including an infrared camera (IR), with control and interpretation functions. Data collected from real-world settings, such as Diabetic Camps, are subjected to statistical analysis, validation, and machine learning for pattern recognition [11]. The development of the entire interface, control system, image analysis, and statistical measures has been achieved through Labview, with additional use of Matlab tools for machine learning and pattern recognition training [72].

2.6 Conclusion

The closing remarks of this chapter emphasize the transformative impact of infrared Imaging within the medical realm, with a particular emphasis on its potential to develop diagnosis techniques and early identification of diabetes. Its non-invasive nature and real-time temperature measurement capability have contributed to the rising popularity of this technology, which has now transcended initial cost constraints to become more widely accessible.

The section also stresses establishing well-structured and standardized data collection and analysis protocols. Such protocols are critical to strengthen the credibility and dependability of infrared thermography as a robust diagnostic tool for diabetes. The discussion

encourages the refinement of experimental protocols and the streamlining of rapid data analysis processes, highlighting the need to implement this technology efficiently in clinical practices.

The importance of correlating infrared thermography results with clinical findings is also acknowledged, highlighting the significance of integrating this innovative technology with traditional medical approaches. The section further highlights the role of affordable infrared cameras in propelling the widespread adoption of this technology, positioning it as an essential asset for various medical applications.

With the above advancements and the growing significance of infrared Imaging, the conclusion of the chapter lays the groundwork for the subsequent exploration of its application in stress and diabetic level monitoring, which is depicted in the next chapter. This seamless link between the potential of technology and its practical implementation in the healthcare sector sets the stage for a deeper understanding of how infrared Imaging can contribute to developing intelligent diagnostic systems and boosting progress in healthcare.

Chapter III

Infrared Imaging of Stress and Diabetic Level Monitoring for Intelligent Diagnosis System

3.1 Introduction

While human society gradually advances society with Systems deployed in all spheres, new technologies and techniques are being used to extend the reach and reliability of healthcare services. New-generation diagnostic tools are enhancing the quality of medical services. Several easy-to-use, efficient tools and systems are emerging. The previous chapter depicted an Innovative approach to using Infrared Imaging in the medical sector.

In order to improve diagnosis through infrared (IR) imaging, computer software for quantitative analysis of IR images has been studied by some investigators for years. This chapter presents an IR image processing system for monitoring the stress level using Infrared (IR) imaging with pattern recognition techniques. The intelligent healthcare system comprises three distinct entities: a temperature-controlled environment, an IR image acquisition system and a Virtual instrument software environment for IR image analysis, Interpretation and Reporting.[11], [12], [13], [14], [49]

3.2 Experimental procedures

3.2.1 Materials and Methods

Fifteen healthy subjects from the CDAC Kolkata (ages 35–52) employee pool participated in this study. As the experiment commenced, the participants were instructed to sit comfortably and maintain stillness. As a preliminary step, 48 emotionally neutral images were shown to them to facilitate a period of relaxation lasting approximately 10 minutes. Subsequently, the participants underwent a "Paced Stroop Test." At the same time, their Infrared Image for Skin Temperature (ST) was recorded from an IR Camera placed in front of the issue and focused on the upper body for face and hand imaging.

In contrast, the right side of the head focused on the right ear and forehead was recorded moving on each response of the 'Stroop Test slides. The subject was asked to respond loudly to the Stroop Test Slide movement in this test. The computer program is designed so that, during the selection process, participants will encounter identifiable segments known to induce the "Stroop Effect." Studies have scientifically shown that this phenomenon can cause cognitive

stress in individuals. The ambient temperature was kept constant during the experiments to ensure the reliability of the changes in ST.

3.2.2 Stress Monitoring

The computerized "Paced Stroop Test" was developed to replicate real-world stress conditions. In human-computer interaction, the stress encountered by users is predominantly mental, with moderate intensity being the norm, as opposed to physical stress, which is less common [73]. The traditional Stroop Colour-Word Interference Test [74] involves naming the colour of a word that denotes a different colour. Our study adapted the classic Stroop test into an interactive format where participants must click on the correct answer instead of verbalizing it. Each word is displayed for 3 seconds per trial. This modification, known as the pacing of the Stroop test, has the potential to heighten the physiological response [75]. If participants fail to respond within the allotted time, the test proceeds to the next trial. This version was created using Microsoft PowerPoint and incorporated bursts of a sinusoidal tone via the laptop's sound system for stimulation at specific time points throughout the protocol, thereby allowing for the precise timing of recorded signals at these critical junctures [76].

The complete experiment comprises eight to ten consecutive sections. In each section, there is an Introductory Segment (IS); a Colour cognition segment (C), colour with matching meaning in memory (CM) in the Stroop words; a Colour Word segment (CW), with mismatched sense and font colour in the Stroop words; a Colour Word with memory test segment (CWM), colour combined word (CCW) and colour combined word memory (CCWM) and a Resting Section (RS). The subject was memorizing the pictures as shown in the previous Stroop Test. If they fail to memorize less than three out of five tests, the CCW and CCWM tests repeat to CCW1, CCWM1, CCW2, and CCWM2. All physiological signals were recorded and synchronised throughout the experiment using the hardware and software setup, which allowed for analysing potential concurrent changes associated with sympathetic activation, commonly linked with 'stress', over the entire procedure.

3.2.3 Diabetes Monitoring

In a controlled environment with a temperature set at approximately 25.5°C, specific body areas selected for imaging were exposed by removing clothing and any metallic adornments, allowing them to acclimatize to the room temperature for 15 minutes. The

environment was carefully regulated to maintain stable temperature, humidity, and air circulation [76]. This setup facilitated the observation of skin temperature changes within a narrow range of 0.05°C to 0.1°C between the targeted area and the surrounding or contralateral body regions. Importantly, this controlled environment ensured that thermal radiation naturally emitted by the human body was not absorbed or scattered by external objects [26].

3.3 Experimental setup: Measurement Procedure in Virtual Instrument

There are two types of postures taken for the experiments. 460- 500 still IR images of total sections were recorded for observations. 10- 12 base images were captured at the initial point (IS). Thirty (30) images on each C test response and 25 images on the CM response (5 images on each memory test) were recorded. Thirty (30) images on CW responses and, 25 images on CWM responses, 50 on each CCW, and 25 on each CCWM test were recorded. The images were recorded on the resting section (RS). Whereas for diabetic patients, the images of different body parts are captured for a specific time. The overall Stress analysis system is shown in the flowchart in Fig 3.1.

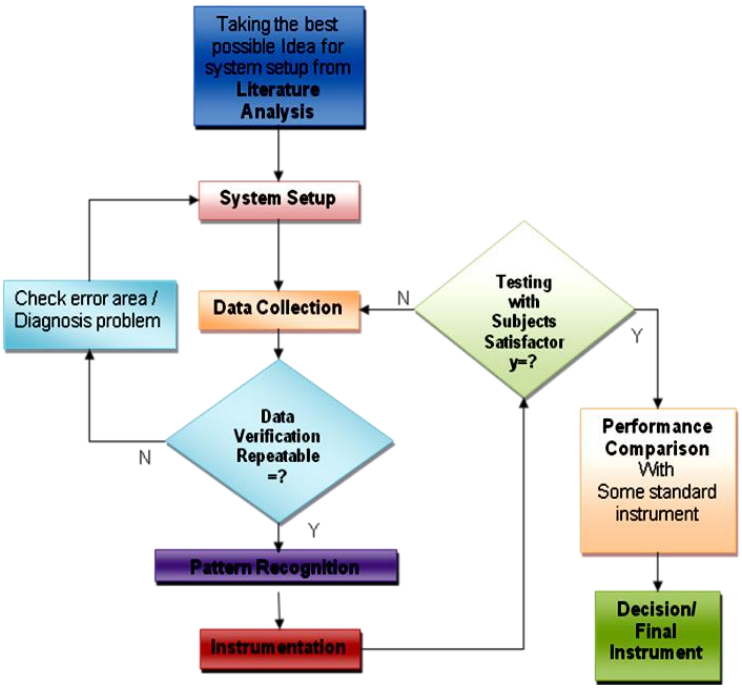

Fig. 3.1: Flow chart for the algorithm of Stress Analysis System

The temperature profile of the ear spreads out as the mental stress increases. Diabetic patients exhibit lower temperature profiles compared to those of individuals without diabetes. This distinction is discerned using LabVIEW-based image analysis techniques encompassing thresholding, particle area calculation within the Region of Interest (ROI), and histogram analysis methods. The application of image processing methodologies is directed explicitly towards ear images. Image segmentation, a fundamental process dividing images into distinct sub-regions or objects, is pivotal in this analysis [20]. Given the variability in particle attributes and light distribution, segmentation is achieved through thresholding to delineate the particles accurately. Diabetic patients exhibit lower temperature profiles compared to those of individuals without diabetes. This distinction is discerned using LabVIEW-based image analysis techniques encompassing thresholding, particle area calculation within the Region of Interest (ROI), and histogram analysis methods. The application of image processing methodologies is directed explicitly towards ear images. Image segmentation, a fundamental process dividing images into distinct sub-regions or objects, is pivotal in this analysis [20]. Given the variability in particle attributes and light distribution, segmentation is achieved through thresholding to delineate the particles accurately. A threshold image g (x, y) is defined as

$$g(x, y) = \begin{cases} 255 & \text{if} \quad f(x,y) > T \\ 0 & \text{if} \quad f(x,y) \leq T \end{cases} \tag{3.1}$$

In this context, let T represent the range of the threshold value. Specifically, T denotes the fluctuating temperature of the ear, encompassing a range within which scanned images are processed using the algorithm. The resultant extracted values are then preserved for subsequent utilization. For instance, the intensity values pertinent to the temperature range of interest are extracted, with thresholding values ranging from 105 to 108. Values exceeding this upper threshold are assigned a value of 0. Notably, patients might adjust their position to attain relaxation following prolonged periods of hesitation. So, the ROI is to be tracked by the Virtual instrumentation procedure. Here, a geometrical shape-based object tracing procedure is followed. A flow chart for the algorithm of image analysis for the proposed system is shown in Fig3.2.

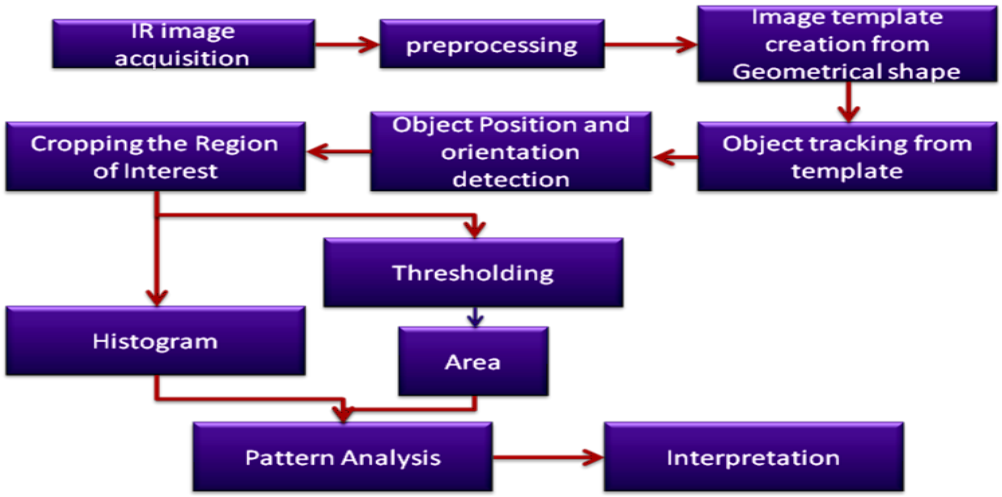

Fig. 3.2 : A flow chart of the image analysis algorithm for the proposed system

The images are acquired by a virtual instrumentation system by the patient's voice response from the microphone to change per slide and capture one image parallelly.

Fig 3.3 shows the Graphical User Interface front panel for the IR image acquisition and parallel stroop test software.

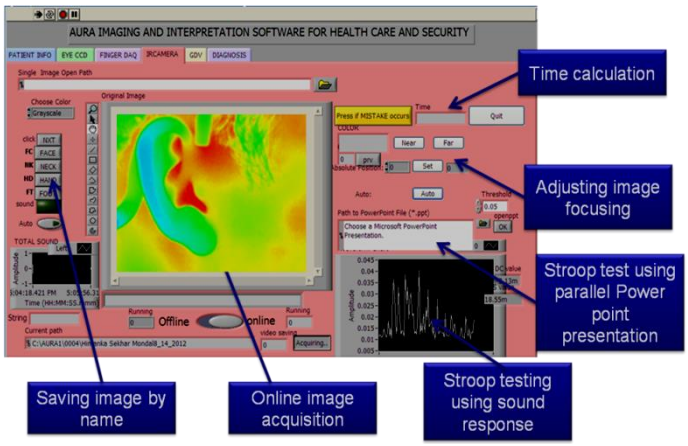

Fig. 3.3: GUI for IR image acquisition with parallel Stroop test for stress analysis.

For diabetic Monitoring, the IR images are captured from different body regions. The nearest value of the subject's core temperature is searched to get the consistent temperature of a subject. According to the expert, the ear lobe, inner canthus points, inner posterior buccal

cavity, and palm are located where interest is highest. The single images of the interested regions of the diabetic subjects are taken and analyzed. The results are compared with the average (non-diabetic) subjects.

3.4 Observations

The processed ear images use observations from the ear images of different segments (IS, C CM, CW, etc.) during Stroop tests and their temperature changes. The area of the corresponding segmented region is extracted for further analysis.

The temperature profile of the face is observed by changing the histogram value (temperature vs. pixel number) along the line drawn on the forehead. The mean temperature increases as mental stress increases.

Fig 3.4 shows the ear images of different segments of the Stroop test with the corresponding area with increasing and decreasing profiles, calculated by total area measurements in pixels after thresholding a specific temperature region.

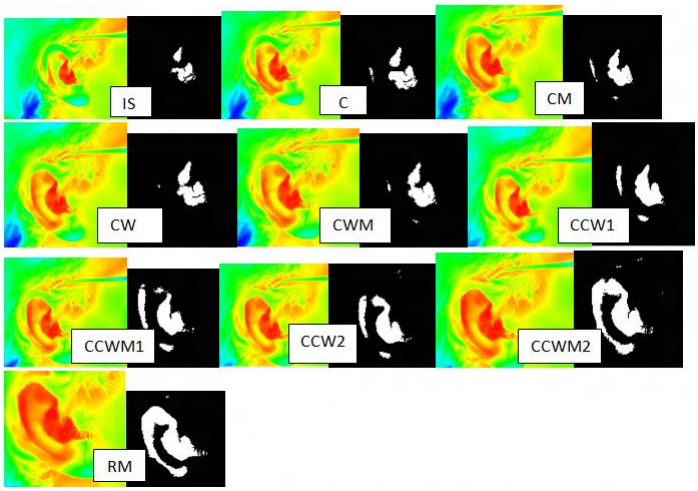

Fig. 3.4: Processed image of the human ear with area calculation for the corresponding thermal profile

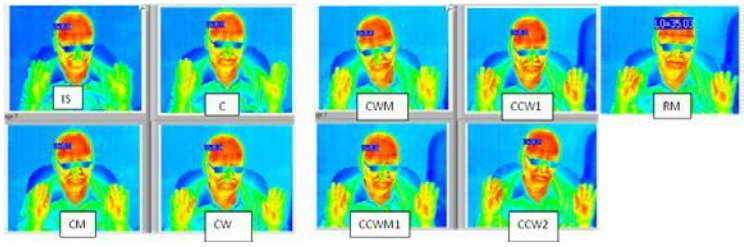

Fig. 3.5: Face images with corresponding lines on the forehead with mean temperature profile

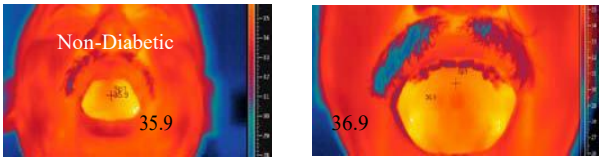

Fig. 3.6: Thermal profile of Non-Diabetic and Diabetic patients

Observations provide the information that the thermal profile of diabetic patients has less thermal distribution than non-diabetic patients. Fig 3.5 depicts the face images with corresponding lines on the forehead with the mean temperature profile. Fig 3.6 shows the corresponding inner posterior buccal cavity images of two subjects. The first image is of a person with diabetes, and the other is from a non-diabetic subject, according to their clinical test reports.

3.5 Results and discussions

All the segmented temperature regions are distinguished in their surface area calculations from the number of pixels in a particle. After the connected component labelling algorithm, the particle size can be extracted by the pixels measured in the particle [20]. Fig. 3.7 shows the image area calculation of the corresponding segmented particles of all IR images. The subjects were asked about the level of stress they felt during the Stroop test after completing all the tests. The level of stress they felt was recorded on a 0 to 10 scale. Fig. 3.8 represents the plot of the image area analysis from IR images and the questionnaire output on a scale of 0 to 1 for all the segments.

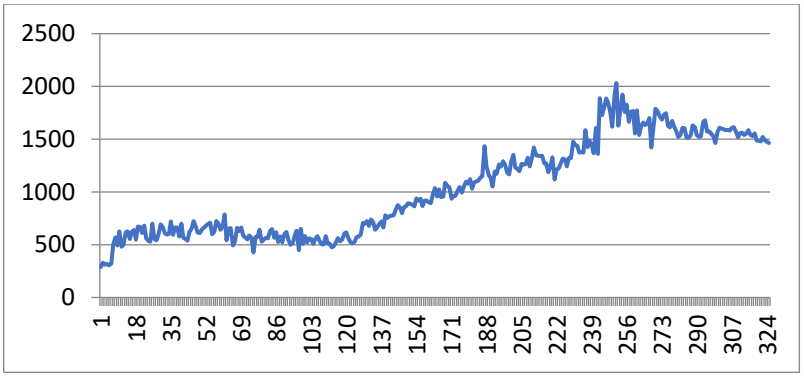

Fig. 3.7: Area of the segmented particles of all IR images

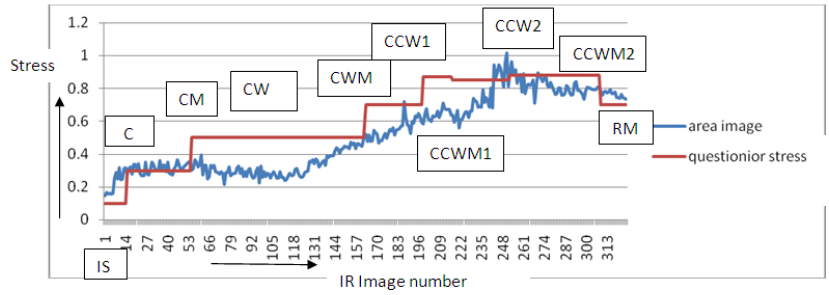

Fig. 3.8: Plot of IR image area analysis vs. questionnaire output from different stress levels of Subjects

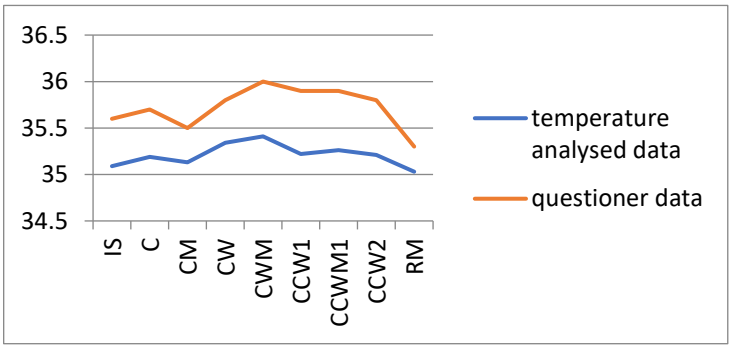

Fig. 3.9 : Questionnaire versus temperature analysis from IR image

The face temperature profile is also observed to confirm changes in the thermal effect on the skin in this context. The histogram value of temperature vs. pixel number along a line drawn on the forehead shows the same effect. Fig 3.9 shows the questionnaire stress output versus mean temperature analysis from the histogram value drawn from a line on the forehead image. The temperature of image histogram analysis falls in 35 to 36 scales, so the questionnaire output is scaled to that range.

Graphs from the outputs prove that the thermal profile acquired from the IR images follows the stress conditions that the subject felt during the whole session. The ear imaging is recorded from a close distance, and the head movements do not affect the analysis very much for the image Analysis system's constant tracking of the ROI area. However, an observation reflects that in the ear, the temperature change with stress sustains longer than that of the forehead.

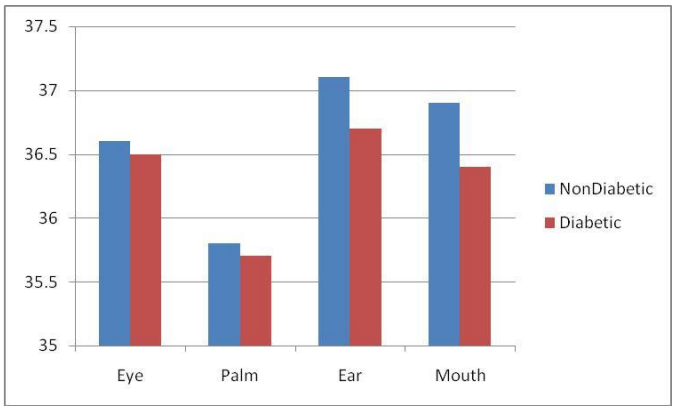

Fig. 3.10 : Graphical representation of the thermal profile of non-diabetic vs diabetic subjects.

The distribution of thermal profiles in various anatomical locations, such as the inner canthus points (Eye), palm, ear lobe, and inner posterior buccal cavity (mouth) among diabetic and non-diabetic patients, is illustrated in Fig 2.10, highlighting temperature variations.

Between the two postures, the face images are taken from a more considerable distance than ear imaging, so the minute change in temperature has been considered to avoid the distribution of emissivity in the whole image instead of the region of interest. The subjects move their head left to right as per relaxation of body requirements, reflecting the difficulty in line histogram tracking for the second posture. Whereas the ear imaging is recorded from a close distance, the head movements from left to right do not affect the analysis very much. However, an observation reflects that in the ear, the temperature change with stress sustains longer than that of the forehead. Seven subjects of the fifteen people responded to the Stroop test with mild psychological stress in these tests. Their feelings of stress level and IR image analysis report also followed the response graph of Fig 2.8, which proves the authenticity of this work with the other research in both ways.

3.6 Conclusion

The closing statements of this chapter highlight the conformity of IR image analysis with the questionnaire outputs of the segments, emphasizing the need for further verification with an expanded pool of subjects to ensure reliable outcomes and highlighting the significance of body temperature as a reflection of human energy emission from physical organs, primarily metabolism. The discussion emphasizes how the infrared camera effectively detects changes in the subject's skin temperature through continuous Monitoring and modulation.

Furthermore, the chapter reports the initial experiments and presents the system's fundamental design. Drawing on experiments conducted on fifteen subjects, the chapter corroborates the comparison of stress levels in terms of the subject's thermal profile using IR images, aligning with the expected results. So far, we have experimented on fifteen subjects and compared the stress level in terms of the thermal profile of the subject using an IR image. A response matches our expectations[13]. It envisions the fully developed system's non-invasive utility in hospitals and office environments for early diagnostics of various diseases, particularly in stress management, showcasing the potential of intelligent healthcare infrastructure.

The forthcoming chapter aligns with this trajectory by delving into developing an IR image processing-based technique for detecting oral cancer. It emphasizes the pressing need for an accurate and sensitive molecular-based diagnostic tool for early screening systems, positioning IR image analysis as a pivotal approach. Early cancer detection is crucial. Infrared imaging plays a significant role in alerting patients to potential cancers, potentially improving survival rates. It also acknowledges the challenges associated with the interpretation of thermograms, emphasizing the recent advancements in infrared technology and image processing and the improved understanding of IR images based on pathophysiology, which have prompted renewed interest in infrared imaging for cancer detection.

Chapter IV

Development of IR image processing-based Oral Cancer detection technique

4.1 Introduction

Early oral cancer diagnosis can significantly improve patient survival rates and reduce medical costs. There is an urgent need for an accurate and sensitive molecular-based diagnostic tool for early oral cancer screening systems based on IR image analysis [77] [78][79]. This chapter reports an experimental study on oral cancer detection techniques. Literature available on cancer and complexities in diagnostics has led to the main work, i.e., Infrared (IR) imaging technique and how to implement IR imaging technology in detecting oral cancer diseases. The same sample IR images are analyzed using IR image processing techniques in a Virtual Instrumentation environment. The practical application of these developmental techniques is yet to be confirmed. IR image analysis and interpretation with subjects will decide whether these techniques are practically feasible for usable system development. Early diagnosis of any form of cancer is the key to improving the survival rate [78] [80]. Infrared imaging or thermography-based systems are essential screening tools that can warn a patient of cancer quite a few years in advance. Although the application efforts and research on Infrared thermal imaging in cancer studies started as early as 1961, it has not widely recognized the premature status of technology, the superficial understanding of infrared (IR) images. The experimental process is established based on the latest advancements in infrared technology, image processing capabilities, and the interpretation of IR images assisted by pathophysiology [81]. These have spurred renewed interest in using infrared imaging, particularly for cancer detection. An early cancer diagnosis is vital. Tumours appear as hotspots in infrared images due to cancer cell's high metabolic rate and temperature [82]. The existence of asymmetry in temperature distribution indicates the presence of a tumour.

4.1.1 Image acquisition

Infrared (thermal) cameras measure the infrared, or thermal, energy emitted from any human object. Infrared cameras can solve some scientific and industrial application development requirements that the visible spectrum of light sensors cannot solve [80]. Defects can be detected easily in the infrared spectrum for some applications. An infrared camera can be used to check the oil level in the compressor, especially if there is a temperature differential. National Instruments devices help acquire and process thermal images. Images are collected from infrared cameras along with some high-resolution digital cameras. The thermal images are analyzed with IMAQ Vision image analysis functions.

4.1.2 IR image Acquisition, Processing and Analysis

The emission measurement software system contains an infrared camera that captures body images.

The setup involves an online image-capturing process and preliminary image analysis simultaneously. Following image capture on a computer (offline mode), statistical output extraction occurs, and the data is forwarded for machine learning. The algorithm for image control and analysis is detailed as follows.

The thermal camera captures images using the NI Vision Development Module and FLIR Thermo-Vision LabVIEW Toolkit. LabVIEW employs a high-pass filter to eliminate impulse noise from each image.

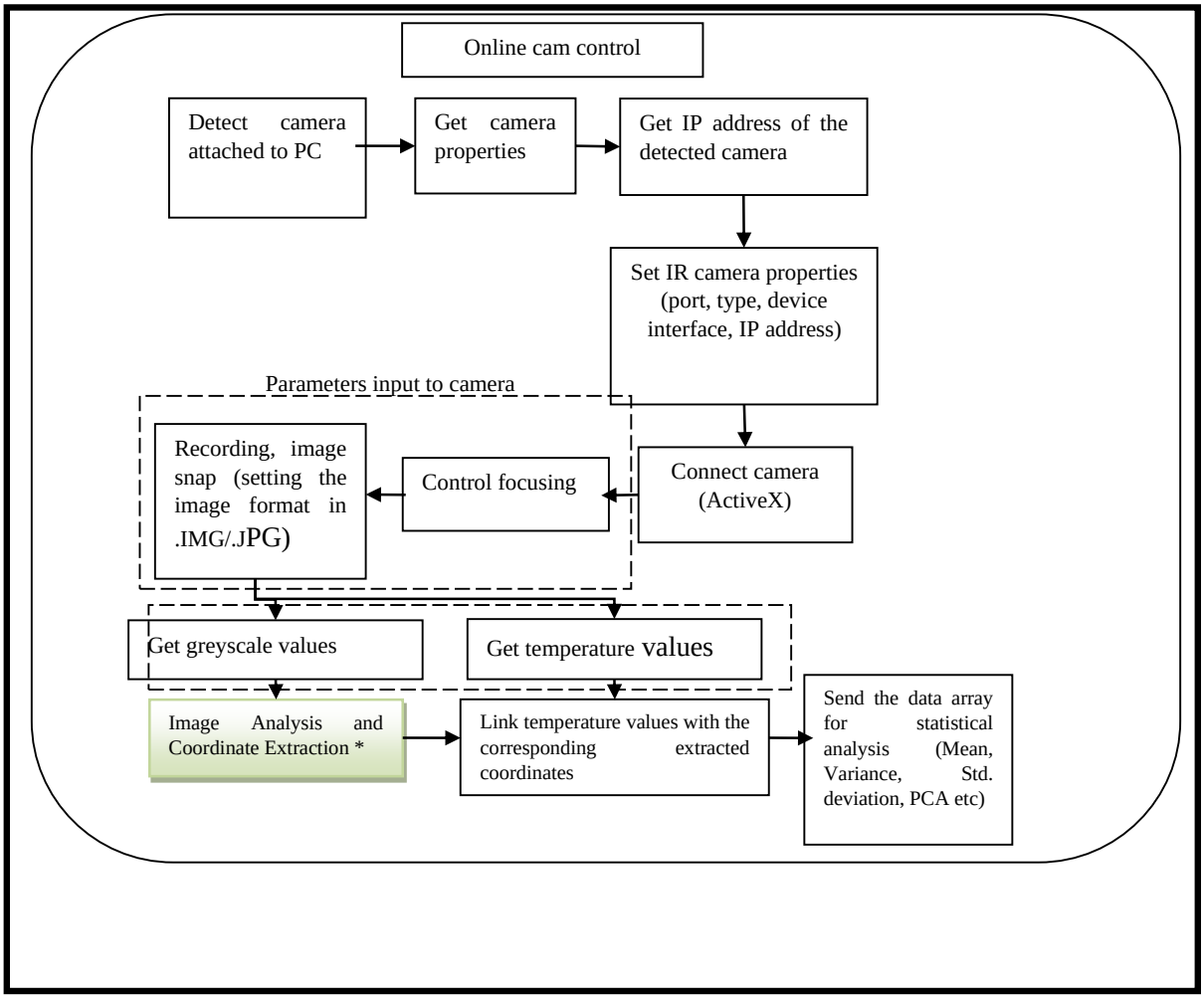

Fig. 4.1 : IR Online Image Capturing Algorithm

The required controls are received from the LabVIEW image processing and vision development module, the Thermo-Vision toolkit provided by FLIR, and the Infrared device. The infrared image differs from the superficial image data as the images are separated into temperature data and image files. The image file is used for offline processing of body part tracking and extracting the masked image for further uses. The online IR Image capturing and control module is shown in Fig. 4.1. The captured IR image is analyzed using image processing tools in LabVIEW, shown in Fig. 4.2.

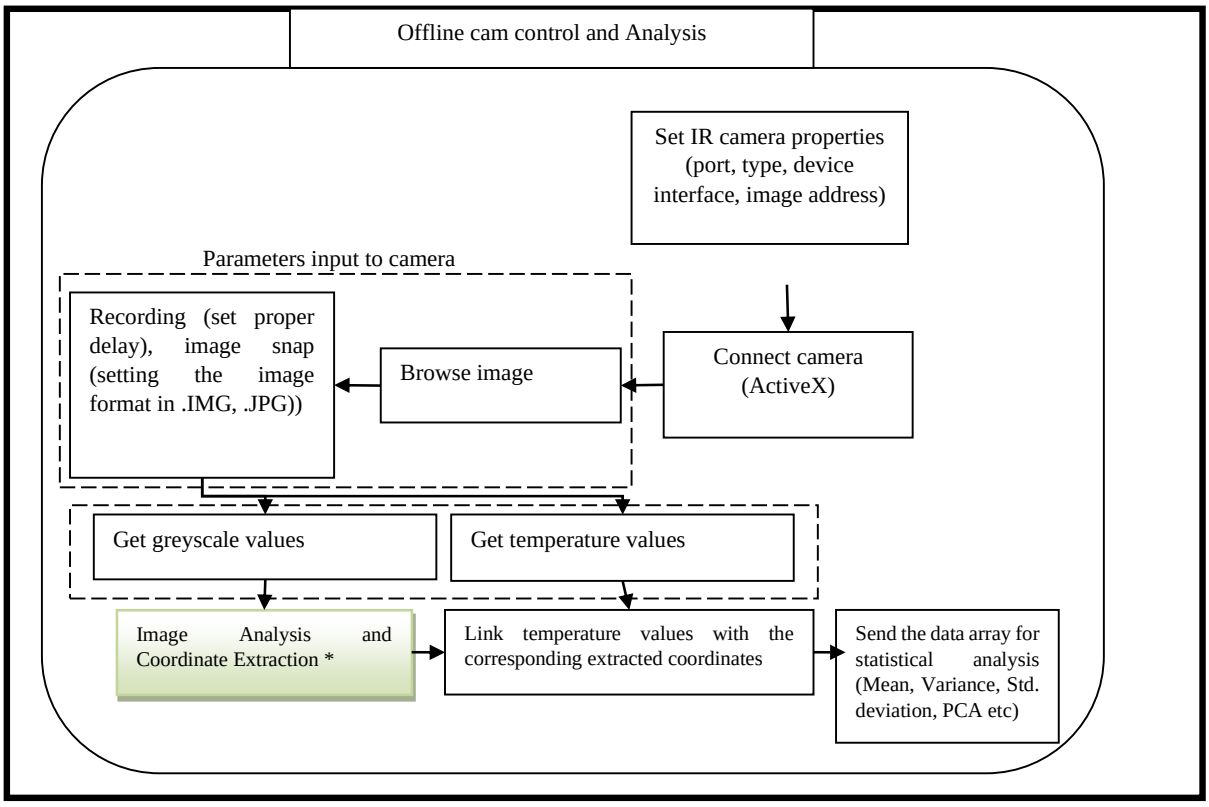

Fig. 4.2 : offline Image Analysis Algorithm for IR imaging

4.1.3 Thermo-Vision LabVIEW Toolkit

The Thermo-Vision LabVIEW Toolkit is a VI (virtual instrument) for cameras supporting alarms, measurement function and I/O functionality. LabVIEW VIs is used as sub-VIs to manage communications with a FLIR IR camera in digital mode. Temperature images are generated from images acquired through LabVIEW. The LabVIEW IR Measurement and Display tools are used to analyze the temperatures of the imaged objects.

LabVIEW Toolkit provides the functions needed to:

- Set up communications between LabVIEW VI and the FLIR IR camera
- Capture and gather images via FireWire™ or Ethernet interfaces
- Adjust the camera configuration parameters and focus as we view a live image
- Control the camera calibration
- Send any other camera command to the camera
- Generate an actual temperature image from a 16-bit image acquired using the Cameras FireWire™ or Ethernet interfaces.
- Close the communications to the IR camera.

4.2 Feature Extraction for IR Image Analysis

4.2.1 Image processing Features

In computer vision and image processing system, a feature is a valuable piece of information for solving computational tasks in machine learning and pattern recognition. However, image processing has a highly developed collection of features. Features are specific structures in the image, such as points, edges or objects [83]. Features may also result from a general neighbourhood operation or feature detection technique. Various features relate to motion in image sequences [84]. These may pertain to shapes defined based on curves or boundaries separating different regions in the image. Alternatively, they may relate to the properties of a particular region in the image.

The concept of features is quite broad, and the selection of features for a computer vision system can vary considerably depending on the specific issue. There are two approaches when defining features in an image using local neighbourhood operations, also known as feature extraction [83]. One produces local decisions on whether a feature of a particular type exists at a specific image point, while the other yields non-binary data. When there are only a few detected features, it is essential to distinguish between local decisions and binary images. The result of a feature detection process can be expressed as collections of linked or separate

coordinates corresponding to the image locations where features were identified, frequently with sub-pixel precision.

4.2.2 Feature detection

Regarding computer vision and image processing, feature detection involves analyzing specific characteristics at every point within an image to identify distinct features. These features are subsets of the image domain. Feature detection refers to techniques that compute abstract representations of image information and make local decisions at each image point to determine whether a particular type of image feature exists at that point or not. The features that are obtained are a part of the image domain. Feature detection is a technique used to compute abstract representations of image information and assess whether a specific type of image feature exists at each point. The features identified are a subset of the overall image domain. Often isolated points, continuous curves or connected regions. A feature is an essential aspect of an image that serves as a foundation for computer vision algorithms, but there is no set definition for what qualifies as a feature. Defining a feature can vary depending on the problem or application. The quality of the feature detector heavily affects the effectiveness of algorithms. It should be able to detect the same feature in multiple images for repeatability.

Pixel analysis in feature detection confidently identifies the presence of features in an image. If this is part of a more extensive algorithm, it will usually analyze only the image within the area of the features. Applying a Gaussian kernel to process the input image in a scale-space representation smoothly is imperative. This critical step helps to calculate image features by using local image derivative operations.

Advanced algorithms are used to focus on specific areas of an image to streamline feature detection when time is limited. Many feature detectors have been developed for this purpose. Depending on the features detected, computational complexity, and repeatability, the variations can be significant.

4.2.3 Feature Extraction

After detecting features, a specific image patch related to the feature set is extracted locally. This process of Extraction requires a significant amount of image processing. After analyzing the image, attributes are extracted and combined to create a feature descriptor or vector. Different methods exist for feature description, such as N-jets and local histograms

(scale-invariant feature transform is an example of a local histogram descriptor). The feature detection step also provides supplementary attributes like edge orientation and gradient magnitude in edge detection or polarity and strength of the blob in blob detection [84].

When feature extraction is done without local decision-making, the result is often called a feature image. A featured image essentially shares the same spatial or temporal variables as the original image [85], [86]. However, instead of holding information about intensity or colour, the pixel values contain data about image features. Hence, a feature image is processed similarly to an ordinary image captured by an image sensor. Feature images are frequently computed as integrated steps in algorithms for feature detection.

4.3 System Overview

4.3.1 Work Flow of the System

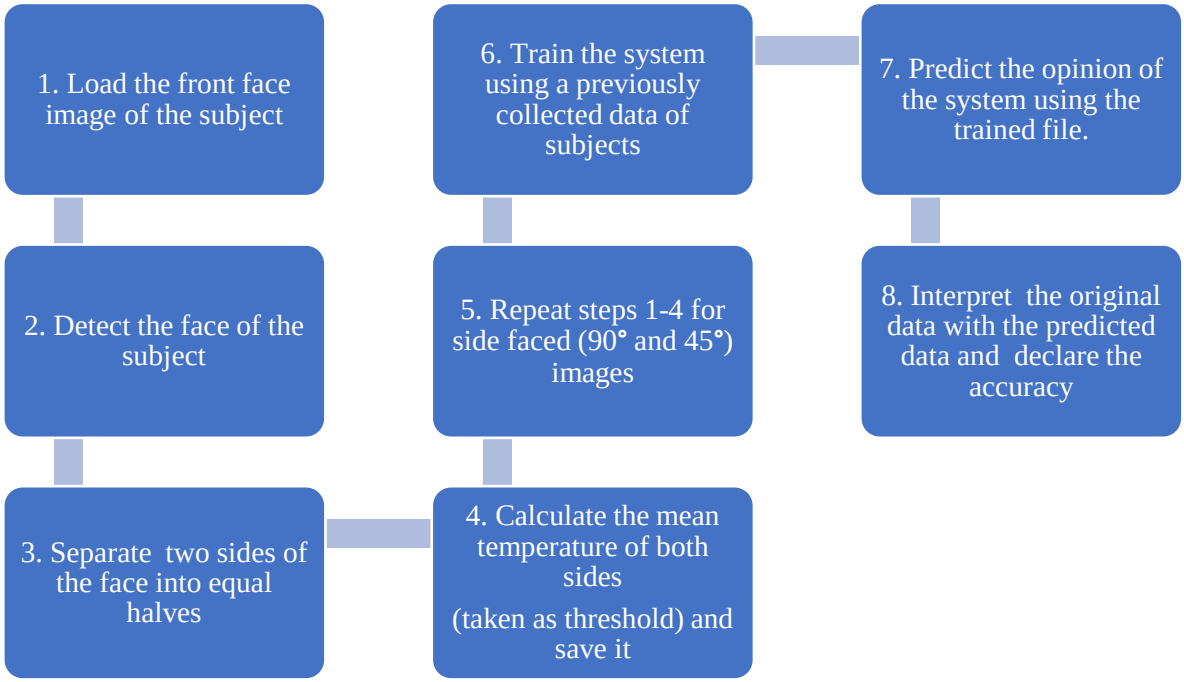

Fig. 4.3 : Workflow of the entire system

4.3.2 Data Flow Diagram (DFD) of the System (Level 1)

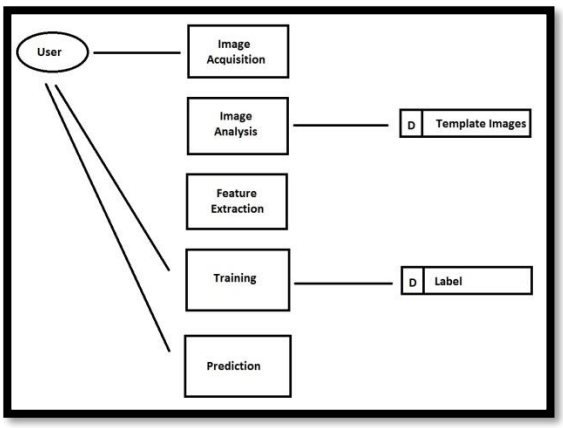

Fig. 4.4 : DFD (Level-1) of the system

4.3.3 Context-Free Diagram (CFD) of the System

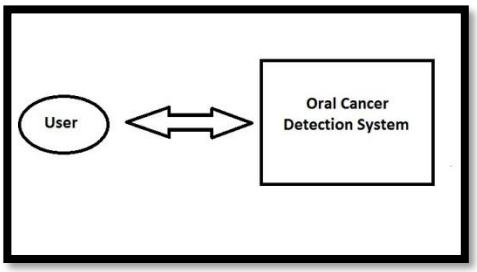

Fig. 4.4.1: CFD of the system

4.3.4 Feature Extraction of Front-Faced image

Input:

Fig. 4.5 : Thermogram of a subject

Output:

Fig. 4.6 : Two parts of the face after thresholding

Fig. 4.7 : Final output of the algorithm for Extracting features from the front-faced image

4.3.5 Feature Extraction of Side Faced image (90 and 45 °)

Input:

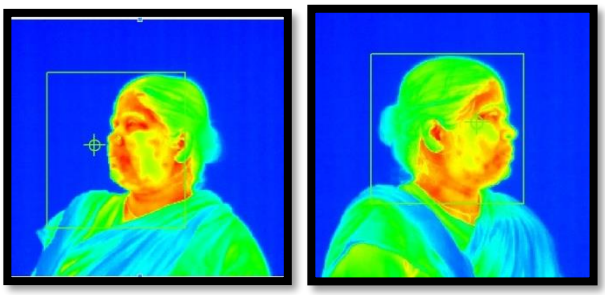

Fig. 4.8 : Thermogram of the subject from a 45 ° angle (left and right side)

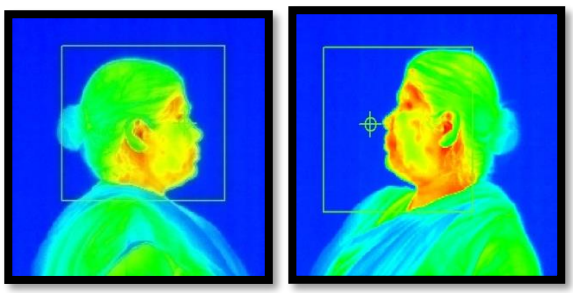

Fig. 4.9: Thermogram of the subject from a 90 ° angle (left and right side)

Output:

Fig. 4.10 : Threshold image of the woman from a 45° angle (left and right side)

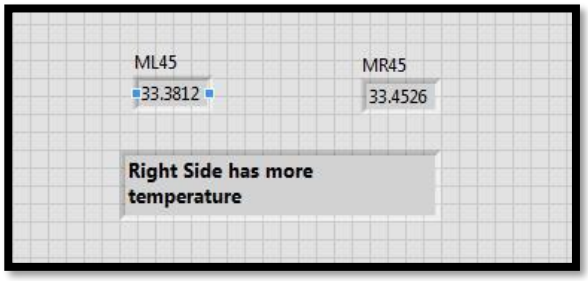

Fig. 4.11: Final output for extracting the features from Side-Faced image (45°) algorithm

Fig. 4.12 : Thermogram of a subject from a 90° angle (left and right side)

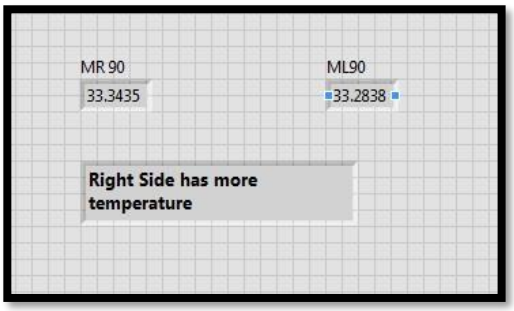

Fig. 4.13 : Final output for extracting the features from Side-Faced image (90°) algorithm

4.3.6 System Training

Output:

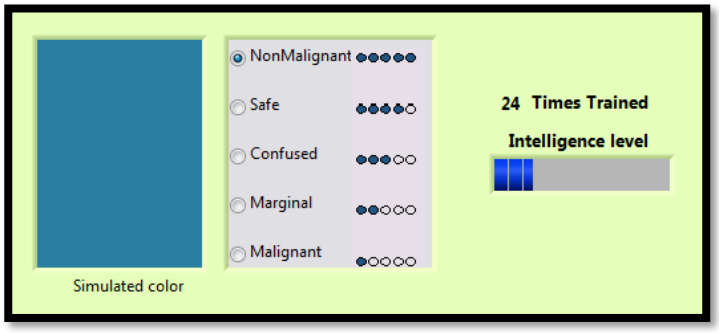

Fig. 4.14 : Output of the training algorithm

4.3.7 Prediction from the system

Output:

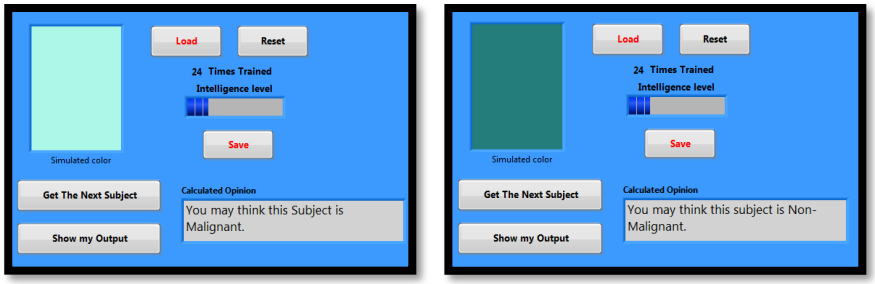

Fig. 4.15 : Output of the prediction algorithm

4.3.8 Screenshots of VI-based Oral Cancer screening software

4.3.8.1 Front Panel View

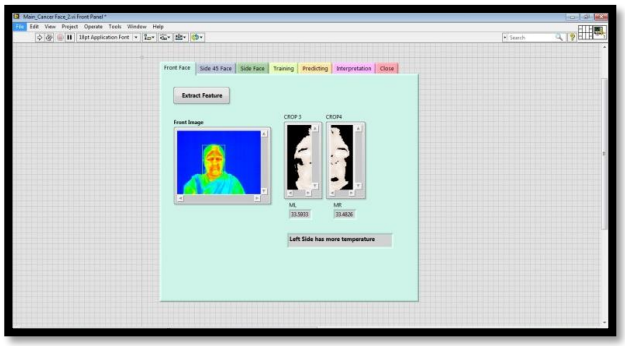

Fig. 4.16 : Front Panel showing the feature extraction from the front face image

Fig. 4.17 : Front Panel showing the feature extraction from the side face (90°) image

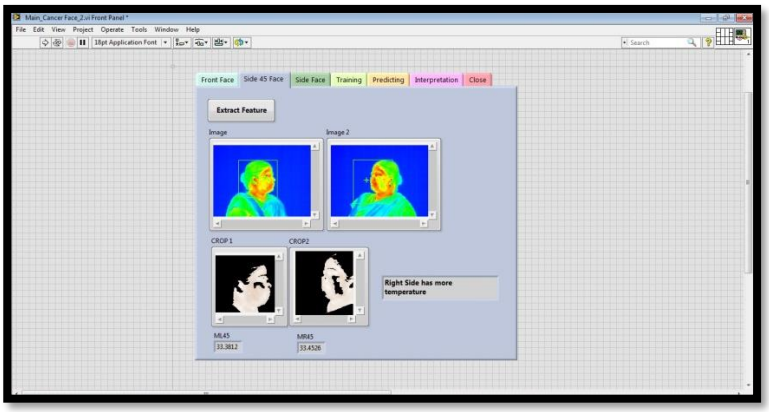

Fig..4.18 : Front Panel showing the feature extraction from the side face (45°) image

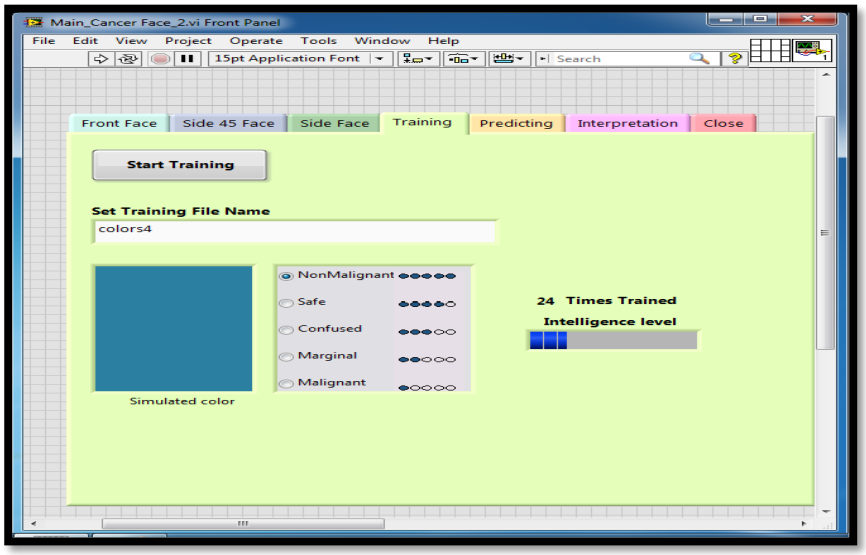

Fig. 4.19 : Front Panel showing the training module of the system

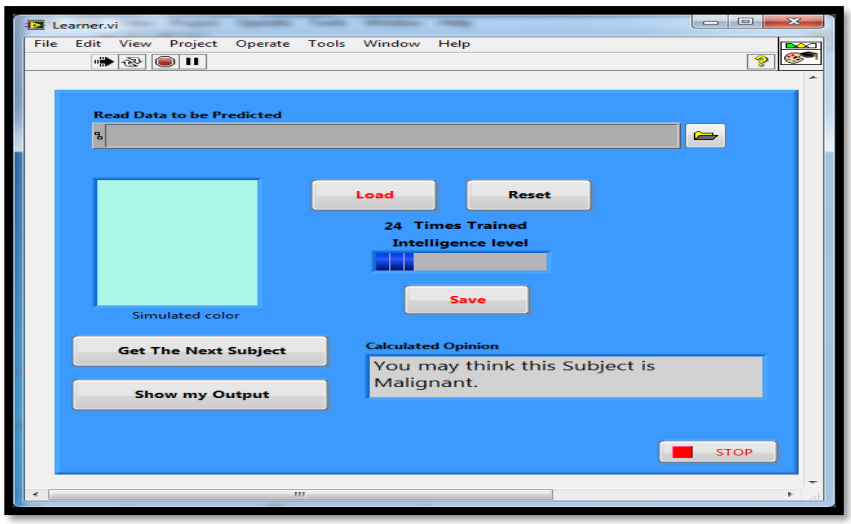

Fig. 4.20 : Front Panel showing the prediction module of the system

4.3.9 VI Block Diagrams of the Software

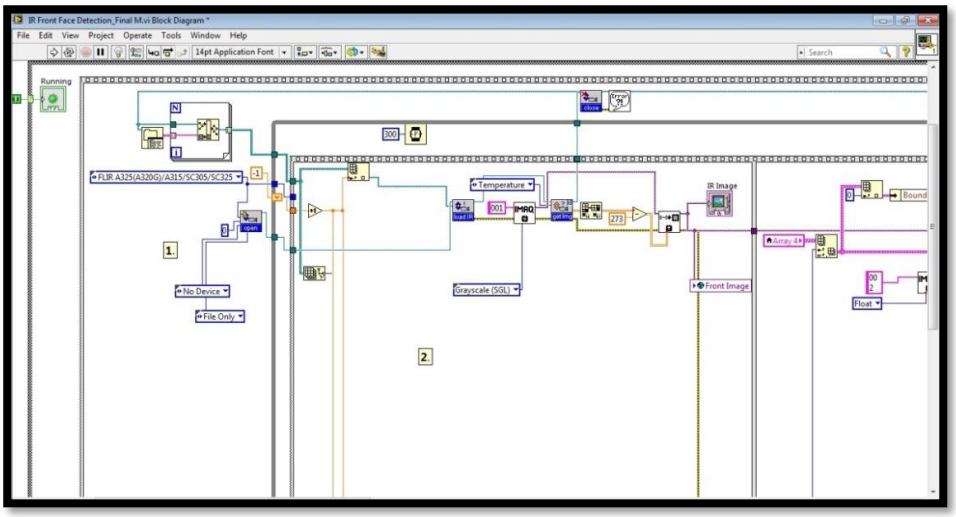

Fig. 4.21 : Block diagram for Front face feature extraction (1 and 2)

1: This part of the VI loads the files sequentially for further operation.

2: This part of the VI converts the temperature values in each image from Kelvin to Celsius to better understand the user.

4.4 Issues in Oral Image Capturing

The infrared (IR) camera faces limitations when attempting to access the buccal cavity of the mouth, posing challenges in creating a comprehensive system for determining its focal

area. A standard IR camera with dimensions of 143×195×95mm (4.2×7.9×4.9in) and a focal length of 24.6 mm (25°) has a lens size much larger than that of the buccal cavity, preventing proper entry into this region.

Primarily, the problem arises in capturing images of the hidden portions of the mouth, which are crucial for diagnosis. Due to the focal area of the IR image and the minimum focus distance, the imaging system struggles to capture close-up images effectively, resulting in defocused images. As a result, infrared imaging primarily focuses on the outer surface of the oral cavity and its surrounding areas [58] [30].[87].

4.5 Images of some Oral Cancer Subjects

Following images are some sample of the subjects for front-face data collection on Oral cancer analysis.

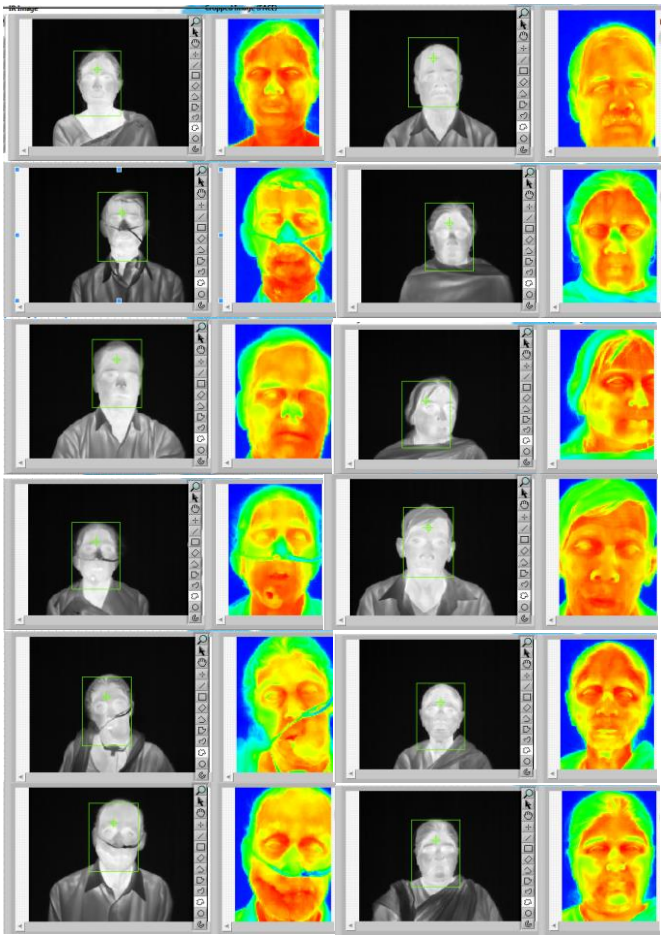

Fig. 4.22 : Sample images of the subjects for the front-face data collection on Oral cancer

Infrared (IR) images are acquired from five distinct perspectives: frontal, from 45 degrees to the right and left, and 90 degrees to the left and right. Notably, all these images are captured

from external viewpoints of the face. This approach proves efficient for detecting complexities present on the exterior surface of the face. However, employing an IR camera with an appropriate focal length becomes crucial for complexities within the inner cavities where their effects have yet to extend to the outer surface. This section will delve into the outcomes and subsequent discussions.

4.6 Results

The current system captures thermal images from an IR camera, which follows the image acquisition and analysis method. It then extracts the mean value of each side of a face image within a threshold value from the images for further processing. It then uses this feature to train the system, after which any data can be fed to predict from the system. We tested our method on 24 subjects.

4.6.1 System Performance

The system's efficiency is measured by a population-based case-control study on the current subjects for 12 subjects. One side of the face is considered one case. 24 cases with five different angles are taken for the total evaluation. The study results are shown in Table 4.1.

Table 4.1: System Performance

Total positive	4
Total Negative	12
False Positive	6
False Negative	2
Sensitivity	66.67%
Specificity	66.67%
Positive Predictive Value	40%
Negative Predictive Value	85.71%
Accuracy	66.66%
False Negative ratio	33.33%
False positive ratio	33.33%
LR+	+2
LR-	0.5
Diagnostic Odd Ratio	4

In all the above equations, the True Positive is represented as TP, the True Negative is represented as TN, the False Positive is represented as FP, and the False Negative is represented as FN.

4.6.2 Discussion on Result

An automated system has been implemented to generate decisive opinions on any relevant data set. The system has been developed to become an integral part of the overall diagnostic system to utilize the Genfis property appropriately [87]. The current data set was obtained from Cachar Cancer Hospital, Silchar, where a data collection program on random patients was executed. The system has been trained on collected data.

A virtual instrumentation module using LabVIEW has been developed for inclusion in Virtual instrumentation architecture to implement intelligent medical diagnostic systems using infrared imaging.

The algorithm that has been developed so far using Genfis can be beneficial for future research work, which can be used for

- Implementation of SVM (Support Vector Machine) classifier in LabVIEW.
- Comparison of the performance of Genfis and SVM
- Integrating various modules to implement an intelligent virtual instrumentation system for medical diagnosis using an infrared thermography technique

4.7 Conclusion

The concluding segment of the previous chapter highlights the initial findings that have laid a foundational level of confidence, drawing from practical experiments and literature studies. It emphasizes the need for specialized, practical research studies and the indispensable guidance of dental experts to ensure the integration of IR imaging and image processing techniques in oral cancer detection. Additionally, it acknowledges the ongoing collaborations with oral cancer specialists and hospitals, underscoring the pivotal role of collective expertise and partnerships in advancing the efficacy and applicability of the proposed systems.

This paves the way for the subsequent exploration, wherein Chapter V presents a widespread investigation of the potential applications of infrared imaging in diabetes and breast cancer screening.

The next chapter explores how infrared imaging can be used to develop an early detection framework for diabetes and breast cancer. By leveraging advancements in image processing, data acquisition methodologies, and machine learning techniques, the chapter aims to establish a robust and precise screening system that can significantly contribute to the timely diagnosis and management of these critical medical conditions.

Emphasizing the significance of the ear cavity region for diabetes screening and drawing from existing research on the application of infrared imaging in various body regions, the chapter highlights the depth of knowledge and the promising possibilities offered by this technology. Furthermore, the discussion highlights the collaborative efforts between research institutions and medical facilities, showcasing the importance of collective expertise in driving the evolution of practical diagnostic tools. The chapter also anticipates exploring innovative non-invasive breast imaging methods, accentuating the potential for enhanced accuracy in detecting abnormalities through sophisticated data analysis and machine learning algorithms.

Chapter V

Exploring the potential use of infrared imaging in medical diagnosis: comprehensive framework for diabetes and breast cancer screening

5.1 Introduction

This chapter reports an all-inclusive approach combining infrared (IR) imaging for diabetes screening tools and breast cancer screening systems. The selection of the ear cavity region as an essential body region for diabetes screening, as well as advances in image processing, data acquisition, and machine learning, contribute to the accuracy and effectiveness of the proposed system. The findings of this study have important clinical implications and provide insights into the potential of infrared imaging in the diagnosis of type 2 diabetes. For breast cancer detection, the data acquisition technique used four pilot studies (PS1, PS2, PS3, and FS) to acquire infrared images for breast cancer screening. Each pilot study employed specific settings and modifications to simplify data collection, analysis, and optimization for breast cancer detection [51].

The research consisted of two main parts: selecting regions of interest for infrared imaging in diabetes-related equipment using the most influential body parts and developing a non-contact, non-invasive breast imaging method using infrared technology. In the first part, the study builds on previous work on region selection for infrared imaging. Various research groups have investigated how infrared imaging can assess the temperature of different body regions, such as the surface of the eye, foot, cornea, toes, and skin, for diabetes-related applications.

5.2 Methods

5.2.1 Diabetes Screening Methodology

Capturing infrared images of different body parts, such as the face, neck, hands, legs, and ears, was the primary focus of screening diabetes. The imaging setup and data acquisition exercise were conducted at a Chennai hospital. An Arduino Uno microcontroller with an integrated data acquisition system based on a temperature sensor was developed to account for changes in ambient temperature, which helps to normalize the effects of temperature changes caused by environmental factors.

Special precautions were taken during data collection to ensure accurate imaging results. Selected areas of the body are stripped naked and free of any metallic ornaments or objects. Subjects were allowed to acclimate for 15 minutes in an air-conditioned room at approximately 25.5°C while maintaining controlled temperature, humidity, and airflow. This step aims to

capture skin temperature changes within the range of 0.05 °C to 0.1 °C between the affected area and the surrounding or contralateral area.

Data collection was performed in two sessions: a fasting blood draw and a postprandial (PP) blood draw with a two-hour interval between two so that data could be collected from 12 to 13 subjects daily. Infrared image processing employs various techniques, including manual, semi-automatic, and fully automatic Region of Interest (ROI) selection. Manual ROI selection involves cropping an ear template from an infrared image. In contrast, semi-automatic ROI selection allows the user to accept or reject the coordinate region suggested by the software. Fully automatic ROI selection uses image registration and feature extraction algorithms to select ROIs. Fig. 1 shows the automatic selection of the ear cavity area by image processing technology, data acquisition and analysis of the heat distribution in the diabetic "ear" area. Image processing algorithms such as thresholding and morphological operations are used to extract thermal information of the affected area. Fig. 2 shows a flowchart of an image analysis algorithm using the image processing system of the diabetes screening system.

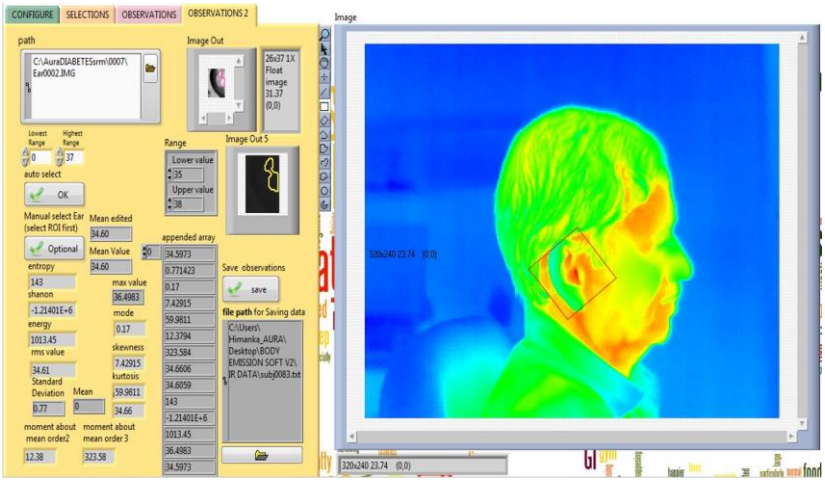

Fig. 5.1 : Data Collection and analysis of Thermal profile of “ear” zone for Diabetic Patient

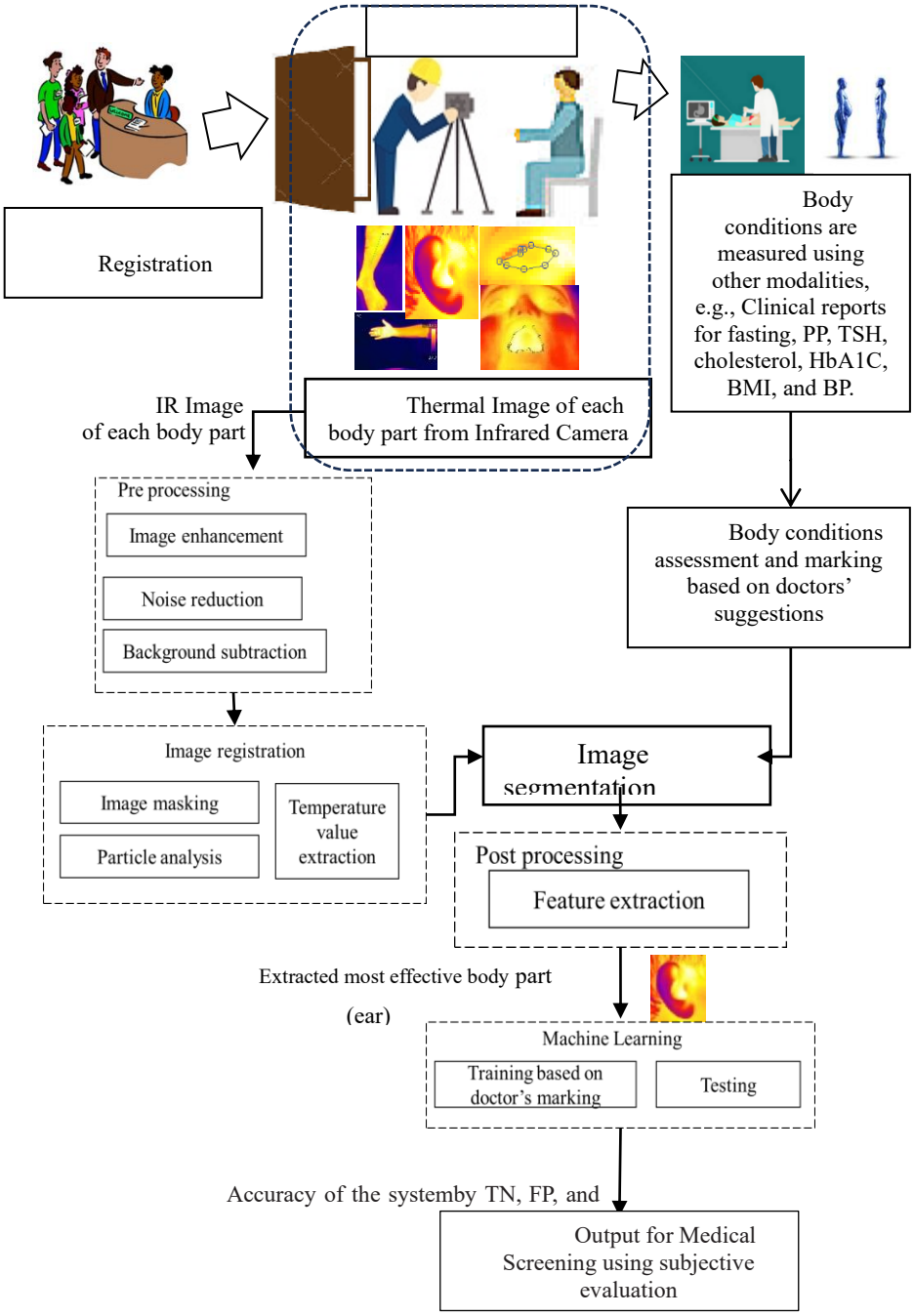

Fig. 5.2 : Diagram for Infrared image processing and Machine vision system for Diabetes Screening

Image analysis techniques include thresholding to segment particles based on pixel intensity values. Virtual instrument software tracks regions of interest through shape-based object-tracking techniques. The temperature values extracted from the ROI are saved for further analysis. Feature extraction techniques include a generalized "Hough transform" algorithm to extract geometric shape features, which are then trained as geometric shape

patterns. Statistical image analysis algorithms record mean temperature, standard deviation, median, mode, skewness, kurtosis, moments, root mean square (RMS), entropy, energy, and maximum temperature values for each infrared Image as a function of the ROI. Feature ranking was done using the Euclidean distance and information gain theory method.

Machine learning-based classification was performed using the statistical features extracted from the thermal arrays as input. The top three features are selected using a feature ranking algorithm and trained using an SVM learning algorithm for classification and analysis. Other classification algorithms, including BPNN, RBF NN, and PNN, were also tested during the software development phase. The SVM algorithm exhibits better and more consistent classification accuracy on image databases.

5.2.2 Breast cancer screening methodology

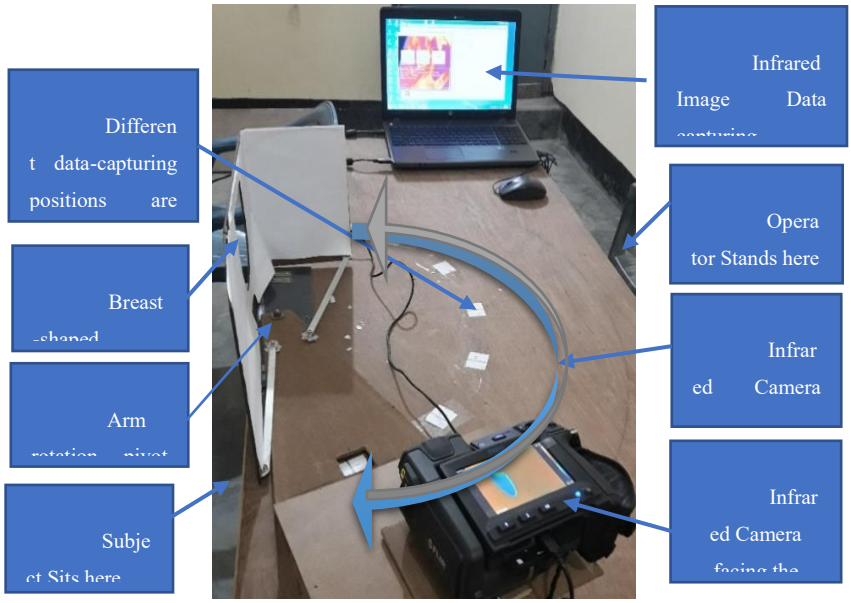

Fig. 5.3 : Breast cancer screening Setup for Rotational Thermography

In the case of Breast Cancer detection, the data collection techniques employed four pilot studies (PS1, PS2, PS3, and FS) to obtain IR images. Each pilot study utilized specific setups and modifications to optimize the data acquisition. For example, PS1 and PS2 involved subjects seated in front of cameras with raised hands. At the same time, PS3 introduced a modified setup with the Camera moving in a semi-circular arc to focus on one breast while covering the other with an infrared-proof barrier. The FS employed rotational thermography, with the patient's

breasts positioned one at a time through a breast-shaped grooved hole for IR imaging. Fig. 3 shows the Breast cancer screening setup using rotational thermography.

Data analysis techniques were crucial in breast cancer screening using thermal imaging. The data analysis techniques were integrated into the system at various stages of development to ensure optimal performance. Previous studies needed to integrate data collection protocols and analysis algorithms, resulting in suboptimal system performance. This study followed the intelligently designed data collection protocols to integrate with IR image processing techniques.

In the FS pilot study, a data collection protocol was developed to overcome limitations in previous studies. The IR image processing techniques were integrated into the data analysis process, where clustering methods were used to segment the images and extract the Region of Interest (ROI). K-means clustering was applied to other image features using the mean temperature of each ROI as a discriminative feature. The clustering method was optimized based on experimental validation with consulting doctors, and seven clusters were finalized for analysis. Fig. 4 shows the ROI of detected abnormality on IR breast images captured from different angles.

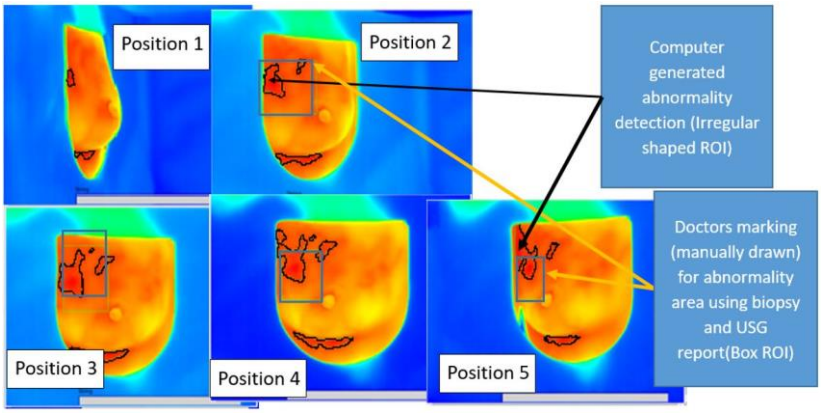

Fig. 5.4 : ROI of detected abnormality on IR breast images captured from different angles

Regarding IR image feature-based analysis, PS1 and PS2 conventionally analyzed IR images by extracting features such as mean, median, mode, standard deviation, histogram, and maximum value. However, no reference was made to IR images acquired via other modalities.

In the PS3 pilot study, the primary reference for analysis was ultrasound (USG) and biopsy reports obtained through other modalities. Clustering based on infrared images was used for segmentation, and the average temperature of each ROI was used as a discriminator. The clustering method was gradually improved, and seven clusters were finalized based on experimental validation by consulting doctors.

In the FS pilot study, the analysis was accomplished after integrating the temperature-controlled enclosure into the system. The differences in IR images acquired at different ambient temperatures were used as the key discriminating feature for analysis. This analysis technique effectively detected temperature variations associated with breast cancer.

The methodologies for cancer detection using IR imaging incorporated specific data collection techniques tailored for each pilot study. Modifications and optimizations were made to address challenges and improve imaging results. Integrating data collection protocols with IR image processing techniques ensured complete analysis at every stage of development.

By employing clustering methods, extracting key features, and leveraging temperature variations, these methodologies aimed to enhance the accuracy of breast cancer detection using IR imaging. Experimental validation and consultation with medical professionals were crucial in refining the techniques and achieving more reliable results.

Therefore, the methodologies for diabetes and cancer detection using IR imaging encompassed various steps, including imaging setup, data collection, IR image processing, feature extraction, and data analysis. These methodologies aimed to optimize the performance of the IR imaging system, contributing to accurate diabetic screening and early detection of breast cancer. Integrating machine learning algorithms and consultation with domain experts were critical in achieving more reliable and effective results in both research areas. Table 1 briefly details different aspects of the methodology and compares Infrared imaging-based Diabetes and cancer detection.

Table 5.1: Comparison chart of methodology used for Infrared imaging-based diabetes and breast cancer detection

Methodology	Diabetes Detection	Cancer Detection
Imaging Setup and Data Collection	A data collection setup was created at SRM Hospital and Cachar Cancer Hospital using an IR camera to capture images of different body regions. Image analysis was done using LabVIEW software.	Data collection techniques were employed in four pilot studies (PS1, PS2, PS3, and FS) for breast cancer screening—specific setups and modifications utilized for optimal data acquisition.
Temperature Control and Image Capture	Subjects were acclimated to a temperature-controlled room for 15 minutes. Skin temperature variations were captured in the range of 0.05°C to 0.1°C.	Various setups are used in different pilot studies. FS implemented rotational thermography with temperature variations.
Data Collection Plan	Two sessions: fasting blood sample collection and postprandial blood sample collection. Approximately 12 to 13 subjects per day.	Varied data collection techniques were used in different levels (PS1, PS2, PS3, and FS) of studies.
Infrared Image Processing Techniques	Manual, semi-automated, and full-automated ROI selection methods. Image processing algorithms (thresholding and morphological operations) were used.	Integration of data collection protocols and analysis algorithms. IR image processing techniques are integrated at every stage of development. Clustering methods were used for segmentation and ROI extraction.
Analysis and Information Extraction Techniques	Thresholding and shape-based object tracing techniques were employed. Temperature values are stored for further analysis.	IR image-based clustering is used for segmentation. The mean temperature of ROI was used as the discriminating feature.

Feature Extraction Techniques	Generalized "Hough Transform" algorithm used for geometric shape features. Statistical image analysis algorithm recorded various features. Extraction of features like mean, median, mode, standard deviation, and histogram. Gradual improvement and finalization of the clustering method.	Feature extraction based on mean temperature and clustering methods. Seven discrimination clusters have been extracted.
Machine Learning Classification	Statistical features used as input for machine learning algorithms. The SVM algorithm demonstrated better classification accuracy.	Analysis based on IR image features and discrimination using clustering for machine learning algorithm (SVM) is used.
IR-Image Feature-Based Analysis Technique	Statistical Features (mean, median, mode, standard deviation, and maximum value) were extracted.	Integration of temperature-controlled enclosure. Differences in IR images acquired at different ambient temperatures are used as discriminating features.
Overall Aim	Development of diabetic screening system using non-invasive, no touch method for improved medical diagnostics and early disease detection.	An intelligently designed data acquisition protocol and integration with infrared imaging technology achieve optimal system performance for breast cancer screening.

5.3 Results and Discussion

The study highlights the potential of IR imaging-based diabetes screening where the ear cavity zone takes a significant role and the potential of IR imaging-based screening systems in detecting breast cancer. The research shows that advances in data collection techniques, image analysis, and machine learning algorithms can improve accuracy and efficiency.

5.3.1 Diabetes Screening using IR Imaging

The research studied 243 human subjects from different diabetic camps in India. The data was collected with SRM Medical College Hospital and Cachar Cancer Hospital. Ethical clearance was obtained from the ethics committee, and informed consent was obtained from all subjects. The study group comprised 129 males and 114 females aged between 19 and 91.

5.3.2 Feature Extraction and Classification

A statistical image analysis algorithm was developed for the "infrared image analysis module." The algorithm automatically plots the mean, standard deviation, median, mode, skewness, kurtosis, moments, root mean square (RMS), entropy, energy, and maximum temperature values of a Region of Interest (ROI) on an infrared image as statistical value. These statistical values are considered as discriminators for classification using machine learning algorithms.

5.3.3 Gender-Specific Classification

The three most significant features for males were identified as Standard Deviation, Mean, and Root Mean Square (RMS), while they were different for females. As a result, separate machine learning algorithms were developed for classifying males and females. The experimental database determined the best features based on blood biochemical reports and infrared image output. It was observed that changes in the database might interchange the ranking position of features, but the basic algorithm remained the same.

5.3.4 Thermal Profile Distribution

The thermal profile distribution of diabetic and non-diabetic patients were compared in specific body regions, including the inner canthus points (Eye), ear, palm, cavity, and inner posterior buccal cavity (Mouth). The temperature difference between diabetic and non-diabetic subjects was approximately 0.5 degrees centigrade. These findings supported previous research using thermography for diabetic patients, prompting further optimization of body regions for

better results; here, the earlobe shows a significant differentiation between diabetic and non-diabetic subjects.

5.3.5 Classifier Performance

A population-based cross-sectional and case-control study was conducted to evaluate the performance of the diabetes screening system. Sensitivity, specificity, positive predictive value (PPV), negative predictive value (NPV), accuracy, false negative rate (FNR), false positive rate (FPR), and diagnostic odds ratio (DOR) were calculated for each study group. The overall accuracy rate of Diabetes screening with fasting data was 70.62%, and that of Diabetes screening with postprandial data was 67.08%. Table 2 shows the results of the diabetes screening study phase of a population-based cross-sectional and case-control study of fasting and PP.

Table 5.2: Comparison of Results from Each Study Phase for diabetes screening

	Population-based fasting cross-sectional and case-control studies (243 subjects)	Population-based PP cross-sectional and case-control studies (243 subjects)
Sensitivity (%)	53.968	53.846
Specificity (%)	81.443	76.344
Positive predictive Value (PPV)%	65.385	61.404
Negative predictive value (NPV)%	73.148	70.297
Accuracy (%)	70.625	67.089
FNR	46.032	46.154
FPR	18.557	23.656
LR+	2.908	2.276
LR-	0.565	0.605
Diagnostic Odd Ratio (DOR)	5.146	3.765

5.3.6 Breast Cancer Detection using IR Imaging

A novel non-contact and non-invasive breast imaging method was developed for breast cancer detection. This method captured all abnormalities presented by the subjects and introduced a rotational thermography setup for better visualization of the affected area.

5.3.7 Data Collection and Analysis

Data was collected from four pilot studies where PS1 was for 71 subjects, PS2 was done on ten subjects, PS3 was done on 37 subjects, and the final study (FS) was done on 119 subjects. A double-blind test was conducted during PS3 to FS. Clustering techniques were done using K-median, and a support vector machine (SVM) learning algorithm was used for feature extraction and classification.

5.3.8 Classifier Performance

The accuracy of the developed system for screening breast abnormalities and detecting malignant tumours was 93.27% for the FS data set. The sensitivity and specificity were 86.67% and 97.30%, respectively. These results demonstrated the effectiveness of the proposed IR image acquisition and analysis technique for breast cancer detection. Table 3 shows the Results from the Study Phases for the Breast Cancer screening system for Population-based cross-sectional and case-control studies PS3 and FS.

Table 5.3: Comparison of Results between PS3 Study Phases and FS for Breast Cancer screening system

	Population-based PS3 cross-sectional and case-control studies (37 subjects)	Population-based Final System FS cross-sectional and case-control studies (119 subjects)
	Female	Female
Sensitivity (%)	90.00	86.67
Specificity (%)	82.61	97.30
Positive predictive Value (PPV)%	69.23077	95.12
Negative predictive value (NPV)%	95	92.30
Accuracy (%)	84.84848	93.27
FNR	10	13.33
FPR	17.3913	2.70
LR+	5.175	32.06
LR-	0.121053	0.13
Diagnostic Odd Ratio (DOR)	42.75	234

Therefore, the research presents promising results for diabetes screening and breast cancer detection using IR imaging. Advanced image processing and machine learning approaches offer accurate and efficient medical diagnoses, indicating the potential for clinical

applications in the future. Further research and optimization of the proposed method could improve healthcare and early detection of diseases.

5.3.9 Discussion

The approach presented in this study provides insights into infrared imaging for diabetes screening and breast cancer detection. The findings contribute to developing a comprehensive framework for data acquisition and automated analysis methods and illustrate the importance of joint research in medical thermography.

5.4 Conclusion

In conclusion, it reflects the validation of infrared imaging as a promising tool for thoroughly screening Diabetes and breast cancer. It emphasizes the potential of automated image processing and machine learning techniques to enhance the accuracy and efficiency of infrared image-based systems for medical diagnosis. The discussion emphasizes the necessity for further studies to validate and refine this all-inclusive approach, advocating for the development of standardized protocols and extensive clinical trials to determine the effectiveness and reliability of infrared imaging in diabetes screening and breast cancer detection. Additionally, it highlights the imperative of addressing challenges related to quantifying malignancy temperature levels and ensuring the training of qualified healthcare professionals in using infrared imaging techniques.

The subsequent chapter delves into a detailed exploration of efficient infra-red image processing and machine-learning algorithms for breast cancer screening. It delves into the significance of non-invasive imaging techniques, particularly thermal imaging, in the context of early breast cancer detection. The chapter features the diverse approaches employed in developing efficient breast cancer screening software by drawing on various studies focusing on diverse methodologies, such as feature extraction, image segmentation, and deep learning techniques. Furthermore, it highlights incorporating rotational thermographic imaging, colour-based infrared image processing, and machine learning algorithms to create a non-invasive and no-pain breast cancer screening system. The chapter's emphasis on data collection, image processing, and machine learning highlights the importance of an integrated approach in achieving accurate and efficient results in the context of breast cancer screening.

Chapter VI

Efficient Infra-Red Image Processing and Machine Learning Algorithm for Breast Cancer Screening

6.1 Introduction

Breast cancer is a significant global health concern, and early detection is crucial for improving survival rates. This article examines non-invasive imaging techniques for breast cancer detection, focusing on thermal imaging. The article reviews studies investigating different methods for detecting breast cancer using thermal imaging, including feature extraction, image segmentation, and machine learning. It concludes that developing efficient and accurate breast cancer screening software requires an integrated approach to data collection, image processing, and machine learning algorithms [50].

Additionally, the article presents an innovative technique for developing breast cancer screening software using Rotational Thermographic Imaging, Color-based Infrared Image Processing, and a Machine Learning algorithm. The proposed system aims to provide a non-invasive and comfortable way for patients in sitting positions with complete breast imaging, thereby reducing the chances of missing abnormalities.

The proposed breast cancer screening method employs dynamic temperature-based data collection and rotational thermography. Image processing and machine learning techniques extract relevant features from the captured images. A broad dataset of thermal images was amassed, and relevant features were extracted and used to train a machine-learning model. The developed screening system was tested on an increasing patient population in a clinical setting deployed at a hospital. The algorithm's performance was evaluated using several metrics, including sensitivity (82.14%), specificity (98.33%), and accuracy (93.27%). The results demonstrate that the proposed algorithm achieved high accuracy and sensitivity, making it a promising tool for breast cancer screening.

6.2 Methodology and Algorithm

The present study proposes an innovative method for detecting breast cancer using infrared imaging. The data collection involves dynamic temperature-based data collection and rotational thermography using an Infrared camera in a semi-circular arc on an arm-based arrangement, with 32 thermal IR images captured for each subject. A table top mechanical arrangement focuses on

one breast at a time, and the other breast is isolated from the camera view by covering it with an infrared-proof barrier.

6.2.1 Data collection system with hardware and software interface

The data collection unit developed is a tabletop unit with a semi-circular template hole grooved on the front wall. The subject sits in front of the unit, and one breast is placed in the template opening. The Infrared Camera is positioned 1 meter away, the minimum focal length of the Infrared Camera (Infratec Variocam) used here. The IR camera position can be changed to 180 degrees by maintaining the same distance from the focused breast and pointing towards it. The Infrared images are collected in 7 positions for each breast, named 0° (IR image 1), 30° (IR image 2), 60° (IR image 3), 90° (IR image 4), 120° (IR image 5), 150° (IR image 6), and 180° (IR image 7) for the right breast and 180° (IR image 8), 150° (IR image 9), 120° (IR image 10), 90° (IR image 11), 60° (IR image 12), 30° (IR image 13), and 0° (IR image 14) for the left breast. During the data collection, the 90° (IR image 4) position of the right breast and 90° (IR image 11) position of the left breast are analyzed in real-time to extract the mean body temperature. The ambient temperature is then varied to change breast temperature by 2°C, and another set of IR images is collected in the same positions. This data collection process is referred to as dynamic Infrared Imaging.

6.2.2 Interface for doctor's marking on ROI with clinical validation

The data is collected in a hospital environment in an air-conditioned 10'X12' room. The patient reports to a registration desk, where the patient's history and other details are recorded in a questionnaire form. Then, infrared, USG, /Mammography images are collected individually, maintaining all the necessary precautions for each modality. A clinical summary report is prepared using the doctor's advice, and all the records are stored in a proper database or file. A software interface is developed to mark each suspected image to assist doctors. Doctors mark malignant areas on the IR images based on USG/mammography and biopsy reports (Figs.6.7 and 6.8). The overall picture of IR imaging-based data collection analysis and decision-making is shown in Fig 6.1 as an example.

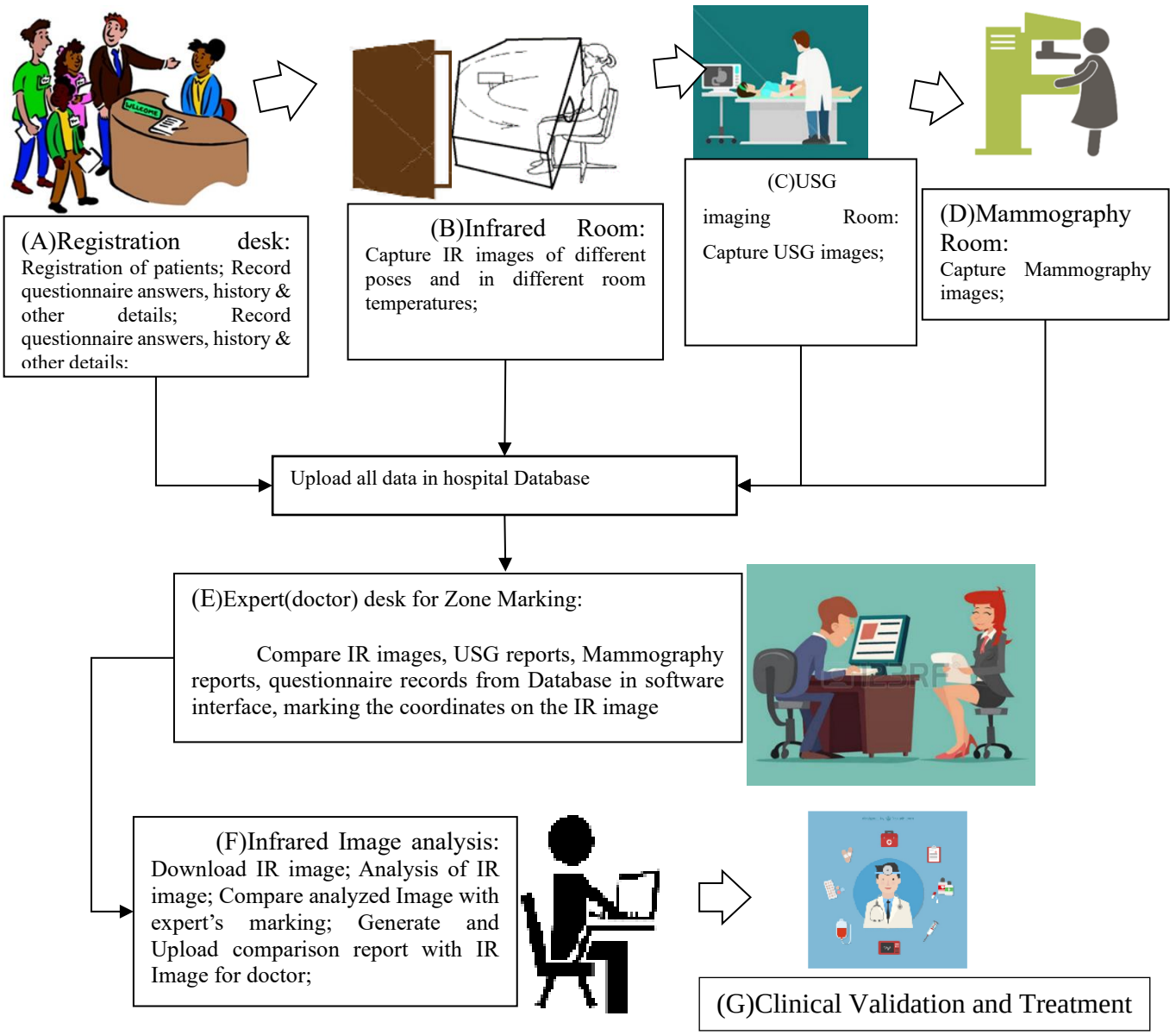

Fig. 6.1: IR imaging-based data collection, analysis and decision-making

6.2.3 Data analysis with Image processing and Machine Learning techniques

The first step was to collect a large dataset of breast thermal images using an infrared camera that captures the temperature distribution on the surface of the breast. These images were carefully selected to ensure that a wide range of variables, such as age, race, and breast size, were represented in the dataset.

Once the images were collected, the next step was to pre-process them using various image processing techniques to correct for artifacts such as noise, distortion, and non-uniformity. These

pre-processing steps may vary depending on the application and the characteristics of the analyzed images. However, some standard techniques include image enhancement, noise reduction (GLCM or Wavelet techniques both can be used in this case; Wavelet techniques have been used), image segmentation, image registration, and background subtraction. The overall steps of IR Image analysis with Image processing and Machine Learning techniques are shown in Fig 6.2. These steps were designed to ensure the accuracy and quality of the data analyzed during the pilot study phases and supported by the feedback of the concerned experts and doctors. The Image Segmentation Algorithm developed for abnormality detection (Fig 6.3) is an innovative technique for extracting features, which have been discussed in detail in the following sections.

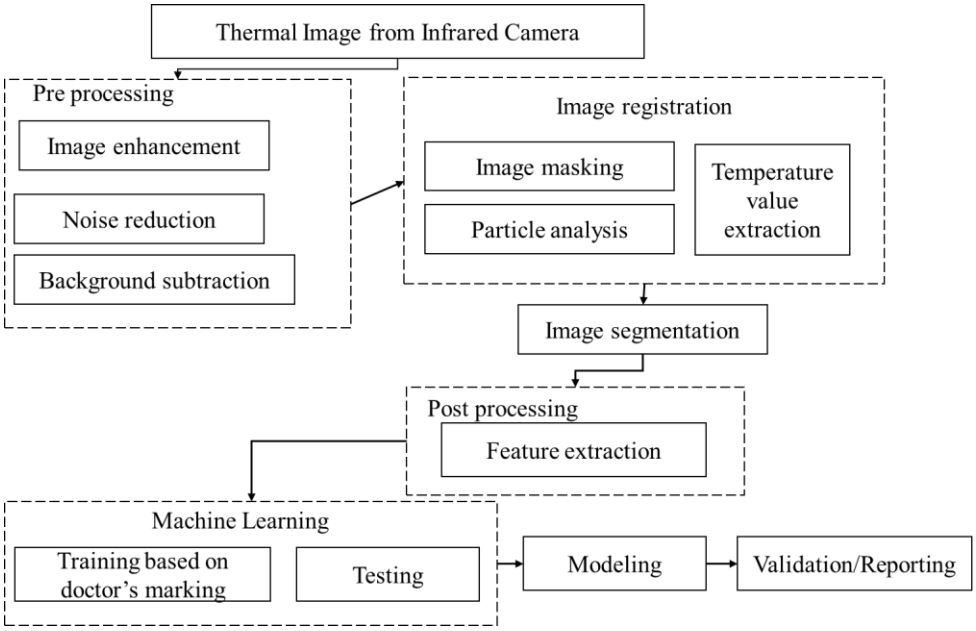

Fig. 6.2 : IR Image analysis with Image processing and Machine learning techniques

After preprocessing, relevant features were extracted from the thermal images using feature extraction techniques and statistical analysis. These features were carefully selected based on their potential to identify patterns that may indicate the presence of breast cancer. The extracted features were then used to train a machine-learning model on the dataset.

Selecting an appropriate machine learning algorithm was an essential step in this process, as different algorithms have varying levels of accuracy and speed. In addition, hyperparameters were optimized to improve the machine learning model's performance, and the dataset was split into training and validation sets to ensure the model's accuracy.

Once the model was developed, it was tested and validated on a separate test dataset, evaluating various performance metrics such as accuracy, sensitivity, specificity, and area under the curve (AUC). The developed breast cancer screening system was then implemented in a clinical setting by testing the system on a larger patient population, integrating it with existing clinical workflows, and validating its performance against established standards.

The Infrared Image capturing tools were developed using LabVIEW (Laboratory Virtual Instrument Engineering Workbench) image processing and vision development module with a Thermovision toolkit provided by FLIR with an Infrared image-capturing device and one Software Development Kit (SDK) provided by Infratech Variocam. The infrared image differs from the superficial image data as the images are separated into temperature data and image files. The image file is used for body part tracking and extracting the masked image for further use, as shown in Fig 6.4 and Fig 6.5. The captured IR image is analyzed using image processing tools in Labview.

6.2.4 Development of software Algorithm for breast abnormality detection

In their literature, Krithika Venkataramani, Lalit K. Mestha, L. Ramachandra, S.S. Prasad, et al. showed semi-automated cancer tumour detection on IR using colour-based tumour location. They used the unsupervised k-means algorithm to obtain three colour clusters from the chromaticity of the L*a*b* colour space, i.e., on the a*b* layers (M. Etehad Tavakol et al. [8]. A similar algorithm has been developed using the LabVIEW environment.

During the development, another algorithm was necessary to develop for tumour detection. The algorithm is inspired by "Brain Tumour Detection Using Colour-based K-Means Clustering Segmentation'" by M.N. Wu et al. [48]

The overall algorithm was developed by combining these algorithms, as shown in Fig 6.3.

A greyscale tumour image to colour image conversion from pseudo colour reference, detecting tumours using the k-means clustering algorithm, was developed.

Necessary modifications have been made to implement the "tumour detection algorithm of 8-bit greyscale MRI image" Pramanik et al. implement in 16-bit IR images for breast tumour detection.

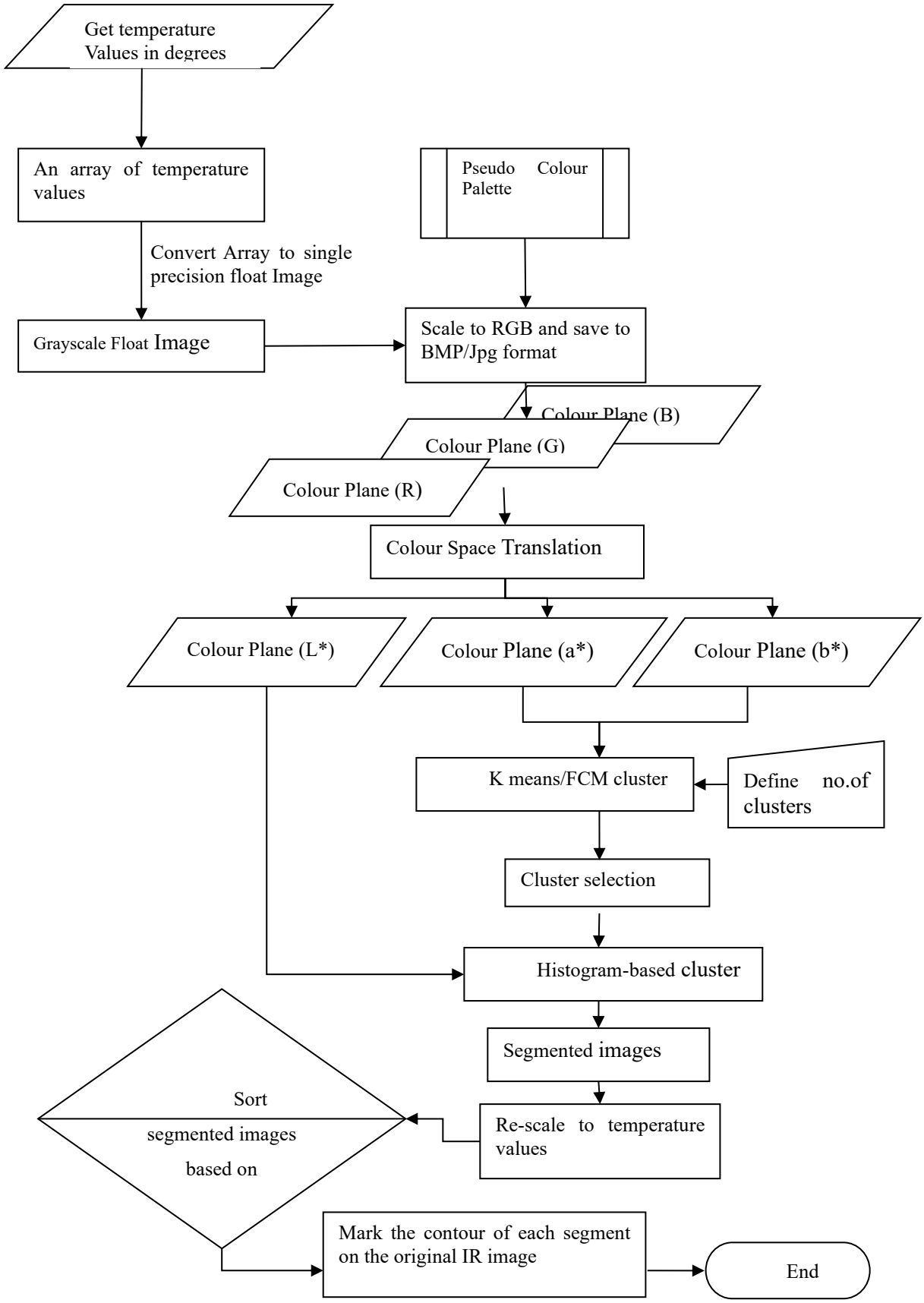

Fig. 6.3 : Algorithm developed for abnormality detection

A Virtual Instrumentation-based Infrared Image analysis program is developed. A greyscale tumour image to colour image conversion from pseudo colour reference, detecting tumour using FCM (Fuzzy C-Means) clustering algorithm, was developed. The algorithm is inspired by "Brain Tumour Detection Using Colour-based K-Means Clustering Segmentation'" by Ming-Ni Wu et al . The tumour detection algorithm is developed using the "tumour detection algorithm of 8-bit greyscale MRI image". Here, an 8-bit greyscale MRI Image was modified to implement it in a 16-bit IR Image. The same was improved by replacing k means with FCM clustering techniques. Their "Centroid" values sort the clusters. The highest Centroid value is the Region of Interest of our algorithm. Accordingly, all the images formed by the clusters are also sorted and processed further. The clustered images are used as "Mask images" in further Image processing. The outer region of extracted masks is used as an outline of a particular clustered temperature zone, which in turn is used to extract the mean temperature and corresponding area of the zone, as depicted in Fig. 6.6 and Table 6.1. These values are used as features of a particular temperature zone in the Machine Learning algorithm, which is discussed later. The following image reflects FCM-based clusters and corresponding masks in Infrared images.

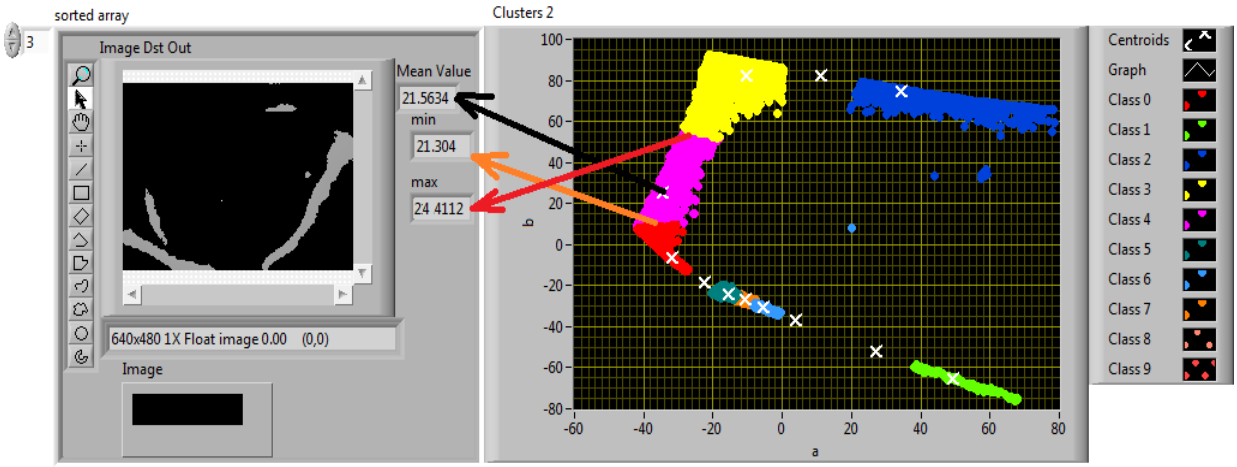

Fig. 6.4: Extracting the masked image

If a pixel in the image mask has a non-zero value, the corresponding pixel in the inspection image is processed, and it is not processed otherwise. Therefore, here, the outline of the ROI is non-uniform and can be of any size. For this reason, the Mask-based outline algorithm has been developed as a background using the LabVIEW Vision Development Module. In Fig. 6.5 below, one Mask and the corresponding Region of Interest are drawn in the software interface on the IR images.

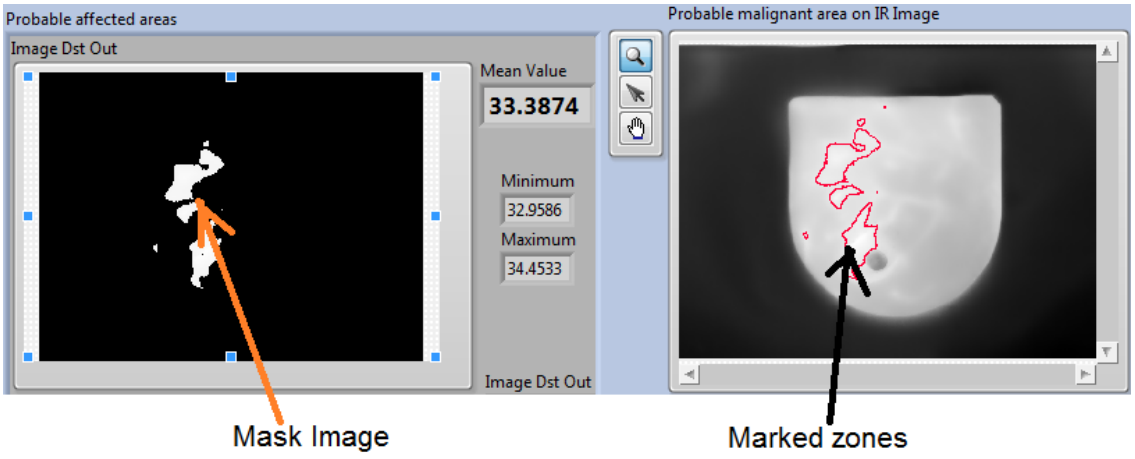

Fig. 6.5 : Infrared image masking: extracting the temperature from the subject area

The temperature values of the corresponding masked image are used as features in this system. In addition, the masked images are the root of the temperature cluster zones, used as features for machine learning algorithms during IR image analysis.

The number of pixels of each Mask corresponding to every zone of the temperature cluster has been recorded. The number of pixels is the "area" of a particular zone. The total number of pixels in an image is 640 X 480. If a particular zone has 7962 pixels, it is spread over a 2.59 per cent image area. The distribution of different area zones that correspond to different temperatures in bar plots of four defined colours is shown in Fig 6.6.

The colour bars have also been defined to reflect the severity of temperature formation due to abnormalities. In each coloured plot, the top plot shows the percentage area of a particular temperature zone in the lower plot. In addition, the mean temperature value of each zone has been recorded in a database for each subject.

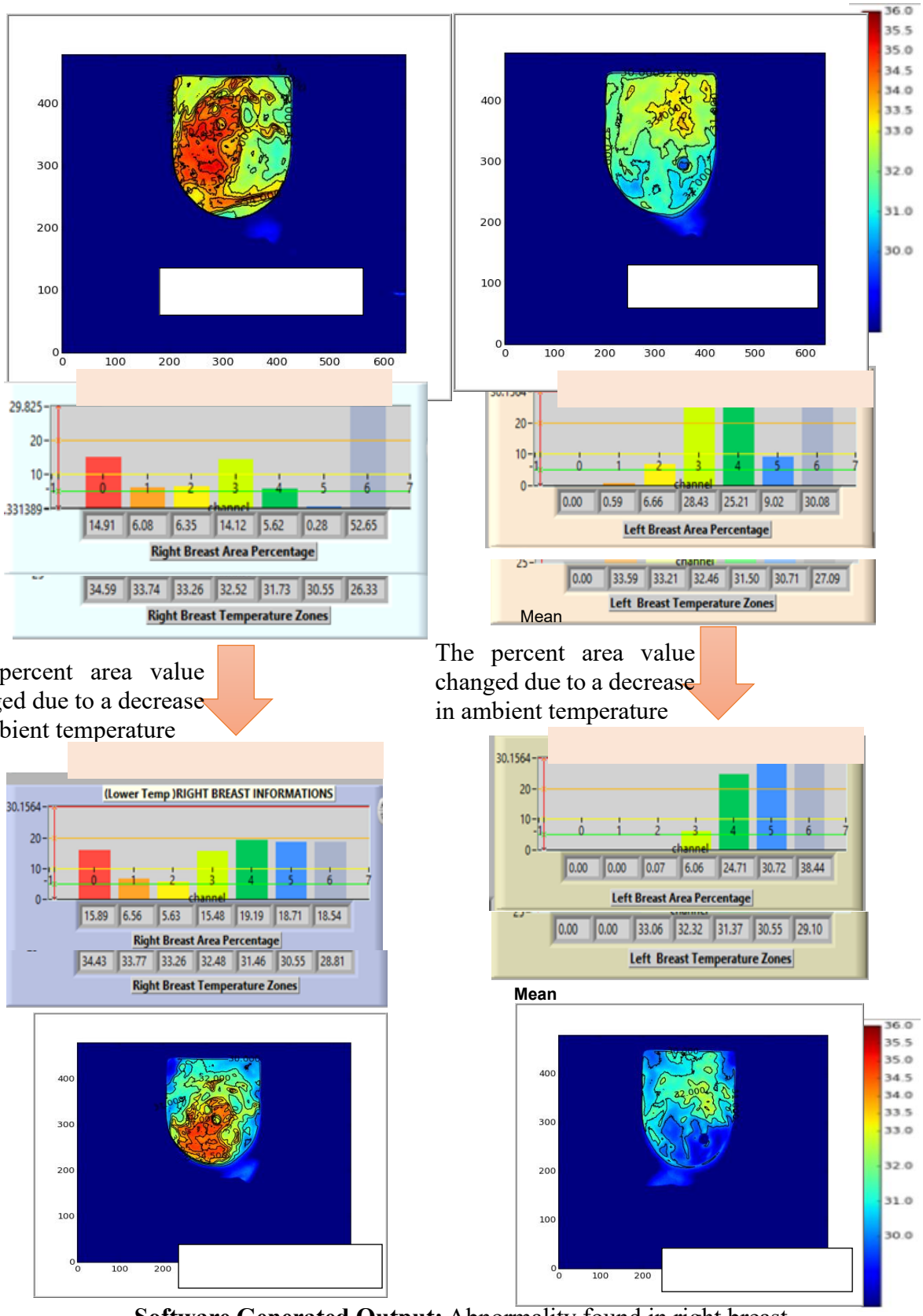

Software Generated Output: Abnormality found in right breast

Fig. 6.6 : Plotting for distribution of different area zones in different colour codes

Fig 6.6 includes screenshots demonstrating the front viewing angle of a subject, accompanied by an area-temperature bar plot. The bar plot illustrates the distribution of different area zones using different colour codes based on the analysed IR images of the left versus right breast with varying ambient temperatures. Fig 6.7 shows a sample Clinical report with doctor's remarks, and Fig 6.8 shows the software interface for Doctor's Manual Marking vs. Automatic Marking by Image Analysis software.

6.2.5 Clinical summary

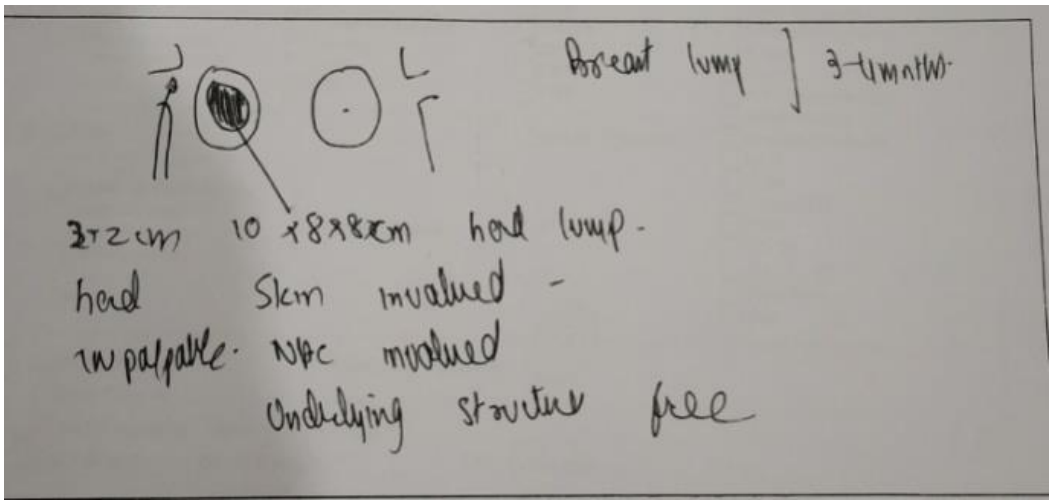

Fig. 6.7: Sample Clinical report with doctor's remarks

Doctor's remarks: Cancer on Right Breast, Left Breast is normal.

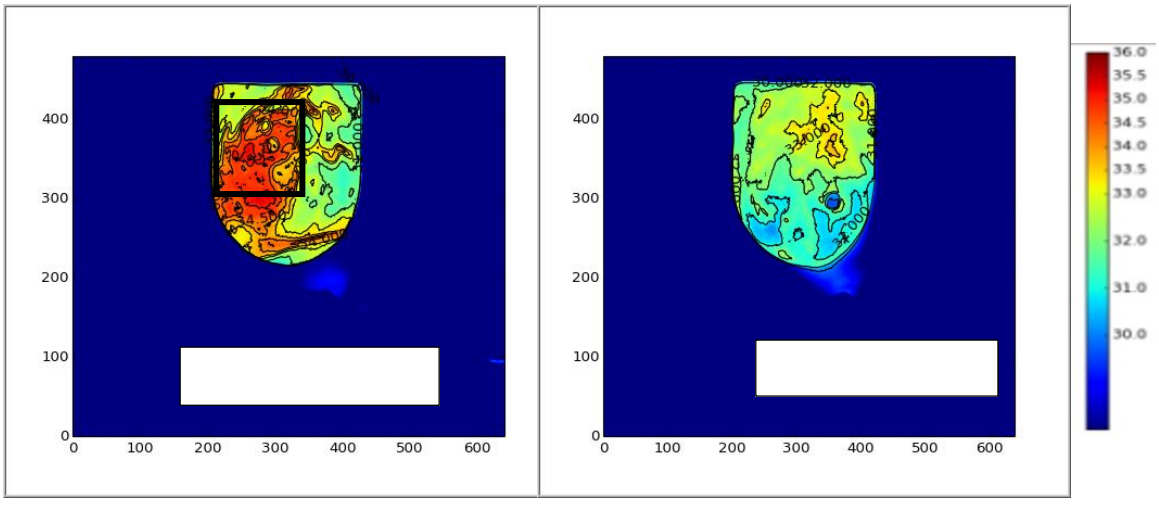

Fig. 6.8: Doctor's Manual Marking vs. Automatic Marking by Image Analysis Software

Doctor's manual marking on Breast Images based on USG/ Mammography :(Box marking on right breast Image)

6.2.6 Development of Machine Learning model

The database is created for all images of each subject and is trained with the Machine Learning algorithm Fig 6.9. The mean temperature of each ROI has been used as a discriminating feature interpreted as different body temperature zones. IR-image FCM clustering method is used at this stage for the clustering of features [48] [18],[17]. Improvement of the clustering method has gradually optimized the number of clusters from 20 to 7 based on the experimental validation by the concerned doctor's marking, which was related to the actual abnormality found in the USG and Biopsy reports. These 7 clusters have been used as features in machine learning algorithms for further processing. The clustering technique was improved from K-means to FCM for optimization in the number of clustering. Fuzzy C-Means (FCM) is a clustering algorithm that belongs to the category of fuzzy clustering methods. It is used to partition a dataset into a predefined number of clusters based on the similarity of the data points within each cluster. In FCM, each data point is assigned a membership value for each cluster rather than a crisp assignment to a single cluster. It allows overlapping clusters and a data point to belong to more than one cluster. The membership values are calculated using a fuzzy membership function, which assigns a membership degree to each cluster data point. The FCM algorithm iteratively adjusts the membership values and cluster centroids to minimize the objective function, which measures the error between predicted and actual cluster assignments. The algorithm stops when the error reaches a predetermined threshold or when a predetermined number of iterations has been reached. Here, each mask image is considered a cluster, and the predicted centroid membership is the mean temperature of the corresponding cluster. The predefined number of clusters was considered as 7.

For machine learning, an NN (Neural Network) based back propagation learning algorithm has been implemented [9] [19] [15]. The backpropagation algorithm is a supervised learning algorithm to train artificial neural networks. The error between the predicted output and the desired output is minimized by adjusting the weights and biases of the connections. The backpropagation algorithm works by feeding an input through the network, calculating the output, comparing the output to the desired result, and then adjusting the weights and biases of the connections between the neurons in the network to reduce the error between the predicted output and the desired output. It is repeated for each input in the training dataset, and weights and biases are updated after each iteration. The backpropagation algorithm is an iterative process. The weights and biases are updated until the error between the predicted and desired output is minimized until the error reaches a predetermined threshold. Once the training is complete, the network can predict new

data. In the NN-based algorithm, extracted values of 7 clusters were used as input for 3 Hidden Layers, and outputs were rated as abnormal and normal for Malignant and Benign subjects.

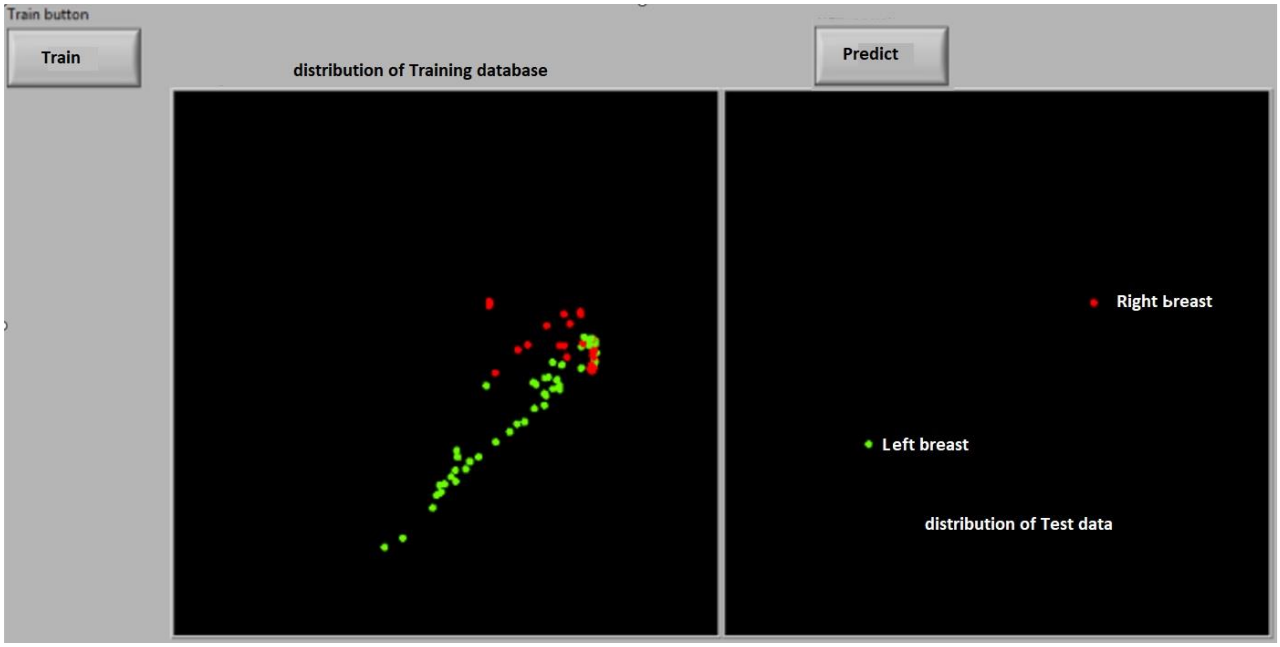

Fig. 6.9 : Screenshot of Prediction module using Machine Learning Algorithm

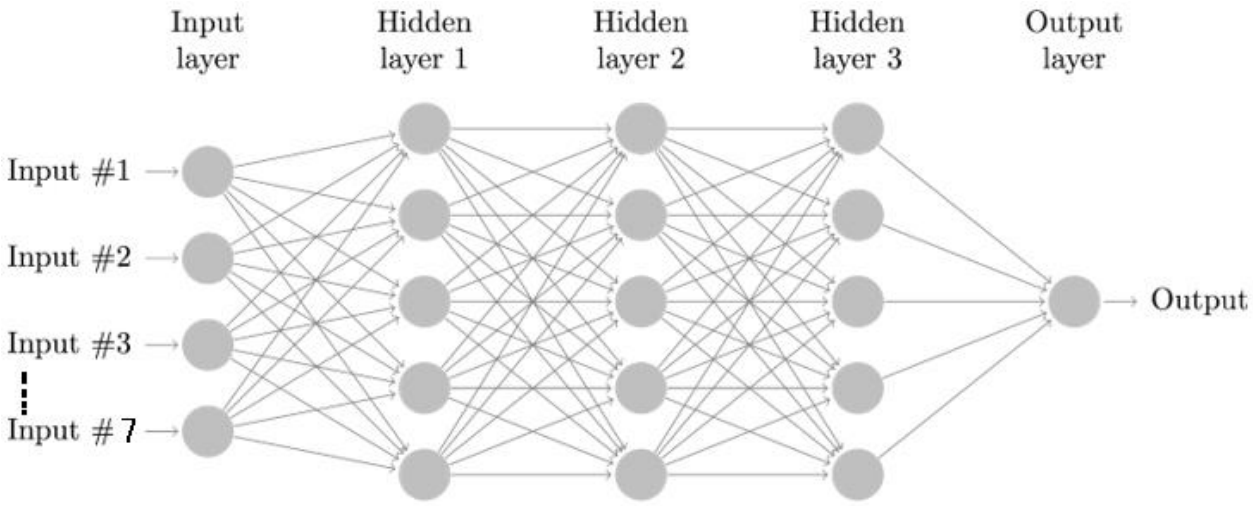

Fig. 6.10: Conceptual diagram of BP Neural network module used

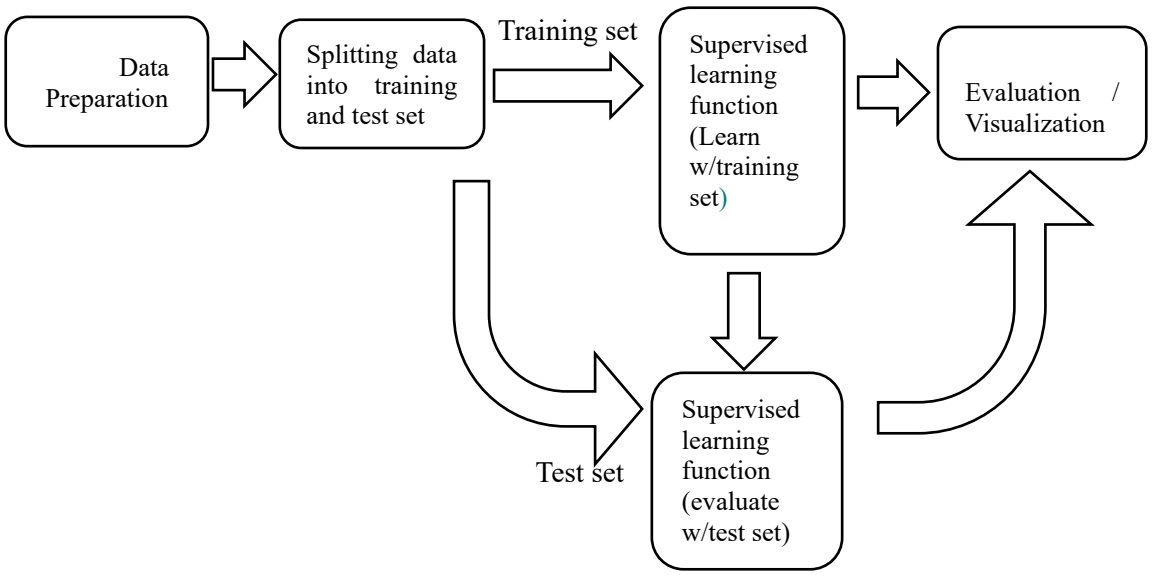

Fig. 6.11: Conceptual diagram of the Machine Learning Toolkit for supervised learning implemented in the LabVIEW environment

A prediction module has been developed in a virtual instrumentation environment for a subject corresponding to Right and left images, which shows the abnormal and normal images concerning the current training database for a new Infrared image. A Screenshot of the Prediction module using a Machine Learning Algorithm is shown in Fig 6.9. The Conceptual diagram of the Back Propagation Neural network module used here is shown in Fig 6.10. Finally, a Conceptual diagram of the Machine Learning Toolkit for supervised learning used in the LabVIEW environment is shown in Fig 6.11.

6.3 Results and Discussion

This part of the thesis has analyzed two sets of collected data.

The first data set was collected during the 'Pilot Study ' of 33 subjects. Afterwards, modifications were made to the data collection protocol, ROI extraction, and IR image analysis techniques. The second set of data for the final study consists of 119 subjects.

Thirty-three (33) subjects at two different room temperatures were collected during the pilot study. The datasets were analyzed and validated for performance measures under the guidance of Oncologists using the double-blind testing method. In addition, a lab view-based program has been developed for analyzing infrared images and temperature using doctor's markings and ultrasound

reports as a reference. Six (6) subjects showed probable abnormalities. The confusion matrix for the training and testing dataset is depicted in Fig. 6.12.

In Fig. 6.12, the first two diagonal cells show the trained network's number and percentage of correct classifications. For Pilot study cases,19 subjects are correctly classified as benign, and 9 are correctly classified as abnormal among 33 total cases (Table 6.1).

Table 6.1: Prediction percentage from output class of Pilot Study using the developed algorithm

Sl. no	Study name	A pilot study (33 cases)	
	Case type	Benign	Malignant
	Type of subjects from Clinical summary	23	10
	Correctly classified using the developed algorithm	19	9
	Misclassified using the developed algorithm	4	1
	Percentage of Correctly classified in overall cases	82.60%	90.00%
	Percentage of misclassification in overall cases	17.40%	10.00%

The image below reflects the output of the Neural Network Pattern Recognition tool depicting classification results on the said database. Fig. 6.12.

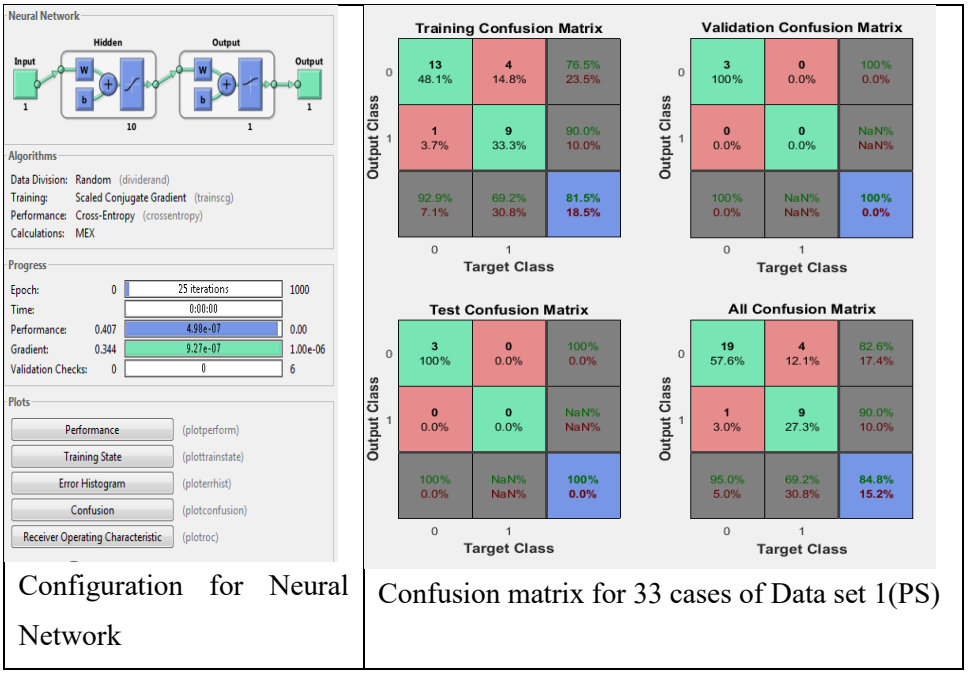

Configuration for Neural Network

Confusion matrix for 33 cases of Data set 1(PS)

Fig. 6.12: NN-based classification result for breast abnormality detection.

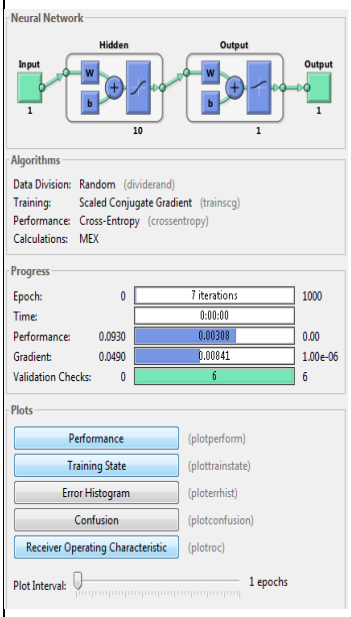

Configuration for Neural Network	Confusion Matrix for 119 cases of the final dataset

Fig. 6.13: Neural Network-based classification result of training and testing dataset for breast abnormality detection for Final Dataset.

During the Final Study, data were collected from 119 subjects. First, the data collection system was improved by introducing a rotational dynamic data collection unit in a temperature-controlled enclosed chamber and using an improved image processing algorithm. Then, for machine learning, an NN-based back propagation algorithm was implemented.

For comparison between the pilot study (PS) and the final study dataset, these 119 subjects' data were also processed in neural network-based classification. Where confusion matrix Fig. 13 shows improved performance with 93.27% accuracy.

In Fig. 13, the first two diagonal cells show the trained network's number and percentage of correct classifications. For the final study cases, 72 subjects are correctly classified as benign, and 33 are correctly classified as abnormal out of 119 subjects (Table 6.2).

Table 6.2: Prediction percentage from output class of Final study using the developed algorithm

Sl.no	Study name	The final study (119 cases)	
1	Case type	Benign	Malignant
2	Type of subjects from Clinical summary	72	39
3	Correctly classified using the developed algorithm	70	33
4	Misclassified using the developed algorithm	2	6
5	Percentage of Correctly classified in overall cases	97.3%	86.7%
6	Percentage of misclassification in overall cases	2.7%	13.3%

The performance in recognition can be evaluated by the following factors: Accuracy (AC), Sensitivity (SE), and Specificity (SP) of detection. They are defined as follows:

1. Classification accuracy is dependent on the number of samples correctly classified.

$$AC = \frac{TP + TN}{TP + FP + TN + FN} \tag{6.1}$$

2. Sensitivity is a proportion of positive cases well detected by the test.

$$SE = \frac{TP}{TP + FN} \tag{6.2}$$

3. Specificity is a proportion of negative cases well detected by the test.

$$SP = \frac{TN}{TN + FP} \tag{6.3}$$

Where TP is the number of true positives, FP is the number of false positives, TN is the number of true negatives, and FN is the number of false negatives.

The following table shows the result of the Performance Analysis of Data set 1(PS) vs. Dataset 2(Final study dataset) of collected IR image data from Cachar Cancer Hospital Silchar, Assam.

Performance Analysis of Data set 1(PS) vs Dataset 2(Final study dataset):

Table 6.3: Population-based case-control Study on PS for 33subjects vs. final study for 119 subjects

Diagnostic Information	Number of Cases: 33(Pilot Study dataset)	Number of Cases: 119(Final study Dataset)
TP	9	39
TN	19	72
FP	4	2
FN	1	6
Sensitivity	90.00	86.67
Specificity	82.61	97.30
Accuracy	84.84	93.27

The system design and developed algorithm are unique, so comparing the system with other researchers' output is difficult. This part of the thesis compares the work from earlier designs to the final design.

The accuracy of the pilot study was 84.84%, which improved with the modified data collection procedure and data analysis algorithm for the Final system to 93.27 % for screening of breast abnormality and detecting malignancy (Table 4). Further, note that the number of data sets in the final study is more significant than in the pilot study. The study encountered some challenges, such as a small initial sample size, which was later expanded to 119 subjects for the final study, and a limited geographical scope restricted to a hospital in the North Eastern state of India, as well as a lack of diversity in terms of age, race, and ethnicity. In addition, there was potential human error during data collection, image processing, and analysis, as well as a lack of long-term follow-up, which may impact the generalization, applicability, and effectiveness of the study findings and developed algorithm. However, I plan to address these limitations in future follow-up studies to enhance their research quality further. The system is installed in a hospital in the NE state of India, where mass-level screening, as well as validation of output of the IR-based system, is done using biopsy reports for final product deployment. The system's performance for the Final study dataset with innovative image acquisition and analysis techniques has produced better results, which were vetted by the doctors.

6.4 Conclusions

Using Infrared imaging for breast cancer detection is an innovative, non-invasive, and no-touch system. The breast cancer screening system uses Rotational Thermographic Imaging, Color based on infrared image processing, and Feed Forward Backpropagation classifier in Machine Learning. The key concept in this system is to offer a technique for complete breast imaging, leading to fewer chances of missing an abnormality with the best comfort of a subject in a sitting position and a non-contact, non-invasive way. The developed software is already copyrighted. Moreover, the system is deployed in Cachar Cancer Hospital, Silchar, for regular data collection. This part of the thesis introduces this unique method for developing Breast cancer screening software using Rotational Thermographic Imaging, Colour-based infrared image processing, and Machine Learning algorithms. This part of the thesis compares the work from earlier designs to the final design. The accuracy of the pilot study was 84.84%, which improved with the modified data collection procedure and data analysis algorithm for the final system to 93.27% for screening of breast abnormality and detecting malignancy. Further, note that the number of data sets in the final study is more significant than in the pilot study. The system is installed in a hospital in the NE state of India, where mass-level screening, as well as validation of the output of the IR-based system, is performed regularly. The results show encouraging outputs toward developing a system that can be integrated by the developed software using the algorithms used in this part of the thesis. Moreover, the satisfaction of the concerned oncologists made this part of the thesis relevant and valuable to the common mass towards the development of breast cancer screening devices and deployment all over India.

Ethical Information

The study was done and approved by CCHRC and the number is : CACHAR CANCER HOSPITAL AND RESEARCH CENTRE IRB/Ethics Committee bearing approval number CCHRC/IRB/01/2019/254

Chapter VII

Conclusion and future work

7.1 Conclusion

The principal objective of this work is to explore the use of infrared (IR) thermal imaging techniques for monitoring and screening critical human ailments in a non-invasive way. This research activity has explored the possibilities of establishing a new marking in stress assessment, diabetes level tracking, breast cancer screening, and oral cancer detection by employing the potential of InfraRed (IR) thermal imaging methodologies.

The systematic exploration of the elaborate interaction between stress patterns, physiological responses, and thermal profile distributions has illuminated new pathways for personalized patient care and enhanced disease management. The research has provided an opportunity to explore the underlying mechanisms of human physiological responses to stress by deciphering the complex relationship between stress-induced autonomic nervous system responses and subtle variations in skin perfusion.

By integrating advanced image processing algorithms and new machine-learning techniques, the research has established a robust framework for the automated identification and precise delineation of Regions of Interest (ROIs) in IR images. This research demonstrates a commitment to developing precise, efficient, and user-friendly medical diagnostic solutions.

The study has been made to achieve precise and accurate medical diagnoses by utilizing advanced data acquisition systems, intelligent feature extraction, and pattern classification systems. Integrating the Genfis property within the diagnostic system has played an important role in enhancing the system's robustness and adaptability, so much necessary within clinical settings.

Developing and fine-tuning the infrared imaging-based system required meticulous consideration of the sample objects' imaging distance, angle, and height. Accurately calibrating the IR imaging format ensures reliable data capture, preventing distortions or discrepancies.

The introduction of the unique dynamic temperature-based data collection approach and rotational thermography in the context of breast cancer screening has significantly augmented the accuracy and effectiveness of the screening process, providing a solution for early detection

and timely intervention in cases of breast cancer disease. Efficient imaging algorithms and intelligent data analysis techniques have paved the way for early detection and intervention of breast cancer. The entire system encompasses intelligent medical diagnostic modules with a newly developed virtual instrumentation architecture for an automated system to generate firm opinions on any relevant subject dataset. The system's design was crucial for the diagnostic process, utilizing the Genfis property appropriately [87]. The data collection program was conducted on random patients at Cachar Cancer Hospital in Silchar, resulting in the current dataset. The system was trained using the collected data set.

LabVIEW software was used to develop a virtual instrumentation module that implements intelligent medical diagnostic systems for oral cancer detection using infrared imaging.

All required clinical settings were meticulously followed and adhered to ethical guidelines and best practices during the investigations. A rigorous data collection and analysis process was implemented. [14], [50], [51][81]

The proposed IR imaging paradigm was validated through testing in diverse clinical settings. The careful development of the system and further refinement of the developed image-processing software can address varying environmental conditions and clinical complexities.

Highlights of the research work carried out and reported in previous chapters of the thesis are briefly presented below for reference.

7.1.1 Development of an Innovative Approach in Infra-red Imaging for Medical Applications

Chapter II describes the innovative approach in infra-red imaging for medical applications.

The study discusses the correlation between pathology and infrared imaging, research planning, thermal image acquisition, image processing techniques, and intelligent image segmentation.

RoI detection using Dynamic Contour Evolution:

This section highlights the RoI detection method through Dynamic Contour Evolution, which implemented a precise automated LabView-based virtual instrument software module. This work employs dynamic contour evolution based on level-set and active contour models to identify Region of Interest (ROIs) on the side faces of 85 subjects. This process, encompassing two stages of dynamic thresholding and application of the Geometric Pattern Matching algorithm, has led to attaining 95% accuracy in extracting the highest temperature region of the ear for subsequent temperature analysis.

Feature Extraction, Statistical Analysis, and Neural Network Modelling:

This involves extracting Statistical features from the thermal distribution of the ear zone. It includes measuring properties such as mean, standard deviation, mode, median, root mean square, maximum value, and other relevant features. After extraction, statistical analysis is performed on the features to differentiate between diabetic and non-diabetic subjects. Tools like SPSS, Unscrambler, Matlab, and LabView are utilized for this purpose. The analysis involved creating models for pattern classification and correlation assessments. This led to using machine learning algorithms, such as Support Vector Machines, Back Propagation Neural Networks, Radial Basis Function Neural Networks, Probabilistic Neural Networks, and Bayes Classifiers. Subjects were then categorized as diabetic or non-diabetic based on extracted features using the above algorithms. Classifier performance was compared across different classifiers using parameters like accuracy, sensitivity, and specificity, with the Bayes classifier demonstrating the highest average accuracy among all classifiers. The evaluation has been done on the male and female groups separately.

Development and results of Neural Network predictive models:

Neural Networks were employed to predict temperature profiles based on extracted features. These features, obtained from 85 diabetic and non-diabetic subjects, were reduced to four key elements using Principal Component Analysis. The subsequent implementation of Neural Networks yielded a model with an overall accuracy of 81.2%, as demonstrated through a confusion matrix and a Receiver Operating Characteristic (ROC) Curve. Various

classification algorithms were employed, and their corresponding overall accuracies were presented. The study, involving 243 human subjects across different diabetic camps and climatic conditions in India, was done through collaborative efforts with medical institutions and the continuous refinement of software for diverse image data. The algorithm for statistical image analysis was implemented to capture statistical values of the region of interest, which played a crucial role in classification via machine learning algorithms.

Development of Pattern Recognition Tools for IR Imaging-based Health Monitoring software:

Image processing and pattern recognition algorithms were integrated to develop software modules and tools for monitoring human health. These tools underwent iterative improvements based on feedback obtained from hospital-based data collection and validation activities. The feature selection process involved comparing various classification techniques using feature ranking methods. Specialized tools for pattern recognition have been explicitly enhanced for software used in imaging body emissions. These tools combine hardware and software components, including an infrared camera, to collect data in real-world settings such as Diabetic Camps. The LabVIEW software modules were modified to create an interface and control system, perform image analysis, and generate statistical measures. Machine learning and pattern recognition training were done using Matlab tools.

7.1.2 Development of Infra-red Imaging-based Stress and Diabetic Level Monitoring System

Specific applications of infrared imaging for Stress and Diabetic Level Monitoring of human subjects are considered in Chapter III. This new approach differs from conventional methods by using infrared imaging, an interactive Stroop test, and temperature-controlled conditions. It is a non-invasive method that can effectively monitor stress levels and evaluate thermal changes related to diabetes. It diverges from traditional and integrated diagnostic approaches, providing a comprehensive means of evaluation.

Implementation of Combined solution of IR-imaging and interactive Stroop Test for stress level monitoring:

Infrared imaging with pattern recognition techniques has been integrated to create a non-invasive and comprehensive method beyond traditional diagnostic approaches. The study involves a computerized "Paced Stroop Test," adapted to simulate real-world stress environments, synchronized with IR image acquisition for skin temperature analysis. The experimental setup consists of a temperature-controlled environment, an IR image acquisition system, and virtual instrument software for analyzing, interpreting, and reporting IR images. The combined solution provided a holistic understanding of stress levels and assessed diabetes-related thermal changes in human subjects.

Design and implementation of a Diabetes monitoring system using IR-Imaging:

The same was done by exploring the process of capturing IR images from different body parts, including the ear lobe, inner centre points, inner posterior buccal cavity, and palm, to monitor diabetic patients over a specific period.

Development of Experimental setup:

The measurement Procedure in the Virtual Instrument deals with the details of the experimental setup, including the capture of around 500 still IR images in various postures, the recording of base images at the initial point, and an interactive Stroop test was applied to assess stress levels, forming a non-invasive and comprehensive approach for monitoring stress levels and evaluating diabetes-related thermal changes.

7.1.3 Development of Oral Cancer Detection Technique using IR Image Processing

The techniques for developing Oral Cancer detection methods using IR Image Processing are described in Chapter IV. The data collection methodology was followed based on earlier works from the literature. The current work reflects implementing an automated system to generate decisive opinions on the collected data set. The system utilizes a fuzzy logic approach, which becomes an integral part of the diagnostic system**.**

Feature Extraction for IR Image Analysis:

This section deals with extracting relevant features from infrared (IR) images. Temperature variations indicating oral cancer were identified by studying patterns, thermal irregularities, and anomalies in captured images. Several image processing techniques, such as edge detection, gradient analysis, and temperature thresholding, were employed to enhance the precision of feature extraction.

System overview:

This section details the workflow and architecture of the developed oral cancer detection system. This includes the step-by-step process from image acquisition to prediction, covering elements like Computational Fluid Dynamics (CFD), Data Flow Diagrams (DFD), and training techniques. The fuzzy logic approach has been introduced into the system, which has played an essential role in the decision-making process based on the collected data set. The section provides a comprehensive report on how each component contributes to the diagnostic system.

Issues in Oral Image Capturing:

This section addresses the practical challenges encountered while capturing infrared images of the oral cavity. It highlights the limitations posed by the size of standard IR camera lenses in reaching the buccal cavity. The study emphasizes the inherent difficulty in designing a foolproof system that effectively captures images from the inner regions of the oral cavity. The limitations of the IR camera, specifically its focal area and minimum focus distance, are outlined in imaging the critical hidden portions of the mouth.

Performance measure:

This part describes the evaluation methods of the developed system through a series of metrics. Sensitivity, specificity, positive and negative predictive values, accuracy, and false positive and false negative ratios are discussed. It also provides insights into how well the system can identify true positive and true negative cases, the trade-offs between sensitivity and specificity, and the overall diagnostic efficiency. The section introduces metrics like likelihood and diagnostic odds ratios to understand system performance.

7.1.4 Potential Use of Infra-red Imaging in Medical Diagnosis - Comprehensive Framework for Diabetes & Breast Cancer Screening

A framework for screening diabetes and breast cancer using IR imaging is elaborated in Chapter V. The work consisted of two main parts: selecting Region of Interest (ROI) for infrared imaging in diabetes and Breast cancer-related equipment using the most significant body parts and developing a non-contact, non-invasive breast imaging method using infrared technology.

Diabetes screening methodology:

This involves capturing infrared images from specific body parts such as the face, neck, hands, legs, and ears. A precise data acquisition system is developed by using an Arduino Uno microcontroller with a temperature sensor. This integration shows the utilization of embedded systems in the Diabetes Screening Methodology for accurate data acquisition.

Data Collection and Analysis Techniques:

The exercise is systematically carried out in a controlled environment at Chennai-based hospital. Subjects acclimate to a temperature-controlled room for 15 minutes, and two sessions, comprising fasting and postprandial blood draws, are conducted daily on 12 to 13 subjects. Various ROI selection methods and image processing algorithms, including thresholding, are employed to enhance the accuracy of data analysis.

In-depth analysis incorporates statistical and feature extraction techniques, employing a "Hough transform" algorithm. The classification process is enriched with the application of machine learning, specifically utilizing the Support Vector Machine (SVM) algorithm. The IR-image feature-based analysis involves extracting statistical features for a comprehensive analysis of the captured infrared images.

Breast Cancer Screening Methodology:

This involves conducting four pilot studies, each utilizing specific setups to optimize infrared image data collection. The method integrates data collection and analysis techniques, employing advanced clustering methods for segmentation and Region of Interest (ROI)

extraction. Improving breast cancer detection accuracy is a crucial focus, and innovative data analysis approaches are integrated with infrared imaging technology to achieve this goal.

Data Collection Techniques:

Four pilot studies are executed with tailored setups, including subjects sitting with raised hands, a camera moving in a semi-circular arc, and rotational thermography. These helped to improve data acquisition for breast cancer screening.

Integration of Data Collection and Analysis Techniques:

Data analysis techniques are seamlessly incorporated into the system, ensuring optimal performance. Clustering methods are utilized for segmentation and ROI extraction, with optimizations based on experimental validation.

Reference-Based Analysis Techniques:

In pilot studies PS1 and PS2, conventional analysis involves extracting features like mean, median, mode, and standard deviation. In PS3, ultrasound and biopsy reports are used as references, employing clustering for segmentation and average temperature of each ROI as a discriminative feature.

Temperature-Controlled Enclosure:

In the FS pilot study, a temperature-controlled enclosure is integrated, utilizing differences in IR images at various ambient temperatures as a key discriminating feature.

IR Image Feature-based Analysis Technique:

Statistical features such as mean, median, mode, standard deviation, and maximum value for IR image-based analysis are employed to develop the system.

Optimizations and Improvements:

Continuous modification and optimization techniques address challenges, improving imaging results based on experimental validation and consultations with medical professionals.

Creation of Comparative Chart for Infrared Imaging-based Diabetes and Breast Cancer Detection:

The same is created by systematically comparing the methodologies used in the screening processes for both diseases. This chart covers imaging setup, data collection, temperature control, processing techniques, analysis methods, feature extraction, machine learning-based classification and overall aims. It serves as a valuable tool to highlight similarities and differences, aiding in the optimization and refinement of both screening methods.

This comparison led to developing a common framework for Diabetes and Breast Cancer Screening using Infrared (IR) imaging. The approach includes designing a unified framework, establishing a standard imaging setup, implementing standardized data collection protocols, ensuring temperature control, employing consistent image processing techniques, applying standardized analysis methods, developing a comparative chart for systematic evaluation, integrating advanced technologies, and iteratively optimizing the framework based on feedback and advancements. This structured and integrated approach ensures efficiency and accuracy in diabetes and breast cancer screening.

7.1.5 Efficient Infra-red Image Processing and Machine Learning Algorithm for Breast Cancer Screening

Efficient infrared Image Processing and Machine Learning Algorithms and their implementation methods for Breast Cancer Screening have been discussed in chapter 6. Here, dynamic temperature-based data collection and rotational thermography techniques have been employed for breast cancer screening. Image processing and machine learning techniques extract relevant features from the captured images. A broad dataset of thermal images was collected, and relevant features were extracted and used to train a machine-learning model. The developed screening system was tested on an increasing patient population in a clinical setting deployed at a hospital. The following approaches have been undertaken:

Data Collection System with Hardware and Software Interface:

A table top unit featuring a semi-circular template is utilized to ensure the precise positioning of breasts during infrared image capture. Infrared images are systematically collected at 14 positions for each breast, incorporating dynamic infrared imaging to account

for temperature variation. The system uses LabVIEW, a Thermovision toolkit, and Infratech Variocam for infrared image capturing.

Interface for Doctor's Marking on ROI with Clinical Validation:

A specialized software interface is developed to aid doctors in identifying suspicious areas on infrared images and gathering insights from ultrasound/ mammography and biopsy reports. Comprehensive clinical summaries are created using doctors' advice and stored in a database.

Data Analysis with Image Processing and Machine Learning Techniques:

A dataset of breast thermal images is meticulously collected using an infrared camera. Various image processing techniques, including noise reduction and segmentation, are applied to preprocess the collected images. Using statistical analysis, relevant features are extracted from the thermal images and subsequently utilized to train a machine-learning model.

Development of Software Algorithm for Breast Abnormality Detection:

An algorithm inspired by previous research studies has been created to accurately detect abnormalities.

Abnormality detection in infrared images:

Techniques such as grayscale tumour image-to-colour image conversion and Fuzzy C-Means clustering are employed to detect the abnormalities. The algorithm is adapted to accommodate 16-bit IR images, utilizing clusters as features for subsequent machine-learning processes.

Clinical Summary:

Comprehensive clinical reports are systematically generated, including doctors' remarks and manual markings on breast images. A sample clinical report is presented, identifying cancer in the right breast and confirming the normalcy of the left breast.

Development of Machine Learning Model:

A Neural Network (NN)-based back propagation algorithm is implemented for machine learning, generating a comprehensive database for all images. Fuzzy C-Means clustering is employed to optimize the number of clusters for subsequent machine learning processes. The developed neural network model underwent rigorous testing, validation, and subsequent implementation in a clinical setting.

Performance Analysis:

Performance metrics, encompassing accuracy, sensitivity, and specificity, are systematically employed to evaluate the effectiveness of the developed algorithm. The final study dataset, consisting of 119 subjects, demonstrates enhanced performance, achieving an accuracy rate of 93.27% compared to the pilot study dataset. Here, parameters like sensitivity, specificity, and accuracy values are meticulously calculated and presented for both datasets.

7.2 Future Work

Improvement in system performance requires an increase in the feature set and database. New computational methods are being implemented to yield better results. For research, there has been a frequent search for infrared imaging and earlier studies related to diabetes. Although some medical journals have mentioned specific indications, the exact process has not yet been described. However, the techniques developed as depicted in this thesis are significant advancements in establishing IR imaging in selected medical areas for detection or screening purposes. This non-invasive way of imaging with intelligent processing will make the techniques popular when available in computer-based system solutions.

The following work may be carried out further:

To improve the performance of the presently practised image processing system in cases of diabetic patients in the following aspects:

Innovative Data Collection: Utilize multi-spectral infrared imaging for diverse and comprehensive datasets.

Smart Temperature Control: Investigate inventive methods to minimize variations during image capture and address environmental impact through adaptive control mechanisms.

Advanced Image Processing: Create sophisticated algorithms for precise region-of-interest selection.

Next-gen Machine Learning: Explore advanced algorithms, such as neural networks, to next-gen machine learning algorithms and AI techniques. Develop personalized models, refining gender and age-specific approaches.

Cost-Efficient solution development: Investigate low-cost solutions for infrared imaging, ensuring affordability.

To improve the performance of the oral cancer detection system through a new approach using infrared imaging.

Further experimentation is needed to develop an instrumentation system for a miniaturized infrared camera needed towards a customized data collection system for accurately capturing oral cancer data from inside the mouth, a modified algorithm for the Region of Interest (ROI) selection, contouring and analysis, which will help in practical implementation and validation of the system.

Advanced Imaging and Analysis: Explore other oral imaging and alternative analysis methods for improved feature extraction from thermal images.

Algorithm Optimization: Enhance and optimize machine learning algorithms, comparing Genfis with SVM for increased prediction accuracy.

Expanded Data Set and Validation: Collaborate with diverse healthcare institutions to expand the dataset and conduct thorough performance evaluations. Validate the system through practical application and clinical trials with input from dental experts.

Continuous Improvement and Diversification: Optimize Genfis algorithm based on feedback, adapting it for diverse patient populations and oral cancer types. Collaborate with specialists, emphasizing practical research.

Exploring broader applications in healthcare domains beyond oral cancer would help the proliferation of IR Thermal imaging and analysis techniques.

References

[1] M. Anbar, “Telethermometric Psychological Evaluation By Monitoring of Changes In Skin Perfusion Induced By The Autonomic Nervous System,” 1998

[2] S. Sivanandam, M. Anburajan, B. Venkatraman, M. Menaka, and D. Sharath, “Medical thermography: a diagnostic approach for type 2 diabetes based on non-contact infrared thermal imaging,” *Endocrine*, vol. 42, no. 2, pp. 343–351, Oct. 2012, doi: 10.1007/s12020-012-9645-8.

[3] L.V. Beloussov, and F. A. Popp, “Biophotonics: Non-Equilibrium and Coherent Systems in Biology, Biophysics and Biotechnology,” 1995.

[4] J. J. Chang and F. A. Popp, “Biological organization: A possible mechanism based on the coherence of biophotons,” *Bio photons,* pp. 217–227, 1998.

[5] B.Jezowska-Trzebiatowska, B. Kochel, J.Slawinski, and W. Strek, “Biological Luminescence. Singapore: World Scientific.” 1990.

[6] J. J. Chang and F. A. Popp, “The physical background and the informational character of biophoton emission". Biophotons,” 1998.

[7] C. Zhang, F. A. Popp, and M. Bischof, “Current Development of Biophysics.” in *Hangzhou University Press Hangzhou China*, 1996.

[8] M. Etehad Tavakol, S. Sadri, and E. Y. K. Ng, “Application of K- and Fuzzy c-Means for Color Segmentation of Thermal Infrared Breast Images,” *J Med Syst*, vol. 34, no. 1, pp. 35–42, 2010, doi: 10.1007/s10916-008-9213-1.

[9] M. Etehad Tavakol and E. Y. K. Ng, “Color Segmentation of Breast Thermograms: A Comparative Study.” pp. 69–77, 2017. doi: 10.1007/978-981-10-3147-2_6.

[10] S. Pramanik, D. Banik, D. Bhattacharjee, M. Nasipuri, M. K. Bhowmik, and G. Majumdar, “Suspicious-Region Segmentation From Breast Thermogram Using DLPE-Based Level Set Method,” *IEEE Trans Med Imaging*, vol. 38, no. 2, pp. 572–584, 2019, doi: 10.1109/TMI.2018.2867620.

[11] A. Bandyopadhyay, H. S. Mondal, and A. Hazra, “Infrared Imaging of stress level monitoring for intelligent diagnosis system,” in *2nd International Conference on Biomedical Engineering and Assistive Technologies, BEATS-2012, NIT Jalandhar*, Dec. 2012.

[12] A. Bandyopadhyay, H. S. Mondal, B. Mukherjee, and Dr. A. Chaudhuri, "Intelligent health care system for Stress and Diabetic Level Monitoring using Infrared Imaging," in *CSI Journal of Computing*, Dec. 2012.

[13] A. Bandyopadhyay, H. S. Mondal, B. Mukherjee, and A. Chaudhuri, "Infrared Imaging of Stress and Diabetic Level Monitoring for Intelligent Healthcare System," *CSI Journal of Computing*, vol. 2, no. 1, pp. 66–74, 2013.

[14] A. Bandyopadhyay, H. S. Mondal, and A. Chaudhuri, "Thermal Imaging-Based Diabetes Screening Uses Medical Image Processing Techniques," *International Journal of Engineering Research & Technology (IJERT)*, vol. 3, Nov. 2014.

[15] M. Etehad Tavakol, V. Chandran, E. Y. K. Ng, and R. Kafieh, "Breast cancer detection from thermal images using bispectral invariant features," *International Journal of Thermal Sciences*, vol. 69, pp. 21–36, 2013, doi: 10.1016/j.ijthermalsci.2013.03.001.

[16] M. Garduño-Ramón, S. Vega-Mancilla, L. Morales-Henández, and R. Osornio-Rios, "Supportive Non-invasive Tool for the Diagnosis of Breast Cancer Using a Thermographic Camera as Sensor," *Sensors*, vol. 17, no. 3, p. 497, 2017, doi: 10.3390/s17030497.

[17] R. M. Prakash, K. Bhuvaneshwari, M. Divya, K. J. Sri, and A. S. Begum, "Segmentation of thermal infrared breast images using K-means, FCM and EM algorithms for breast cancer detection," in *2017 International Conference on Innovations in Information, Embedded and Communication Systems (ICIIECS)*, IEEE, 2017, pp. 1–4. doi: 10.1109/ICIIECS.2017.8276142.

[18] K. Venkataramani, L. K. Mestha, L. Ramachandra, S. S. Prasad, V. Kumar, and P. J. Raja, "Semi-automated breast cancer tumour detection with thermographic video imaging," in *2015 37th Annual International Conference of the IEEE Engineering in Medicine and Biology Society (EMBC)*, IEEE, Aug. 2015, pp. 2022–2025. doi: 10.1109/EMBC.2015.7318783.

[19] S. G. Kandlikar *et al.*, "Infrared imaging technology for breast cancer detection – Current status, protocols and new directions," *Int J Heat Mass Transf*, vol. 108, pp. 2303–2320, May 2017, doi: 10.1016/j.ijheatmasstransfer.2017.01.086.

[20] C. Rafael Gonzalez and R. E. Woods, "Digital Image Processing," 2007.

[21] K. Nishide *et al.*, "Ultrasonographic and thermographic screening for latent inflammation in diabetic foot callus," *Diabetes Res Clin Pract*, vol. 85, no. 3, pp. 304–309, Oct. 2009, doi: 10.1016/j.diabres.2009.05.018.

[22] Y. Fujiwara, T. Inukai, Y. Aso, and Y. Takemura, "Thermographic measurement of skin temperature recovery time of extremities in patients with type 2 diabetes mellitus," *Experimental and Clinical Endocrinology & Diabetes*, vol. 108, no. 07, pp. 463–469, Dec. 2000, doi: 10.1055/s-2000-8142.

[23] H. Fushimi, T. Inoue, Y. Yamada, Y. Matsuyama, M. Kubo, and M. Kameyama, "Abnormal vasoreaction of peripheral arteries to cold stimulus of both hands in diabetics," *Diabetes Res Clin Pract*, vol. 32, no. 1–2, pp. 55–59, Apr. 1996, doi: 10.1016/0168-8227(96)01222-3.

[24] S. Sivanandam, M. Anburajan, B. Venkatraman, M. Menaka, and D. Sharath, "Medical thermography: a diagnostic approach for type 2 diabetes based on non-contact infrared thermal imaging," *Endocrine*, vol. 42, no. 2, pp. 343–351, Oct. 2012, doi: 10.1007/s12020-012-9645-8.

[25] B. Kyle, "Stress detection device and methods of use thereof," Feb. 2011

[26] J. Lipkova and J. Cechak, "Human electromagnetic emission in the ELF band," *MEASUREMENT SCIENCE REVIEW*, vol. 5, no. 2, 2005.

[27] V. V. Tuchin, *Handbook of Photonics For Biomedical Science*. 2019.

[28] R. Van Wijk, M. Kobayashi, and E. P. A. Van Wijk, "Anatomic characterization of human ultra-weak photon emission with a moveable photomultiplier and CCD imaging," *J Photochem Photobiol B*, vol. 83, no. 1, pp. 69–76, Apr. 2006, doi: 10.1016/j.jphotobiol.2005.12.005.

[29] V. Beloussov, F. A. Popp, V. Voeikov, and R. VanWijk, "Biophotonics and Coherent Systems," 2000.

[30] N. A. Diakides and J. D. Bronzino, *Medical Infrared Imaging*. CRC Press, 2007. doi: 10.1201/9781420008340.

[31] P. Taneja *et al.*, "Classical and Novel Prognostic Markers for Breast Cancer and their Clinical Significance," *Clin Med Insights Oncol*, vol. 4, p. CMO.S4773, Jan. 2010, doi: 10.4137/CMO.S4773.

[32] T. Szafarowski, J. Sierdzinski, M. J. Szczepanski, T. L. Whiteside, N. Ludwig, and A. Krzeski, "Microvessel density in head and neck squamous cell carcinoma," *European Archives of Oto-Rhino-Laryngology*, vol. 275, no. 7, pp. 1845–1851, Jul. 2018, doi: 10.1007/s00405-018-4996-2.

[33] S. V. Ekkad and P. Singh, "Liquid Crystal Thermography in Gas Turbine Heat Transfer: A Review on Measurement Techniques and Recent Investigations," *Crystals (Basel)*, vol. 11, no. 11, p. 1332, Oct. 2021, doi: 10.3390/cryst11111332.

[34] J. F. HEAD, F. WANG, and R. L. ELLIOTT, "Breast Thermography Is a Non-invasive Prognostic Procedure That Predicts Tumour Growth Rate in Breast Cancer Patients," *Ann N Y Acad Sci*, vol. 698, no. 1, pp. 153–158, Nov. 1993, doi: 10.1111/j.1749-6632.1993.tb17203.x.

[35] W. C. Amalu et al., "Review of Thermography,"

https://www.thermologyclinic.com/for-physicians.

[36] U. Forstermann and W. C. Sessa, "Nitric oxide synthases: regulation and function," *Eur Heart J*, vol. 33, no. 7, pp. 829–837, Apr. 2012, doi: 10.1093/eurheartj/ehr304.

[37] Y. Feng *et al.*, "Breast cancer development and progression: Risk factors, cancer stem cells, signaling pathways, genomics, and molecular pathogenesis," *Genes Dis*, vol. 5, no. 2, pp. 77–106, Jun. 2018, doi: 10.1016/j.gendis.2018.05.001.

[38] F1. Martínez-Arribas, P. L., E. Martín-Garabato , A. Tejerina, R. Lucas , J. Sánchez , and J. Schneider , "Immune-histo-chemistry and flow cytometry technique equipment Proliferation measurement in breast cancer by two different methods ".

[39] M. Vollmer and K. Möllmann, *Infrared Thermal Imaging*. Wiley, 2017. doi: 10.1002/9783527693306.

[40] A. Tah, "Tissue impedance measurement techniques for cancer and malignant tissue detection," in *2014 International Conference on Green Computing Communication and Electrical Engineering (ICGCCEE)*, IEEE, Mar. 2014, pp. 1–4. doi: 10.1109/ICGCCEE.2014.6922221.

[41] N. A. Diakides and J. D. Bronzino, *Medical Infrared Imaging*. CRC Press, 2007. doi: 10.1201/9781420008340.

[42] R. D. Rosenberg *et al.*, “Effects of age, breast density, ethnicity, and estrogen replacement therapy on screening mammographic sensitivity and cancer stage at diagnosis: review of 183,134 screening mammograms in Albuquerque, New Mexico.,” *Radiology*, vol. 209, no. 2, pp. 511–518, Nov. 1998, doi: 10.1148/radiology.209.2.9807581.

[43] J. G. Elmore, M. B. Barton, V. M. Moceri, S. Polk, P. J. Arena, and S. W. Fletcher, “Ten-Year Risk of False Positive Screening Mammograms and Clinical Breast Examinations,” *New England Journal of Medicine*, vol. 338, no. 16, pp. 1089–1096, Apr. 1998, doi: 10.1056/NEJM199804163381601.

[44] R. L. E. W. C. A. William B. Hobbin Jonathan F. Head, *Medical Devices and Systems*, 3rd ed., vol. 25. CRC Press, 2006.

[45] J. R. Keyserlingk, P. D. Ahlgren, E. Yu, N. Belliveau, and M. Yassa, “Functional infrared imaging of the breast,” *IEEE Engineering in Medicine and Biology Magazine*, vol. 19, no. 3, pp. 30–41, 2000, doi: 10.1109/51.844378.

[46] A. Sodi, B. Giambene, P. Miranda, G. Falaschi, A. Corvi, and U. Menchini, “Ocular surface temperature in diabetic retinopathy: a pilot study by infrared thermography,” *Eur J Ophthalmol*, vol. 19, no. 6, pp. 1004–1008, Nov. 2009, doi: 10.1177/112067210901900617.

[47] E. F. J. Ring and K. Ammer, “Infrared thermal imaging in medicine,” *Physiol Meas*, vol. 33, no. 3, pp. R33–R46, Mar. 2012, doi: 10.1088/0967-3334/33/3/R33.

[48] M. N. Wu, C. C. Lin, and C.C. Chang, “Brain Tumour Detection Using Color-Based K-Means Clustering Segmentation,” in *Third International Conference on Intelligent Information Hiding and Multimedia Signal Processing (IIH-MSP 2007)*, IEEE, 2007, pp. 245–250. doi: 10.1109/IIHMSP.2007.4457697.

[49] A. Bandyopadhyay, H. S. Mondal, and A. Chaudhuri, “Intelligent IR based image processing techniques for medical application,” in *Proceedings of 2016 SAI Computing Conference, SAI 2016*, Jul. 2016.

[50] A. Bandyopadhyay, H. S. Mondal, B. Dam, and D. C. Patranabis, “Efficient infrared image processing and machine learning algorithm for breast cancer screening,” *Comput Methods Biomech Biomed Eng Imaging Vis*, pp. 1–13, Jun. 2023, doi: 10.1080/21681163.2023.2225639.

[51] A. Bandyopadhyay, H. S. Mondal, B. Pal, B. Dam, and D. C. Patranabis, “Exploring the potential use of infrared imaging in medical diagnosis: comprehensive framework for diabetes & breast cancer screening ,” *Proceedings of 4th International Conference on Image Processing & Capsule Networks (ICIPCN 2023), Springer Link*, Aug. 2023, doi: 10.1007/978-981-99-7093-3_27.

[52] D. Patel, H. Thakker, M. B. Kiran, and V. Vakharia, “Surface roughness prediction of machined components using gray level co-occurrence matrix and Bagging Tree,” *FME Transactions*, vol. 48, no. 2, pp. 468–475, 2020, doi: 10.5937/fme2002468P.

[53] V. Vakharia, M. B. Kiran, N. J. Dave, and U. Kagathara, “Feature extraction and classification of machined component texture images using wavelet and artificial intelligence techniques,” in *2017 8th International Conference on Mechanical and Aerospace Engineering (ICMAE)*, IEEE, Jul. 2017, pp. 140–144. doi: 10.1109/ICMAE.2017.8038631.

[54] E. H. Houssein, M. M. Emam, and A. A. Ali, “An optimized deep learning architecture for breast cancer diagnosis based on improved marine predators algorithm,” *Neural Comput Appl*, vol. 34, no. 20, pp. 18015–18033, Oct. 2022, doi: 10.1007/s00521-022-07445-5.

[55] E. H. Houssein, Z. Abohashima, M. Elhoseny, and W. M. Mohamed, “Machine learning in the quantum realm: The state-of-the-art, challenges, and future vision,” *Expert Syst Appl*, vol. 194, p. 116512, May 2022, doi: 10.1016/j.eswa.2022.116512.

[56] E. H. Houssein, D. A. Abdelkareem, M. M. Emam, M. A. Hameed, and M. Younan, “An efficient image segmentation method for skin cancer imaging using improved golden jackal optimization algorithm,” *Comput Biol Med*, vol. 149, p. 106075, Oct. 2022, doi: 10.1016/j.compbiomed.2022.106075.

[57] E. H. Houssein, Z. Abohashima, M. Elhoseny, and W. M. Mohamed, “An efficient binary harris hawks optimization based on quantum SVM for cancer classification tasks,” in *The 2nd International Conference on Distributed Sensing and Intelligent Systems (ICDSIS 2021)*, Institution of Engineering and Technology, 2021, pp. 247–258. doi: 10.1049/icp.2021.2680.

[58] E. H. Houssein, M. M. Emam, and A. A. Ali, “An efficient multilevel thresholding segmentation method for thermography breast cancer imaging based on improved chimp optimization algorithm,” *Expert Syst Appl*, vol. 185, p. 115651, Dec. 2021, doi: 10.1016/j.eswa.2021.115651.

[59] E. H. Houssein, D. S. Abdelminaam, H. N. Hassan, M. M. Al-Sayed, and E. Nabil, “A Hybrid Barnacles Mating Optimizer Algorithm With Support Vector Machines for Gene Selection of Microarray Cancer Classification,” *IEEE Access*, vol. 9, pp. 64895–64905, 2021, doi: 10.1109/ACCESS.2021.3075942.

[60] National Instruments Corporation, *NI Vision Concept Manual*. Texas USA: ni.com, 2005.

[61] L. Hargasa, D. Koniara, A. Simonovaa, M. Hriankaa, and Z. Loncovaa, “Novel Machine Vision Tools Applied in Biomechatronic Tasks,” *Modelling of Mechanical and Mechatronic Systems*, 2014, doi: 10.1016/j.proeng.2014.12.134.

[62] C. Li, Chenyang Xu, C. Gui, and M. D. Fox, “Distance Regularized Level Set Evolution and Its Application to Image Segmentation,” *IEEE Transactions on Image Processing*, vol. 19, no. 12, pp. 3243–3254, Dec. 2010, doi: 10.1109/TIP.2010.2069690.

[63] V. Caselles, T. C. F. Catte, and F. Dibos, “A geometric model for active contours in image processing,” Dec. 1993.

[64] R. Malladi, J. A. Sethian, and B. C. Vemuri, “Shape modeling with front propagation: a level set approach,” *IEEE Trans Pattern Anal Mach Intell*, vol. 17, no. 2, pp. 158–175, 1995, doi: 10.1109/34.368173.

[65] A. W. and D. T. M. Kass, “Snakes: Active contour models,” Jan. 187AD.

[66] S.C. Zhu and A. Yuille, “Region competition: Unifying snakes, region growing,and Bayes/MDL for multiband image segmentation,” Sep. 1996.

[67] C. Xu and J. L. Prince, “Snakes, shapes, and gradient vector flow,” *IEEE Transactions on Image Processing*, vol. 7, no. 3, pp. 359–369, Mar. 1998, doi: 10.1109/83.661186.

[68] J. Sethian, “Level Set Methods and Fast Marching Methods,” 1999.

[69] S. Osher and R. Fedkiw, “Level Set Methods and Dynamic Implicit Surfaces,” 2002.

[70] R. B. Pereira, Alexandre Plastino, Bianca Zadrozny, Luiz H. C., and Merschmann, “Information Gain Feature Selection for Multi-Label Classification,” Feb. 2015.

[71] A. Peleki and A. da Silva, “Novel Use of Smartphone-based Infrared Imaging in the Detection of Acute Limb Ischaemia,” *EJVES Short Rep*, vol. 32, pp. 1–3, 2016, doi: 10.1016/j.ejvssr.2016.04.004.

[72] M. H. Tom Mitchell, “Machine Learning,” 1997.

[73] H. Selye, *Selye’s Guide to Stress Research*. Van Nostrand Reinhold, 1980.

[74] J. R. Stroop, “Studies of interference in serial verbal reactions” *J Exp Psychol*, vol. 18, no. 6, pp. 643–662, Dec. 1935, doi: 10.1037/h0054651.

[75] P. Renaud and J.P. Blondin, “The stress of Stroop performance: physiological and emotional responses to colour-word interference, task pacing, and pacing speed,” 1997.

[76] A. Barreto and J. Zhai, “Physiological Instrumentation for Real-time Monitoring of Affective State of Computer Users”.

[77] C. Hildebrandt, C. Raschner, and K. Ammer, “An Overview of Recent Application of Medical Infrared Thermography in Sports Medicine in Austria,” *Sensors*, vol. 10, no. 5, pp. 4700–4715, May 2010, doi: 10.3390/s100504700.

[78] P. Kapoor and S. V. A. V Prasad, “Image processing for early diagnosis of breast cancer using infrared images,” in *2010 The 2nd International Conference on Computer and Automation Engineering (ICCAE)*, IEEE, Feb. 2010, pp. 564–566. doi: 10.1109/ICCAE.2010.5451827.

[79] M. A. S. Ali, G. I. Sayed, T. Gaber, A. E. Hassanien, V. Snasel, and L. F. Silva, “Detection of Breast Abnormalities of Thermograms based on a New Segmentation Method,” Oct. 2015, pp. 255–261. doi: 10.15439/2015F318.

[80] C. Zakian, I. Pretty, and R. Ellwood, “Near-infared hyperspectral imaging of teeth for dental caries detection,” *J Biomed Opt*, vol. 14, no. 6, p. 064047, 2009, doi: 10.1117/1.3275480.

[81] A. Bandyopadhyay, H. Sekhar Mondal, B. Dam, and D. Chandra Patranabis, “An Overview of Infra-red Image Processing Based Oral Cancer Detection Technique,” *Archives of Advanced Engineering Science*, Dec. 2023, doi: 10.47852/bonviewAAES32021844.

[82] S. Chucherd, “Edge detection of medical image processing using vector field analysis,” in *2014 11th International Joint Conference on Computer Science and Software Engineering (JCSSE)*, IEEE, May 2014, pp. 58–63. doi: 10.1109/JCSSE.2014.6841842.

[83] R. Mammone, S. Love, L. Barinov, W. Hulbert, A. Jairaj, and C. Podilchuk, “Preprocessing for improved computer aided detection in medical ultrasound,” in *2013 IEEE Signal Processing in Medicine and Biology Symposium (SPMB)*, IEEE, Dec. 2013, pp. 1–3. doi: 10.1109/SPMB.2013.6736776.

[84] V. Bhateja, G. Singh, A. Srivastava, and J. Singh, “Speckle reduction in ultrasound images using an improved conductance function based on Anisotropic Diffusion,” in 2014 International Conference on Computing for Sustainable Global Development (INDIACom*)*, IEEE, Mar. 2014, pp. 619–624. doi: 10.1109/IndiaCom.2014.6828036.

[85] M. Chakraborty, S. Mukhopadhyay, A. Dasgupta, S. Patsa, N. Anjum, and J. G. Ray, “A new approach of oral cancer detection using bilateral texture features in digital infrared thermal images,” in *2016 38th Annual International Conference of the IEEE Engineering in Medicine and Biology Society (EMBC)*, IEEE, Aug. 2016, pp. 1377–1380. doi: 10.1109/EMBC.2016.7590964.

[86] M. Chakraborty, R. Das Gupta, S. Mukhopadhyay, N. Anjum, S. Patsa, and J. G. Ray, “An introductory analysis of digital infrared thermal imaging guided oral cancer detection using multiresolution rotation invariant texture features,” S. G. Armato and N. A. Petrick, Eds., Mar. 2017, p. 101343D. doi: 10.1117/12.2254322.

[87] H. Surmann and lexander Selenschtschikow, “Automatic generation of fuzzy logic rule bases: Examples I,” in First International ICSC Conference on Neuro-Fuzzy Technologies, Oct. 2002, pp. 75–81.

AsokBandyopadhyay

(Signature of the Candidate)

30/09/2024